NOVEL ENGINEERED COMPOUND SEMICONDUCTOR HETEROSTRUCTURES FOR ADVANCED ELECTRONICS APPLICATIONS

(2)

FINAL REPORT

by

GREGORY E. STILLMAN
NICK HOLONYAK, JR.
JAMES J. COLEMAN

JUNE 22, 1992

U.S. ARMY RESEARCH OFFICE

DAAL03-89-K-0080

UNIVERSITY OF ILLINOIS AT URBANA-CHAMPAIGN

APPROVED FOR PUBLIC RELEASE

DISTRIBUTION UNLIMITED.

REPORT DOCUMENTATION PAGE

Form Approved
OMB No. 0704-0188

1. AGENCY USE ONLY (Leave blank)	2. REPORT DATE	3. REPORT TYPE AND DATES COVERED
	06/22/92	Final April 1, 1989 to March 31, 1992

4. TITLE AND SUBTITLE
Novel Engineered Compound Semiconductor Heterostructures for Advanced Electronics Applications

5. FUNDING NUMBERS
DAAL03-89-K-0080

6. AUTHOR(S)
G. E. Stillman, N. Holonyak, Jr., and J.J. Coleman

7. PERFORMING ORGANIZATION NAME(S) AND ADDRESS(ES)
The Board of Trustees of the University of Illinois
105 Davenport House
809 S. Wright St.
Champaign, IL 61820

8. PERFORMING ORGANIZATION REPORT NUMBER

9. SPONSORING/MONITORING AGENCY NAME(S) AND ADDRESS(ES)
U. S. Army Research Office
P. O. Box 12211
Research Triangle Park, NC 27709-2211

10. SPONSORING/MONITORING AGENCY REPORT NUMBER
ARO 26923.1-EL-SDI

11. SUPPLEMENTARY NOTES
The view, opinions and/or findings contained in this report are those of the author(s) and should not be construed as an official Department of the Army position, policy, or decision, unless so designated by other documentation.

12a. DISTRIBUTION/AVAILABILITY STATEMENT
Approved for public release; distribution unlimited.

12b. DISTRIBUTION CODE

13. ABSTRACT *(Maximum 200 words)*

To provide the technology base that will enable SDIO capitalization on the performance advantages offered through novel engineered multiple-layered compound semiconductor structures, this project has focussed on three specific areas: 1) carbon doping of AlGaAs/GaAs and InP/InGaAs materials for reliable high frequency heterojunction bipolar transistors; 2) impurity induced layer disordering and the environmental degradation of $Al_xGa_{1-x}As$-GaAs quantum-well heterostructures and the native oxide stabilization of $Al_xGa_{1-x}As$-GaAs quantum well heterostructure lasers; and 3) non-planar and strained-layer quantum well heterostructure lasers and laser arrays. The accomplishments in this three year research are reported in fifty-six publications and the abstracts included in this report.

14. SUBJECT TERMS GaAs, $Al_xGa_{1-x}As$, InP, InGaAs, C-doping, impurity induced layer disordering, native oxides, quantum well lasers, strained layer lasers, non planar lasers

15. NUMBER OF PAGES

16. PRICE CODE

17. SECURITY CLASSIFICATION OF REPORT	18. SECURITY CLASSIFICATION OF THIS PAGE	19. SECURITY CLASSIFICATION OF ABSTRACT	20. LIMITATION OF ABSTRACT
UNCLASSIFIED	UNCLASSIFIED	UNCLASSIFIED	UL

NOVEL ENGINEERED COMPOUND SEMICONDUCTOR HETEROSTRUCTURES FOR ADVANCED ELECTRONICS APPLICATIONS

FINAL REPORT

by

GREGORY E. STILLMAN
NICK HOLONYAK, JR.
JAMES J. COLEMAN

JUNE 22, 1992

U.S. ARMY RESEARCH OFFICE

DAAL03-89-K-0080

UNIVERSITY OF ILLINOIS AT URBANA-CHAMPAIGN

APPROVED FOR PUBLIC RELEASE

DISTRIBUTION UNLIMITED.

TABLE OF CONTENTS

Page

STATEMENT OF THE PROBLEM STUDIED 1

SUMMARY OF MOST IMPORTANT RESULTS 2

LIST OF PUBLICATIONS 10

LIST OF PERSONNEL AND DEGREES 15

REPORT OF INVENTIONS 15

APPENDIX A: Abstracts and first page of publications 16

STATEMENT OF THE PROBLEM STUDIED

SEMICONDUCTOR HETEROSTRUCTURES FOR ADVANCED OPTOELECTRONIC INTEGRATED CIRCUIT APPLICATIONS

Gregory E. Stillman, Nick Holonyak, Jr., and James J. Coleman, Center for Compound Semiconductor Microelectronics, University of Illinois, Urbana, IL 61801
(217) 333-8457
June 29-30, 1992

Multiple layer heterostructure devices hold great potential for increased performance of both electronic and optoelectronic devices. To capitalize on this potential, it is essential to develop the epitaxial crystal growth techniques to provide composition, thickness, and doping control and the fabrication techniques that will enable the application of these structures and the devices fabricated from them in future high performance optoelectronic integrated circuits. The SDIO/IST research program in the Center for Compound Semiconductor Microelectronics at the University of Illinois focuses on extending growth fabrication techniques and device designs first proposed and later developed at the University of Illinois. These include the impurity induced layer disordering effect (I^2LD), the use of growth on non-planar patterned substrates, the use of strained layer structures for optoelectronic applications, carbon p-type doping of gallium arsenide and aluminum gallium arsenide using CCl_4 sources, and the development of new crystal growth methods, new device fabrication techniques, and novel device concepts, including the superlattice avalanche photodiode.

The technical approach involves low pressure MOCVD, atmospheric pressure MOCVD, and chemical beam epitaxy CBE/MOMBE for the growth of the structures studied. The specific approaches pursued are innovative and novel in that they originated in research at the University of Illinois. Numerous other university and industrial research programs now parallel the research efforts in these areas at the University of Illinois. The risks/payoffs of this research include the determination of the stability and/or reliability of the AlGaAs/GaAs multiple layer heterostructures and the InGaAs/GaAs strained layer optical devices, as well as an understanding of the physical mechanisms involved in these processes.

The anticipated payoff of this research includes the resolution of issues concerning the mechanisms of I^2LD, the stability/reliability of AlGaAs/GaAs devices related to degradation of high aluminum content lasers and C doping, the use of native oxide for optoelectronic decrease and integrated circuits, the reliability and performance of strained layer lasers on non-planar patterned substrates and the use of C base doping for high reliability heterojunction bipolar transistors.

The refinement of carbon-doped GaAs for use in HBTs has been carried out by using the zero-field time-of-flight technique to study minority carrier transport, and by optimization of the undoped spacer layer thickness in InGaP/GaAs HBTs. A comparison of C-doped and Be-doped GaAs has shown that the minority carrier lifetimes and diffusion lengths are nearly identical, provided that the growth conditions are properly chosen. It was found that the use of 15-25Å spacer layer provided the highest common-emitter current gain (β_{max}~210 for a base doping level of $2.5x10^{19}cm^{-3}$) and nearly ideal behavior (n_{base}~1.15) in these devices.

Carbon doping of $In_xGa_{1-x}As$ grown on GaAs and InP substrates by low-pressure metalorganic chemical vapor deposition using CCl_4 has been investigated for In mole fractions as high as x=0.7. P-type conduction was obtained over the entire composition range studied, with hole concentrations above $1x10^{20}cm^{-3}$ for $x < 0.12$, and as high as $1.6x10^{19}cm^{-3}$ for $In_{0.53}Ga_{0.47}As$ lattice-matched to InP. These high carbon concentrations were achieved by employing very low V/III ratios and low growth temperatures. The alloy composition was found to be dependent on several growth parameters, due to surface reactions (etching) involving chlorine-containing compounds during growth. GaAs and InGaAs samples exhibited an increase in hole concentration upon post-growth annealing, due to hydrogen passivation. $InP/In_{0.53}Ga_{0.47}As$ heterojunction bipolar transistors utilizing a carbon-doped base have been demonstrated. These devices exhibit a dc common-emitter current gain of 250 and an emitter-base junction ideality factor of 1.3 in a structure for which no undoped spacer layer was employed at the emitter-base junction. These preliminary results suggest that C-doping of $In_{0.53}Ga_{0.47}$ may be a suitable alternative to Zn in MOCVD-grown $InP/In_{0.53}Ga_{0.47}As$ HBTs.

SUMMARY OF THE MOST IMPORTANT RESULTS

G.E. Stillman: Statement of Work - Year 1

1. Carbon doping of GaAs, InGaAs, and InP for high-speed optoelectronics

Heavy p-type doping of thin semiconductor layers is important for many compound semiconductor optoelectronic device applications, and C is particularly interesting because of its high solubility and low diffusivity in GaAs. We have grown heavily carbon-doped GaAs and $In_{0.53}Ga_{0.47}As$ by low-pressure metalorganic chemical vapor deposition (MOCVD) using CCl_4 with as-grown hole concentrations as high as $1.3x10^{20}$ cm^{-3} and $1.7x10^{18}$ cm^{-3}, respectively. The behavior of these layers upon short duration anneals at temperatures below the growth temperature has been studied. Post-growth annealing of GaAs at 400°C resulted in a significant increase in the hole concentration for samples doped in excess of $3x10^{18}$ cm^{-3}. The most heavily doped GaAs samples had hole concentrations as high as $4x10^{20}$ cm^{-3} after annealing. The hole concentrations measured after annealing are in approximate agreement with the carbon concentrations deduced using SIMS, suggesting near unity electrical activation of carbon after annealing. All $In_{0.53}Ga_{0.47}As$ layers measured showed a significant decrease in resistivity after annealing, with hole concentrations as high as $1.6x10^{19}$ cm^{-3}. The maximum doping levels given above for GaAs and $In_{0.53}Ga_{0.47}As$ are higher than have been previously reported for C-doping of either material by MOCVD. The annealing behavior observed is explained in terms of hydrogen passivation of carbon acceptors during growth, and reactivation during annealing.

Growth of GaAs and InP and related semiconductor materials using chemical beam epitaxy has also been investigated because of the promise of more precise control of layer thickness and alloy composition through *in situ* measurement techniques.

The transport properties of the epitaxial materials have been investigated using photoluminescence, Hall effect, and zero field time of flight measurements.

1. MOCVD Grown InP/InGaAs HBTs - G.E. Stillman

We demonstrated InP/InGaAs heterojunction bipolar transistors (HBTs) grown by low-pressure metalorganic chemical vapor deposition (LP-MOCVD) in which carbon was used as the base dopant.

This development was reported at the Fourth International Conference on InP and Related Materials in Newport, R.I. April 21-24.[1] This development may ultimately help researchers develop a reliable, high-performance InP/InGaAs HBT process. The Gummel plot for one of these devices is shown in Figure 1. The collector has an ideality factor of 1.01 over six orders of magnitude, whereas the base current exhibits an ideality factor of 1.29. The device has greater than unity common emitter current gain for collector current densities greater than $1x10^{-4}$ A/cm^2.

In 1990 a technique was developed to form high-reliability $Al_xGa_{1-x}As$-GaAs HBT devices using carbon tetrachloride as an efficient source for incorporating high levels of carbon in GaAs during epitaxial growth.[2] This technique is now widely used commercially to make high-reliability HBT devices and heavy p-type doped layers in other GaAs products. It's crucial that the p-type doping level of the base region be as high as possible to ensure low base resistance and good high-speed performance. Currently, HBT fabrication and reliability are limited by the diffusion of the base dopant, Be, out of the narrow base region of the device. Carbon doping of p-type GaAs is preferable to beryllium and zinc doping because carbon has a low atomic diffusion coefficient.[3] Movement of the base doping profile by only a few tens of angstroms into the wide bandgap emitter can drastically affect both the turn-on voltage for the emitter-base junction and the current gain of the device. An undoped region within the base of the HBT, called a set-back layer or spacer layer is often used in MBE Be-doped devices to accommodate any such dopant redistribution during high-temperature growth or processing.

Although the diffusion coefficient of carbon in $In_{0.53}Ga_{0.47}As$ has not yet been determined, the devices recently demonstrated did not employ a spacer layer, yet they exhibited a low base-emitter turn-on voltage and a common-emitter current gain (ß) which is comparable with HBTs doped with Zn and using an optimal 100 Å set-back layer. This is an indication that carbon exhibits a low diffusivity in $In_{0.53}Ga_{0.47}As$ films, too.

Several issues must be addressed before this research can be developed into a reliable, high-performance InP/InGaAs HBT process. Further characterization of the epitaxial layers, including the study of minority carrier properties and the stability of the carbon doping profiles must be carried out.

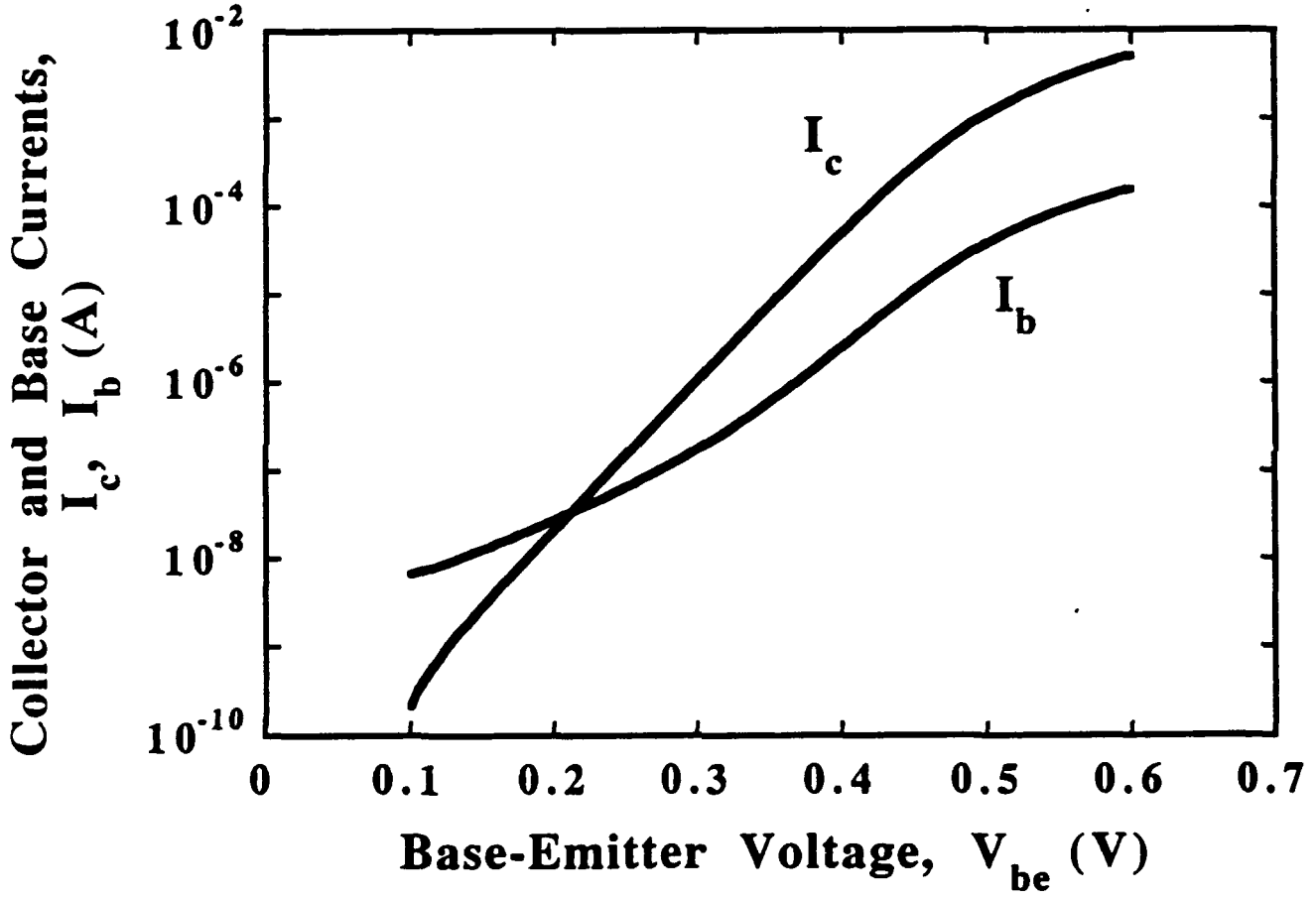
Collector and Base Currents,
I_c, I_b (A)
10^{-2}
10^{-4}
10^{-6}
10^{-8}
10^{-10}
I_c
I_b
0
0.1
0.2
0.3
0.4
0.5
0.6
0.7
Base-Emitter Voltage, V_{be} (V)

The incorporation of hydrogen during growth can also affect the electrical properties of carbon-doped InGaAs, and must be studied further.[4,5] In addition, researchers need to attain higher doping levels (10^{20} cm-3) in order to fabricate high-performance microwave devices. While this research development is but a first step in developing a reliable, high-performance InP/InGaAs HBT process, it has paved the way for collaboration with industry. For example, the Rockwell International Science Center has evaluated dc results, and is presently fabricating high-frequency devices with the University of Illinois, InP-InGaAs HBT material.

2. Native III-V Oxide Technology - N. Holonyak, Jr.

Our work in the SDIO program and a related ARO project has recently been directed towards understanding hydrogenation of high aluminum content III-V semiconductor alloys and formation of intentional stable oxides by deliberately oxidizing, utilizing a high temperature ($\gtrsim$ 400°C) anneal in a wet N_2 atmosphere, high Al-bearing surface layers of quantum well heterostructures. This stable oxide is being investigated for use in optoelectronic device and OEIC fabrication and design.

The degradation of high Al composition AlxGa1-xAs (x>0.7) when exposed to atmospheric conditions has been observed since the time of introduction of AlAs barrier layers in quantum well heterostructures (QWHs) to suppress the effects of alloy clustering.[6] In order to avoid the destructive effects of atmospheric hydrolysis, the AlxGa1-xAs layers are capped with GaAs, which is stable under atmospheric conditions.

The study of the degradation of high composition AlxGa1-xAs under long-term exposure to atmospheric conditions has led to the development of a water vapor oxidation process that provides a potential solution to this and other problems in III-V semiconductor device work.[7] The oxidation procedure involves heating the crystal (with an exposed AlxGa1-xAs layer) to temperatures greater than 400°C in a water vapor ambient created by passing N2 through a water bubbler (maintained at ~100°C).

This process converts the AlxGa1-xAs layer to a stable oxide. In experiments to test the chemically passivating nature of this oxide, a 0.1μm AlAs layer is grown on a GaAs substrate, half of which is immediately oxidized while the other half is left exposed to atmospheric conditions. The

unoxidized layer quickly degrades to a yellowish brown layer and after several months (100 days) shows evidence of a chemical attack as deep as 1μm into the GaAs, 10 times deeper than the original AlAs layer. The oxidized layer, on the other hand, remains intact and shows no evidence of such attack.[8]

One of the most useful properties of any oxide is its ability to mask impurity diffusion, as proven by the Si-SiO2 system and its importance in Si integrated circuit technology. The AlxGa1-xAs native oxides created by the water vapor process are capable of masking both p-type (Zn)[9] and n-type (Si)[10] impurity diffusion. Superlattices with patterned native oxide on the surface are disordered selectively by impurity-induced layer disordering[11] (IILD) in the regions which are not masked by the native oxide (Al0.8Ga0.2As, oxidized at 400°C for 3 hours), while under those regions that are masked by the oxide the superlattice remains intact. The presence of Ga in the oxide layer does not adversely affect its properties since Ga-O and Al-O compounds form structural isomorphs, and Ga2O3 and Al2O3 form solid solutions over the entire compositional range.[12]

As well as using native oxides on III-V semiconductors to mask impurity diffusion, devices have also been made employing native III-V oxides. Single and multiple stripe-geometry $Al_xGa_{1-x}As$-GaAs quantum well heterostructure laser diodes using the native oxide to delineate the gain region have been fabricated.[13,14] When the contact stripes of these devices are separated, one contact on the substrate and the other only on oxide, the I-V characteristics of the oxide itself clearly show an open circuit, indicating that the oxide is a good insulator.

The oxide has also been shown to reduce leakage currents in quantum well heterostructure laser diodes made by IILD.[15] Instead of depositing a dielectric such as SiO2 or Si3N4 after the usual IILD processing, the disordered regions (which consist of exposed Al0.8Ga0.2As) are oxidized. The result is a low threshold (Ith=5mA) self-aligned device which combines the advantages of IILD and native oxidation. The GaAs contact stripes remain exposed during the oxidation process and are unoxidized because GaAs has a significantly lower oxidation potential than high Al composition AlxGa1-xAs. This makes the oxidation process selective to Al-bearing semiconductors.

The native oxide has also been used in strained-layer systems. Ten-stripe quantum well heterostructure laser diode arrays with good performance (Ith=95mA for ten 5 μm stripes) have been

made in the AlxGa1-xAs-InyGa1-yAs-GaAs system.[16] The oxide is formed from the AlxGa1-xAs confinement layer. Additional strain is not introduced by the native oxide.

The oxidation technique is not limited to the AlxGa1-xAs system. Laser diodes from another Al-bearing III-V semiconductor, In0.5(Al0.9Ga0.1)0.5P-In0.5Ga0.5P, have also been made.[17] In these devices the native oxide is formed from the In0.5(Al0.9Ga0.1)0.5P. A higher oxidation temperature is required (T=500°C) because of the lower Al and higher P content of this layer. In spite of the early state of this work, the native oxidation process has proven useful in many applications. The importance of the native oxide in the Si integrated circuit industry makes further study of the analogous system in III-V compound semiconductors necessary.

3. Single growth step DFB laser developed - J.J. Coleman

Distributed feedback (DFB) lasers have received special attention recently for optoelectronic integrated circuit (OEIC) applications because they provide an integrable alternative for the conventional cleaved facet Fabry-Perot etalon and they provide a high degree of modal and spectral stability with drive current.

Most DFB lasers have been fabricated by forming a feedback grating parallel to the growth plane - either below or above the active region - during a growth interruption or by coupling the evanescent field to a lateral grating in complex multiple-growth structures.

We have developed* a relatively simple distributed feedback laser ridge waveguide quantum well heterostructure laser in which DFB gratings are formed along the ridge by direct write electron beam lithography and reactive ion etching in a single post-MOCVD growth step.

The operation of this DFB ridge laser combines the lateral optical confinement of the ridge waveguide with distributed feedback from gratings etched along the side of the laser stripe.

The ridge configuration with etched gratings into an InGaAs-GaAs-AlGaAs strained layer quantum well laser structure is shown schematically Figure 3.

A portion of the structure is removed in this figure to illustrate that the gratings are etched through the AlGaAs top confining layer and close to the strained layer active region.

The gratings form a lateral effective index step which assists in lateral optical confinement as in a conventional ridge laser structure. The gratings also provide optical feedback when the period of the grating is designed to satisfy the Bragg condition within the gain spectrum.

Emission spectra for on-axis (110) uncoated devices show residual Fabry-Perot modes as well as an additional peak corresponding to the Bragg reflector at a single wavelength. The presence of a single mode which does not shift with increasing drive current demonstrates the effect of distributed feedback in these structures.

The additional presence of the Fabry-Perot modes in both structures is due to the high reflectivity of the facets and the fact that the DFB wavelength is displaced from the peak of the gain profile.

Adjustment of the gain profile to coincide with the DFB wavelength, reduction of the facet reflectivity by greater misorientation and facet coatings, and increased gain from multiple quantum wells can all be used to optimize this device.

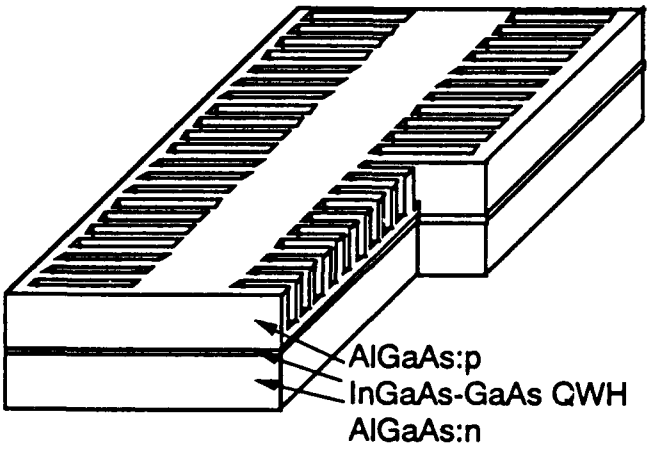

A schematic diagram of a distributed feedback ridge waveguide laser. A portion of the structure is removed in this figure to illustrate that the gratings are etched through the AlGaAs top confining layer and close to the strained layer active region.

REFERENCES

1. S.A. Stockman, A.W. Hanson, G.E. Höfler, A.P. Curtis, and G.E. Stillman. Presented at the Fourth International Conference on Indium Phosphide and Related Materials, April 21-24, 1992, Newport, Rhode Island.
2. B.T. Cunningham, M.A. Haase, M.J. McCollum, and G.E. Stillman, *Appl. Phys. Lett.*, **54**, 1905 (1989).
3. B.T. Cunningham, L.J. Guido, J.E. Baker, J.S. Major, Jr., N. Holonyak, Jr., and G.E. Stillman, *Appl. Phys. Lett.*, **55**, 687 (1989).
4. S.A. Stockman, A.W. Hanson, and G.E. Stillman, *Appl. Phys. Lett.*, **60**, 2903 (1992).
5. S.A. Stockman, A.W. Hanson, G.E. Höfler, K.C. Hsieh, and G.E. Stillman. To be published.
6. N. Holonyak Jr. et al. Phys. Rev. Lett., vol. 45, p. 1703, 1980.
7. J.M. Dallesasse et al. Appl. Phys. Lett., vol. 57, p. 2844, 1990.
8. A.R. Sugg et al. Appl. Phys. Lett., vol. 58, p. 1199, March 1991.
9. J.M. Dallesasse et al. Appl. Phys. Lett., vol. 58, p. 974, March 1991.
10. N. El-Zein et al. J. Appl. Phys., vol. 70 p. 2031, August 1991.
11. D.G. Deppe et al. J. Appl. Phys., vol. 64, R93, Dec. 1988.
12. E.M. Levin et al. Phase Diagrams for Ceramists (The American Ceramics Society, Columbus, Ohio), Fig. 2008, P. 551 (1964), Fig. 1927, p. 527 (1964), Fig. 4965, p. 426, 1975.
13. J.M. Dallesasse et al. Appl. Phys. Lett., vol. 58, p. 394, Jan. 1991.
14. J.M. Dallesasse et al. Appl. Phys. Lett., vol. 58, p. 834, Feb. 1991.
15. F.A. Kish et al. Appl. Phys. Lett., vol. 58, p. 1765, April 1991.
16. T.A. Richard et al. Appl. Phys. Lett., vol. 58, p. 2390, May 1991.
17. F.A. Kish et al. Appl. Phys. Lett., vol. 59, p. 354, July 1991.

LIST OF PUBLICATIONS

DAAL03-89-K-0080

Gregory E. Stillman
(YEAR 1)

Internal photoemission and band discontinuities at $Ga_{0.47}In_{0.53}As$-InP heterojunctions. M.A. Haase, N. Pan, and G.E. Stillman. *Appl. Phys. Lett.*, **54**, 1457 (1989).

Heavy carbon dopingof MOCVD-grown GaAs using carbon tetrachloride. B.T. Cunningham, M.A. Haase, M.J. McCollum, and G.E. Stillman. *Appl. Phys. Lett.*, **54**, 1905 (1989).

Carbon diffusion in undoped, n-type and p-type GaAs. B.T. Cunningham, L.J. Guido, J.E. Baker, J.S. Major, Jr., N. Holonyak, Jr., and G.E. Stillman. *Appl. Phys. Lett.*, **55**, 687 (1989).

Carbon tetrachloride doped $Al_xGa_{1-x}As$ grown by metalorganic chemical vapor deposition. B.T. Cunningham, J.E. Baker, and G.E. Stillman. *Appl. Phys. Lett.*, **56**, 836 (1990).

Al-Ga interdiffusion in heavily carbon-doped $Al_xGa_{1-x}As$-GaAs quantum well heterostructures. L.J. Guido, B.T. Cunningham, D.W. Nam, K.C. Hsieh, W.E. Plano, J.S. Major, Jr., E.J. Vesely, A.R. Sugg, N. Holonyak, Jr., and G.E. Stillman. *J. Appl. Phys.*, **67**, 2179 (1990).

Carbon tetrachloride doped AlGaAs grown by metalorganic chemical vapor deposition. B.T. Cunningham, J.E. Baker, and G.E. Stillman. *J. Electronic Materials*, **19**, 331 (1990).

Carbon impurities in MOCVD InP. G.E. Stillman, B.T. Cunningham, S.A. Stockman, B. Lee, S.S. Bose, I. Szafranek, and J.E. Baker. *Inst. Phys. Conf. Ser. No. 106*: Chapter 2, 63 (1989). Presented at the International Symposium on Gallium Arsenide and Related Compounds, Karuizawa, Japan, September 1989.

(YEAR 2)

Carbon-doped base GaAs/AlGaAs heterojunction bipolar transistor grown by metalorganic chemical vapor deposition using carbon tetrachloride as a dopant source. B.T. Cunningham, G.E. Stillman, and G.S. Jackson. *Appl. Phys. Lett.*, **56**, 361 (1990).

Absence of ^{13}C incorporation in $^{13}CCl_4$-doped InP grown by metalorganic chemical vapor deposition. B.T. Cunninham, J.E. Baker,S.A. Stockman, and G.E. Stillman. *Appl. Phys. Lett.*, **56**, 1760 (1990).

Growth-induced shallow acceptor defect and related luminescence effects in molecular beam epitaxial GaAs. I. Szafranek, M.A. Plano, M.J. McCollum, S.A. Stockman, S.L. Jackson, K.Y. Cheng, and G.E. Stillman. *J. Appl. Phys.*, **68**,754 (1990).

Anomalous luminescence properties of GaAs grown by molecular beam epitaxy. I. Szafranek, M.A. Plano, M.J. McCollum, S.L. Jackson, S.A. Stockman, K.Y. Cheng, and G.E. Stillman. *Materials Research Symposium Proceedings*, **163**, 193 (1990).

Reassessment of acceptor passivation models in p-type hydrogenated GaAs. I. Szafranek, and G.E. Stillman. *Materials Research Symposium Proceedings*, **163**, 483 (1990).

Effects of high source flow and high pumping speed on gas source molecular beam epitaxy/chemical beam epitaxy. M.J. McCollum, S.L. Jackson, I. Szafranek, and G.E. Stillman. *J. Crystal Growth*, **105**, 316 (1990).

Species dependence of passivation and reactivation of acceptors in hydrogenated GaAs. I. Szafranek, and G.E. Stillman. *J. Appl. Phys.*, **68**, 3554 (1990).

Low-temperature defect-induced aging of GaAs grown by molecular beam epitaxy. I. Szafranek, S.A. Stockman, M. Szafranek, M.J. McCollum, M.A. Plano, W.R. Miller, and G.E. Stillman. *Materials Research Society Symposium Proceedings*, **184**, 109 (1990).

Electronic stimulation of acceptor reactivation in p-type hydrogenated GaAs. I. Szafranek, and G.E. Stillman. *Materials Research Society Symposium Proceedings*, **184**, 81 (1990).

Layer intermixing in heavily carbon-doped AlGaAs/GaAs superlattices. I. Szafranek, M. Szafranek, B.T. Cunningham, L.J. Guido, N. Holonyak, Jr., and G.E. Stillman. *J. Appl. Phys.*, **68**, 5615 (1990).

Kinetic effects and impurity incorporation in MBE growth of gallium arsenide. G.E. Stillman, B. Lee, I. Szafranek, M.A. Plano, M.J. McCollum, S.S. Bose, and M.H. Kim. *Defect Control in Semiconductors*, K. Sumino (ed.) Elsevier Science Publishers B.V. (North-Holland) 997 (1990).

Instablility of partially disordered carbon-doped AlGaAs/GaAs superlattices. I. Szafranek, J.S. Major, Jr., B.T. Cunningham, L.J. Guido, N. Holonyak, Jr., and G.E. Stillman. *Appl. Phys. Lett.*, **57**, 2910 (1990).

Hydrogenation of Si- and Be-doped InGaP. J.M. Dallesasse, I. Szafranek, J.N. Baillargeon, N. El-Zein, N. Holonyak, Jr., G.E. Stillman, and K.Y. Cheng. *J. Appl. Phys.*, **68**, 5866 (1990).

(YEAR 3)

Characterization of heavily carbon-doped GaAs grown by MOCVD and MOMBE. S.A. Stockman, G.E. Höfler, J.N. Baillargeon, K.C. Hsieh, K.Y. Cheng, and G.E. Stillman. Submitted to Journal of Applied Physics. (January 1992).

Carbon doping of $In_xGa_{1-x}As$ by MOCVD using CCl_4. S.A. Stockman, A.W. Hanson, and G.E. Stillman. Submitted to Applied Physics Letters. (February 1992)

Passivation of carbon acceptors during growth of heavily carbon doped GaAs and $In_{0.53}Ga_{0.47}As$ by MOCVD. S.A. Stockman, A.W. Hanson, and G.E. Stillman. Submitted to Applied Physics Letters. (February 1992)

Mechanism of light-induced reactivation of acceptors in p-type hydrogenated gallium arsenide. I. Szafranek, M. Szafranek, and G.E. Stillman. *Phys. Rev.B*, **45**, pp. 6497-6508 (1992).

Minority carrier tansport in carbon doped gallium arsenide. C.M. Colomb, S.A. Stockman, S. Varadarajan, and G. E. Stillman. *Appl. Phys. Lett.*, **60**, 65 (1992).

N. Holonyak, Jr.
(YEAR 1)

Stability of AlAs in $Al_xGa_{1-x}As$-AlAs-GaAs quantum well heterostructures. J.M. Dallesasse, P. Gavrilovic, N. Holonyak, Jr., R.W. Kaliski, D.W. Nam, E.J. Vesely, and R.D. Burnham. *Appl. Phys. Lett.*, **56**, 2436 (1990).

Environmental degradation of $Al_xGa_{1-x}As$-GaAs quantum-well heterostructures. J.M. Dallesasse, N. El-Zein, N. Holonyak, Jr., K.C. Hsieh, R.D. Burnham, and R.D. Dupuis. To be published in Journal of Applied Physics.

Hydrogenation of Si- and Be-doped InGaP. J.M. Dallesasse, I. Szafranek, J.N. Baillargeon, N. El-Zein, N. Holonyak, Jr., G.E. Stillman, and K.Y. Cheng. *J. Appl. Phys.*, **68**, 5866 (1990).

Low-threshold disorder-defined buried-heterostructure $Al_xGa_{1-x}As$-GaAs quantum well lasers by open-tube rapid thermal annealing. T.A. Richard, J.S. Major, Jr., F.A. Kish, N. Holonyak, Jr., S.C. Smith, and R.D. Burnham. *Appl. Phys. Lett.*, **57**, 2904 (1990).

Environmental degradation of $Al_xGa_{1-x}As$-GaAs quantum-well heterostructures. *J. Appl. Phys.*, **68**, 2235 (1990).

(YEAR 2)

Hydrolyzation oxidation of $Al_xGa_{1-x}As$-AlAs-GaAs quantum well heterostructures and superlattices. J.M. Dallesasse, N. Holonyak, Jr., A.R. Sugg, T.A. Richard, and N. El-Zein. *Appl. Phys. Lett.*, **57**, 2844 (1990).

Native oxide stabilization of AlAs-GaAs heterostructures. A.R. Sugg, N. Holonyak, Jr., J.E. Baker, F.A. Kish, and J.M. Dallesasse. *Appl. Phys. Lett.*, **58**, 1199 (1991).

Native-oxide stripe-geometry $Al_xGa_{1-x}As$-GaAs quantum well heterostructure lasers. J.M. Dallesasse, and N. Holonyak, Jr. *Appl. Phys Lett.*, **58**, 394 (1991).

Native-oxide-defined coupled-stripe $Al_xGa_{1-x}As$-GaAs quantum well heterostructure lasers. J.M. Dallesasse, N. Holonyak, Jr., D.C. Hall, N. El-Zein, A.R. Sugg, S.C. Smith, and R.D. Burnham. *Appl. Phys. Lett.*, **58**, 834 (1991).

Native-oxide masked impurity-induced layer disordering of $Al_xGa_{1-x}As$ quantum well heterostructures. J.M. Dallesasse, N. Holonyak, Jr., N. El-Zein, T.A. Richard, F.A. Kish, A.R. Sugg, R.D. Burnham, and S.C. Smith. *Appl. Phys. Lett.*, **58**, 974 (1991).

(YEAR 3)

Native-oxide stripe-geometry $In_{0.5}(Al_xGa_{1-x})_{0.5}P$-$In_{0.5}Ga_{0.5}P$ heterostructure laser diodes. F.A. Kish, S.J. Caracci, N. Holonyak, Jr., J.M. Dallesasse, A.R. Sugg, R.M. Fletcher, C.P. Kuo, T.D. Osentowski, and M.G. Craford. *Appl. Phys. Lett.*, **59**, 354 (1991).

Native-oxide-masked Si impurity-induced layer disordering of $Al_xGa_{1-x}As$-$Al_yGa_{1-y}As$-$Al_zGa_{1-z}As$ quantum-well heterostructures. N. El-Zein, N. Holonyak, Jr., F.A. Kish, A.R. Sugg, T.A. Richard, J.M. Dallesasse, S.C. Smith, and R.D. Burnham. *J. Appl. Phys.*, **70**, 2031 (1991).

Diffusion of manganese in GaAs and its effect on layer disordering in $Al_xGa_{1-x}As$-GaAs superlattices. C.H. Wu, K.C. Hsieh, G.E. Höfler, N. EL-Zein, and N. Holonyak, Jr. *Appl. Phys. Lett.*, **59**, 1224 (1991).

Planar native-oxide index-guided $Al_xGa_{1-x}As$-GaAs quantum well heteostructure lasers. F.A. Kish, S.J. Caracci, N. Holonyak, Jr., J.M. Dallesasse, K.C. Hsieh, M.J. Ries, S.C. Smith, and R.D. Burnham. *Appl. Phys. Lett.*, **59**, 1755 (1991).

Native-oxide coupled-cavity $Al_xGa_{1-x}As$-GaAs quantum well heterostructure laser diodes. N. El-Zein, F.A. Kish, N. Holonyak, Jr., A.R. Sugg, M.J. Ries, S.C. Smith, J.M. Dallesasse, and R.D. Burnham. *Appl. Phys. Lett.*, **59**, 2838 (1991).

Visible spectrum native-oxide coupled-stripe $In_{0.5}(Al_xGa_{1-x})_{0.5}P$-$In_{0.5}Ga_{0.5}P$ quantum well heterostructure laser arrays. F.A. Kish, S.J. Caracci, N. Holonyakk, Jr., S.A. Maranowski, J.M. Dallesasse, R.D. Burnham, and S.C. Smith. *Appl. Phys. Lett.*, **59**, 2883 (1991)

J.J. Coleman
(YEAR 1)

High power non-planar quantum well heterostructure periodic laser arrays. M.E. Givens, C.A. Zmudzinski, R.P. Bryan, and J.J. Coleman. *Appl. Phys. Lett.*, **53**, 1159 (1988).

A non-planar quantum well heterostructure window laser. R.P. Bryan, L.M. Miller, T.M. Cockerill, and J.J. Coleman. *Appl Phys Lett.*, **54**, 1634 (1989).

Optical characteristics of high power non-planar periodic laser arrays. C.A. Zmudzinski, M.E. Givens, R.P. Bryan, and J.J. Coleman. *IEEE J. Quantum Elect.*, **QE-25**, 1539 (1989).

Loss in heterostructure waveguide bends formed on a patterned substrate. T.K. Tang, L.M. Miller, E. Andideh, T.M. Cockerill, P.D. Swanson, R.P. Bryan, T.A. DeTemple, I. Adesida, and J.J. Coleman. *IEEE Photonics Tech. Lett.*, **1**, 120, (1989).

High power pulsed operation of an optimized nonplanar corrugated substrate periodic laser diode array. R.P. Bryan, L.M. Miller, T. M. Cockerill, S.M. Langsjoen, and J.J. Coleman. *IEEE J. Quantum Elect.*, **26**, 222 (1990).

Characteristics of step graded separate confinement quantum well lasers with direct and indirect barriers. L.M. Miller, K.J. Beernink, T.M. Cockerill, R.P. Bryan, M.E. Favaro, J. Kim, J.J. Coleman, and C.M. Wayman. *J. Appl. Phys.*, in press.

A self consistent model of a nonplanar quantum well periodic laser array. S.M. Lee, S.L. Chuang, R.P. Bryan, C.A. Zmudzinski, and J.J. Coleman. submitted to *J. Quantum Elect.*

In-phase operation of high power nonplanar periodic laser arrays. R.P. Bryan, T.M. Cockerill, L.M. Miller, T.K. Tang, T.A. DeTemple, and J.J. Coleman. submitted to *Appl Phys. Lett.*

Temperature dependence of compositional disordering of GaAs-AlAs superlattices during MeV Kr irradiation. R.P. Bryan, L.M. Miller, T.M. Cockerill, J.J. Coleman, J.L. Klatt, and R.S. Averback. *Phys. Rev. B15*, **41**, 3889 (1990) and *Mat. Res. Soc. Symp. Proc.*, **198**, p. 79 (1990).

(YEAR 2)

In-phase operation of high power nonplanar periodic laser arrays. R.P. Bryan, T.M. Cockerill, L.M. Miller, T.K. Tang, T.A. DeTemple, and J.J. Coleman. *Appl. Phys. Lett.*, **58**, 113 (1990).

A self consistent model of a nonplanar quantum well periodic laser array. S.M. Lee, S.L Chuang, R.P. Bryan, C.A. Zmudzinski, and J.J. Coleman. *J. Quantum Electon.*, in press.

(YEAR 3)

Characteristics of step-graded separate confinement quantum well lasers with direct and indirect barriers. L.M. Miller, K.J. Beernink, T.M. Cockerill, R.P. Bryan, M.E. Favaro, J. Kim, J.J. Coleman, and C.M. Wayman. *J. Appl. Phys.*, **68**, 1964 (1990).

Depressed index cladding graded barrier separate confinement single quantum well heterostructure laser. T.M. Cockerill, J. Honig, T.A. DeTemple, and J.J. Coleman. *Appl. Phys. Lett.*, **59**, 2694 (1991).

Phase-locked ridge waveguide InGaAs-GaAs-AlGaAs strained-layer quantum well heterostructure laser arrays. K.J. Beernink , L.M. Miller, T.M. Cockerill, and J.J. Coleman. *Appl. Phys. Lett.*, **59**, 3222 (1991).

InGaAs-GaAs-AlGaAs strained-layer distributed feedback ridge waveguide quantum well heterostructure laser array. *Electron. Lett.*, **27**, 1943 (1991).

PARTICIPATING SCIENTIFIC PERSONNEL

The personnel listed below are either graduate research assistants, or post doctoral appointments, as indicated, were supported by this contract. The degrees and dates received are also listed.

Gregory E. Stillman

Brian Cunningham
(Ph.D. 1990)

Timothy Horton

Steven Jackson

Bun Lee
(Ph.D. 1989)

Deepak Sengupta

Stephen Stockman
(M.S. - 1991)

Subadra Varadarajan

Nick Holonyak, Jr.

Steven Caracci
(M.S. - 1992)

Nada El-Zein
(M.S. - 1991)

Fred Kish
(Ph.D. - 1992)

Jo Major, Jr.
(Ph.D. - 1990)

William Plano
(Ph.D. - 1989)

Michael Ries

James J. Coleman

Timothy Cockerill
(M.S. - 1991)

Michael Favaro
(Ph.D. - 1992)

John Honig
(Post Doctoral)

Shing-Man Lee
(Ph.D. - 1992)

Gary Smith

REPORT OF INVENTIONS

NONE

APPENDIX A

PUBLICATIONS

G.E. Stillman

Internal photoemission and band discontinuities at $Ga_{0.47}In_{0.53}As$-InP heterojunctions

M. A. Haase,[a] N. Pan,[b] and G. E. Stillman
Center for Compound Semiconductor Microelectronics, Materials Research Laboratory and Coordinated Science Laboratory, University of Illinois at Urbana–Champaign, Urbana, Illinois 61801

(Received 22 August 1988; accepted for publication 30 January 1989)

Internal photoemission has been observed in the spectral response of specially designed $Ga_{0.47}In_{0.53}As$-InP p^+N^- heterojunction photodiodes. Power-law fits to the internal photoemission as a function of photon energy allow precise determination of threshold energies from which the conduction-band discontinuity is easily and accurately deduced to be $\Delta E_c = 203 \pm 15$ meV at room temperature. These measurements have been performed at temperatures from 135 to 297 K. The temperature dependence of ΔE_c is described by $\partial(\Delta E_c)/\partial T = -0.2 \pm 0.1$ meV/K.

In an effort to characterize the energy-band discontinuities in the technologically important $Ga_{0.47}In_{0.53}As$-InP heterostructure material system, we have studied internal photoemission in p^+N^- heterojunction photodiodes. The techniques employed were first developed in GaAs-$Al_xGa_{1-x}As$ diodes.[1] A number of measurements of the conduction-band discontinuity (ΔE_c) have been previously reported for the $Ga_{0.47}In_{0.53}As$-InP system.[2–10] The results have ranged from 190 to 600 meV, with the most commonly quoted work being that of Forrest and Kim, who measured $\Delta E_c = 190 \pm 30$ meV at room temperature using Kroemer's capacitance-voltage (C-V) technique.[3] More recently, Leu and Forrest examined the subtleties of this technique,[10] and Lang *et al.* used admittance spectroscopy to deduce $\Delta E_c = 250 \pm 10$ meV.[11]

The photodiodes used in the present work were prepared by liquid phase epitaxy. A 4-μm-thick layer of unintentionally doped InP ($n = 4\times10^{15}$ cm^{-3}) was first grown on an n^+-InP substrate. On this layer was grown 2 μm of lattice-matched, Mn-doped $Ga_{0.47}In_{0.53}As$ ($p = 3\times10^{18}$ cm^{-3}), from a melt that was supersaturated by 3 °C. Liquid phase growth under these conditions is known to provide very abrupt interfaces.[12,13] The p^+N^- structure is used to provide near-flatband conditions at the heterointerface (Fig. 1, inset). Diodes were fabricated by evaporating and alloying ohmic contacts and wet chemical mesa etching. The spectral response of these diodes was measured by illuminating them using a grating monochromator with appropriate filters to remove higher order light. The photocurrent was detected using conventional chopper and lock-in amplifier techniques. A pyroelectric detector was used as a reference. Computer-controlled data acquisition was employed, with subsequent corrections for the spectral characteristics of the optics system.

Figure 1 compares the spectral response of one of the heterojunction photodiodes with that of an InP homojunction. Internal photoemission is evidenced by the enhanced response of the heterojunction diode at photon energies between 0.9 and 1.2 eV. At energies between 0.7 and 0.9 eV, a very weak response is observed due to thermionic emission of photogenerated minority electrons over the heterobarrier. At lower temperatures, the response in this region decreased to a level below the sensitivity of our measurement system. The band diagram inset in Fig. 1 illustrates the internal photoemission process observed in these data. The heterojunction is illuminated through the InP substrate with the light of photon energy less than the band gap of InP, but greater than that of $Ga_{0.47}In_{0.53}As$. In this way, hot electrons are generated in the $Ga_{0.47}In_{0.53}As$ near the heterointerface. For sufficiently high photon energies, the photogenerated hot electron has enough kinetic energy to surmount the heterobarrier and be collected, thus generating photocurrent. The lowest photon energy at which this may happen is that corresponding to transitions from the acceptor impurity band, as illustrated in the Fig. 1 inset. By measuring this threshold photon energy $h\nu_T$, one may easily deduce the height of the heterobarrier

$$\Delta E_c \approx h\nu_T - E_g + E_A,$$

where E_g is the band-gap energy of the $Ga_{0.47}In_{0.53}As$ and E_A is the acceptor binding energy (52 meV).[14] Corrections must be made for barrier lowering due to image force[15] and Heine tunneling tails.[16] The latter is a consequence of the charge in the evanescent tails of the $Ga_{0.47}In_{0.53}As$ valence-band states at the heterointerface. The effects of hot-electron tunneling and band bending are also accounted for, but are negligible.

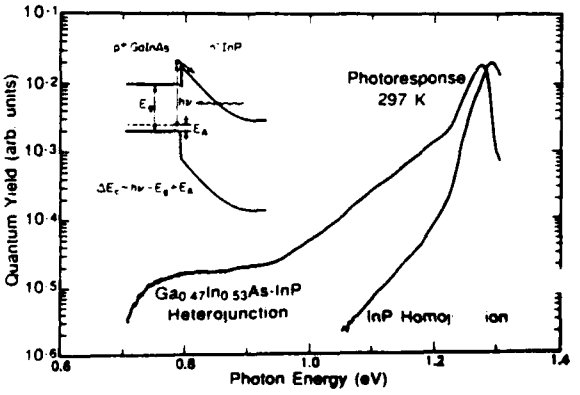

FIG. 1. Measured spectral response of a heterojunction photodiode, compared to that of an InP homojunction. Inset: band diagram showing internal photoemission process.

[a] Present address: 3M Company, 3M Center, St. Paul, MN 55144.
[b] Raytheon Research, 131 Spring St., Lexington, MA 02173.

 0003-6951/89/151457-03$01.00

Heavy carbon doping of metalorganic chemical vapor deposition grown GaAs using carbon tetrachloride

B. T. Cunningham, M. A. Haase,[a] M. J. McCollum, J. E. Baker, and G. E. Stillman
Center for Compound Semiconductor Microelectronics, Materials Research Laboratory, and Coordinated Science Laboratory, University of Illinois at Urbana–Champaign, Urbana, Illinois 61801

(Received 5 December 1988; accepted for publication 28 February 1989)

A mixture of 500 ppm CCl_4 in H_2 has been used to grow heavily doped *p*-type GaAs by low-pressure metalorganic chemical vapor deposition with TMGa and AsH_3 as the group III and V sources, respectively. Carbon acceptor concentrations between 1×10^{16} and 1×10^{19} cm^{-3} were obtained. In addition, abrupt carbon-doping profiles were achieved with no noticeable memory effects. Carrier concentration was studied as a function of CCl_4 flow, V/III ratio, growth temperature, and growth rate using electrochemical capacitance-voltage profiling. Carbon incorporation was found to depend on CCl_4 flow, V/III ratio, and growth temperature. Carbon incorporation had no dependence on the growth rate.

Heavily doped *p*-type layers in GaAs are commonly used in several device structures. They are important in diode lasers and in the base region of heterojunction bipolar transistors (HBTs).[1] Magnesium and Zn are commonly used *p*-type dopants in metalorganic chemical vapor deposition (MOCVD), but these dopants exhibit problems in obtaining abrupt doping profiles due to the adsorption of these reactants on the internal surfaces of the growth chamber and gas lines.[2–4] In addition, rapid diffusion of group IIA and IIB elements in GaAs can also lead to dopant redistribution during growth and subsequent processing.

Carbon has been proposed as an alternative dopant to Mg and Zn.[5–7] Carbon is expected to incorporate only as a shallow acceptor on an As site with very little interstitial incorporation, even at high doping levels.[8] As a result, carbon is expected to have greatly improved diffusion characteristics in comparison to Mg and Zn.[8–11]

Several methods for carbon doping have been proposed. Intentional addition of carbon using a number of hydrocarbon sources has either not been successful, or has led to films of low carbon content.[9,12] One researcher has successfully added carbon to GaAs layers with trimethylarsenic.[8] In this work we show that CCl_4 may be used to controllably obtain *p*-type GaAs with carrier concentrations between 1×10^{16} and 1×10^{19} cm^{-3} in low-pressure MOCVD-grown layers. In addition, we demonstrate that CCl_4 doping yields excellent doping abruptness and does not display the memory effects inherent with Mg and Zn doping. These layers are suitable for high doping applications such as HBTs and diode lasers.

The MOCVD reactor used in this work is an Emcore GS3100. The reactor chamber is constructed of stainless steel, with copper gaskets and Viton O-rings used for all seals. The CCl_4 source, provided by Matheson, was a 500 ppm mixture of CCl_4 in H_2. Trimethylgallium (Alfa), and 100% AsH_3 (Phoenix Research) were the group III and V sources, respectively. All growths were carried out on 2° off (100) oriented GaAs substrates with a substrate rotation speed of 1500 rpm. The reactor pressure was 100 Torr with a total H_2 flow of 9 *l*/min. The growth temperature was varied from 620 to 760 °C, and the growth rate ranged from 700 to 1300 Å/min. The V/III ratio was varied from 32 to 129 in this study. Undoped GaAs samples grown at 700 °C, with a growth rate of 1300 Å/min, an AsH_3 flow of 100 sccm, and a V/III ratio of 64 had *n*-type background carrier concentrations of 1×10^{15} cm^{-3}.

To study the growth temperature, growth rate, and V/III dependence of carbon incorporation, the sequence of layers shown in Table I was grown during a single growth run at a constant temperature. The CCl_4 flow was held constant while the growth rate and V/III ratio were varied independently. Each layer in the sequence had a thickness of about 1 μm, which was sufficient for carrier concentration measurement with a Polaron PN4100 electrochemical profiler. The layer sequence was repeated for growth temperatures between 640 and 760 °C.

The carrier concentration as a function of V/III ratio at three different growth temperatures is shown in Fig. 1 for a CCl_4 flow of 100 sccm. The *p*-type carrier concentration is highest at low V/III ratios, and appears to level out at high V/III ratios for each temperature. A similar trend is typically observed in undoped MOCVD-grown GaAs, so it is not clear to what extent carbon incorporation from the CCl_4 is a function of the V/III ratio. The carrier concentration is less dependent upon the V/III ratio at lower growth temperatures. Figure 1 demonstrates the strong growth temperature dependence of carbon incorporation. By varying the growth temperature between 620 and 760 °C, carrier concentrations ranging from 1×10^{19} to 1×10^{16} cm^{-3} were obtained.

TABLE I. Layer sequence grown at a constant temperature to measure the effects of V/III ratio and growth rate on carbon incorporation with a constant CCl_4 flow rate of 100 sccm. This structure was repeated for temperatures between 640 and 760 °C.

Layer	1	2	3	4
AsH_3 flow (sccm)	50	50	100	100
TMGa flow (sccm)	30	15	30	15
Growth rate (Å/min)	1333	667	1333	667
V/III ratio	32	64	64	128

[a] Present address: 201-IN-35, 3M Center, St. Paul, MN 55144.

 0003-6951/89/191905-03$01.00

Carbon diffusion in undoped, *n*-type, and *p*-type GaAs

B. T. Cunningham, L. J. Guido, J. E. Baker, J. S. Major, Jr., N. Holonyak, Jr., and G. E. Stillman

Center for Compound Semiconductor Microelectronics, Electrical Engineering Research Laboratory, Coordinated Science Laboratory, and Materials Research Laboratory, University of Illinois at Urbana–Champaign, Illinois 61801

(Received 1 May 1989; accepted for publication 5 June 1989)

The effects of background doping, surface encapsulation, and As_4 overpressure on carbon diffusion have been studied by annealing samples with 1000 Å *p*-type carbon doping spikes grown within 1 μm layers of undoped (n^-), Se-doped (n^+), and Mg-doped (p^+) GaAs. The layers were grown by low-pressure metalorganic chemical vapor deposition using CCl_4 as the carbon doping source. Two different As_4 overpressure conditions were investigated: (1) the equilibrium p_{As_4} over GaAs (no excess As), and (2) $p_{As_4} \sim 2.5$ atm. For each As_4 overpressure condition, both capless and Si_3N_4-capped samples of the n^--, n^+-, and p^+-GaAs crystals were annealed simultaneously (825 °C, 24 h). Secondary-ion mass spectroscopy was used to measure the atomic carbon depth profiles. The carbon diffusion coefficient is always low, but depends on the background doping, being highest in Mg-doped (p^+) GaAs and lowest in Se-doped (n^+) GaAs. The influence of surface encapsulation (Si_3N_4) and p_{As_4} on carbon diffusion is minimal.

In order to construct high-gain, high-frequency GaAs/AlGaAs heterojunction bipolar transistors (HBTs), it is necessary to grow a thin, heavily doped *p*-type base layer.[1,2] For GaAs/AlGaAs HBTs grown by metalorganic chemical vapor deposition (MOCVD), the acceptor impurities Mg and Zn are commonly employed in the GaAs base layer. Unfortunately, the large diffusion coefficients associated with these impurities lead to *p-n* junction redistribution, either during crystal growth itself or during subsequent high-temperature processing.[3–5] For example, the diffusion of Zn from the base into the *n*-type emitter changes the emitter-base *p-n* junction location relative to the emitter-base (GaAs/AlGaAs) heterojunction, thereby resulting in degraded HBT perfo ance unless special set back doping layers are used.[5] Recent work has identified carbon as an alternative acceptor to Mg and Zn.[6–10] Because carbon incorporates primarily as a substitutional acceptor on the As sublattice (i.e., low interstitial carbon concentration), it is expected to have a much smaller diffusion coefficient than either Mg or Zn.[6,7,11,12] A detailed understanding of carbon diffusion in GaAs and AlGaAs would be useful for the prediction of the effects of high-temperature processing on HBT and other heterolayer device performance.

In the experiments described here, the effects of background doping, surface encapsulation, and arsenic overpressure (p_{As_4}) on carbon diffusion were studied by annealing (1000 Å) *p*-type carbon doping spikes grown in the center of 1 μm layers of undoped (n^-), Se-doped (n^+), and Mg-doped (p^+) GaAs. Secondary-ion mass spectroscopy (SIMS) was used to measure the carbon depth profiles for both as-grown and annealed samples. In general, the carbon diffusion coefficient is found to be extremely low, but depends on the background doping. The highest carbon diffusion coefficient is observed in Mg-doped (p^+) GaAs, while little or no carbon diffusion is found in Se-doped (n^+) GaAs. The effect of GaAs surface conditions was investigated by employing Si_3N_4 encapsulation and two different As_4 overpressures. These surface conditions had only a minor influence on the carbon diffusion coefficient. Estimates for the carbon diffusion coefficient in undoped (n^-) GaAs and Mg-doped (p^+) GaAs were found by fitting a one-dimensional diffusion equation solution to the measured SIMS carbon depth profiles.

The epitaxial layers used in this work were grown by low-pressure metalorganic chemical vapor deposition (MOCVD) in an Emcore GS3100 reactor on 2° off (100) oriented liquid-encapsulated Czochralski GaAs substrates. All growths were carried out at $T_G \sim 600$ °C, $P_G \sim 100$ Torr, substrate rotation rate ~ 1500 rpm, H_2 flow rate ~ 9 slm, growth rate ~ 1000 Å/min, and V/III ratio ~ 60. Trimethylgallium and 100% AsH_3 were the respective group III and V precursors. Nominally undoped GaAs grown under these conditions is *n*-type with a background carrier concentration of $n^- \sim 1 \times 10^{15}$ cm^{-3}. Layers doped with Mg (*p*-type) using MCp_2Mg have a hole concentration of $p^+ \sim 1 \times 10^{19}$ cm^{-3} as measured by electrochemical capacitance-voltage profiling. Layers doped with Se (*n*-type) using hydrogen selenide have an electron concentration of $n^+ \sim 5 \times 10^{18}$ cm^{-3}. All epilayers are ~ 1 μm in total thickness with the carbon doping spike (1000 Å) located 0.5 μm from the crystal surface. The carbon doping source, a 500 ppm mixture of CCl_4 in high-purity H_2, was turned on only during the growth of the carbon doping spike. The CCl_4 flow rate for each run was sufficient for the growth conditions used to achieve a carbon acceptor concentration of $p \sim 5 \times 10^{18}$ cm^{-3}.

All anneals were performed in evacuated quartz ampoules ($p \sim 10^{-6}$ Torr, vol ~ 3 cm) at 825 °C for 24 h. For each ampoule the sample set (six samples) consisted of a capless and a Si_3N_4-capped sample of the three as-grown crystals (n^-, n^+, and p^+). Pyrolytic decomposition of SiH_4 and NH_3 at 700 °C was used to grow the 1000-Å-thick Si_3N_4 encapsulant. A large As_4 overpressure ($p_{As_4} \sim 2.5$ atm) was achieved by adding 25 mg of elemental As to the anneal

 0003-6951/89/330687-03$01.00

Carbon tetrachloride doped $Al_xGa_{1-x}As$ grown by metalorganic chemical vapor deposition

B. T. Cunningham, J. E. Baker, and G. E. Stillman
Center for Compound Semiconductor Microelectronics, Coordinated Science Laboratory, and Materials Research Laboratory, University of Illinois at Urbana–Champaign, Urbana, Illinois 61801

(Received 26 October 1989; accepted for publication 18 December 1989)

A dilute mixture of CCl_4 in H_2 has recently been shown to be a suitable carbon doping source for obtaining *p*-type GaAs grown by metalorganic chemical vapor deposition (MOCVD) with carbon acceptor concentrations in excess of 1×10^{19} cm^{-3}. To understand the effect of growth parameters on carbon incorporation in CCl_4-doped $Al_xGa_{1-x}As$, carbon acceptor concentration was studied as a function of Al composition, growth temperature, growth rate, and CCl_4 flow rate using electrochemical capacitance-voltage profiling. The carbon incorporation as a function of Al composition, growth temperature, and CCl_4 flow rate was also measured by secondary-ion mass spectroscopy. All layers were grown by low-pressure MOCVD using TMGa and TMAl as column III precursors, and 100% AsH_3 as the column V source. Increased Al composition reduced the dependence of carbon concentration on the growth temperature. Reduced growth rate, which resulted in substantially decreased carbon acceptor concentrations in GaAs, had an insignificant effect on the carrier concentration of $Al_{0.4}Ga_{0.6}As$. A linear relationship between hole concentration and CCl_4 flow rate in $Al_xGa_{1-x}As$ for $0.0\leqslant x\leqslant0.8$ was observed. These results are interpreted to indicate that adsorption and desorption of CCl_y ($y\leqslant3$) on the $Al_xGa_{1-x}As$ surface during crystal growth plays an important role in the carbon incorporation mechanism.

Carbon is an attractive alternative to conventionally used *p*-type impurities in MOCVD, such as Mg and Zn, due to its low diffusion coefficient.[1–7] Diffusion of *p*-type impurities is of particular concern in laser diode structures which are subjected to high-temperature annealing for impurity diffusion in impurity-induced layer disordering (IILD). *Diffusion of p-type dopants into the active region of* a quantum well heterostructure (QWH) laser or into the emitter of an *Npn* heterojunction bipolar transistor (HBT) has been shown to result in degraded device performance.[8,9] Carbon incorporation from the methyl radicals associated with the column III growth precursors has been used to obtain carbon doping of diode laser structures grown by MOCVD.[5] However, carbon doping from a source separate from the growth precursors may be more desirable, as it allows greater flexibility in the choice of growth parameters.

A dilute mixture of CCl_4 in H_2 has been used successfully as a *p*-type dopant source for low-pressure metalorganic chemical vapor deposition (MOCVD) growth of GaAs with carbon acceptor concentrations as high as 4×10^{19} cm^{-3}.[1,10] HBT structures grown by MOCVD with the thin *p*-type (<1000 A) base region heavily doped with CCl_4 ($p=2\times10^{19}$ cm^{-3}) and a current gain cutoff frequency as high as $f_t=30$ GHz have been reported.[11] *p*-type doping of $Al_xGa_{1-x}As$ in MOCVD-grown heterojunction diode laser structures is another potentially important application of CCl_4 doping. CCl_4 doping may be used to obtain $Al_xGa_{1-x}As$ with higher carbon acceptor concentration than can be obtained solely with carbon incorporation from the growth precursors in MOCVD-grown layers.

Because CCl_4 has not been extensively studied as a dopant source, little is understood about the gas phase and/or surface decomposition reactions which result in carbon incorporation. Thus, a knowledge of how Al composition affects carbon acceptor concentration under various growth conditions would be useful for understanding the CCl_4 decomposition mechanism, in addition to providing experimental data for the growth of device structures.

To determine the effect of growth parameters on carbon incorporation in CCl_4-doped $Al_xGa_{1-x}As$, carbon acceptor concentration was studied as a function of Al composition, growth temperature, growth rate, and CCl_4 flow rate through electrochemical capacitance-voltage profiling of the hole concentration. The carbon incorporation as a function of Al composition, growth temperature, and CCl_4 flow rate was also measured by secondary-ion mass spectroscopy (SIMS).

All layers were grown by low-pressure MOCVD in an Emcore GS3100 reactor using TMGa and TMAl as column III precursors and 100% AsH_3 as the column V source. The carbon doping source was a 1500 ppm mixture of CCl_4 in H_2. All growths were done on 2° off (100) liquid-encapsulated Czochralski GaAs substrates at a pressure of ~100 Torr, total H_2 flow rate of ~9 slm, and a substrate rotation speed of ~1500 rpm.

The carbon acceptor concentration was studied as a function of growth temperature by keeping the Al composition ($x=0.0, 0.2, 0.4, 0.6, 0.8$), growth rate ($R_G\sim1000$ A/min), and CCl_4 mixture flow rate (50 sccm) fixed during a single growth run while the growth temperature was increased in steps after the growth of ~0.5 μm at each temperature ($640\,^{\circ}C\leqslant T_G\leqslant810\,^{\circ}C$). A 2 min growth pause under AsH_3 and H_2 was used between layers while the growth temperature was increased to a new value. The carbon acceptor concentration as a function of CCl_4 flow rate was studied by keeping the Al composition ($x=0.0, 0.4, 0.8$), growth rate ($R_G\sim1000$ A/min), and growth temperature ($T_G=600\,^{\circ}C, 700\,^{\circ}C$) constant during a single growth run while decreasing the CCl_4 mixture flow rate after each ~0.5 μm of growth. The flow rate was limited to a maximum of

 0003-6951/90/090836-03$02.00

preventing recontamination of the substrate but is not considered as the main cause of carbide formation in our experiments.

In conclusion, we have conclusively demonstrated interfacial formation of β-SiC during epitaxial growth of Si by RTCVD. Improper substrate cleaning procedures followed by high-temperature prebake leads to carbide formation. By employing proper surface cleaning procedures, the formation of β-SiC can be prevented even when the base pressure is not ultrahigh vacuum.

[1]J. Borland, M. Gangani, R. Wise, S. Fong, Y. Oka, and Y. Matsumoto, Solid. State Technol. **31**, 111 (1988).
[2]T. J. Donahue and R. Reif, J. Appl. Phys. **57**, 2757 (1985).
[3]T. Sugii, T. Yamazaki, T. Fukano, and T. Ito, IEEE Electron. Dev. Lett. **EDL-8**, 528 (1987).
[4]B. S. Meyerson, F. K. LeGoues, T. N. Nguyen, and D. L. Harame, Appl. Phys. Lett. **50**, 113 (1987).
[5]T. Ohmi, T. Ichikawa, T. Shibata, K. Matsudo, and H. Iwabuchi, Appl. Phys. Lett. **53**, 45 (1988).
[6]J. F. Gibbons, C. M. Gronet, and K. E. Williams, Appl. Phys. Lett. **47**, 721 (1985).
[7]C. M. Gronet, J. C. Strum, K. E. Williams, and J. F. Gibbons, Appl. Phys. Lett. **48**, 1012 (1986).
[8]M. L. Green, D. Brasen, H. Luftman, and V. C. Kannan, J. Appl. Phys. **65**, 2558 (1989).
[9]S. K. Lee, Y. H. Ku, and D. L. Kwong, Appl. Phys. Lett. **54**, 1775 (1989).
[10]F. Wong, C. Y. Chen, and Y.-H. Ku, Mater. Res. Soc. Symp. Proc. **146**, 217 (1989).
[11]C. M. Gronet, C. A. King, W. Opyd, J. F. Gibbons, S. D. Wilsen, and R. Hull, J. Appl. Phys. **61**, 2407 (1987).
[12]S. Reynolds, D. W. Vook, and J. F. Gibbons, Appl. Phys. Lett. **49**, 1720 (1986).
[13]I. H. Khan and R. N. Summergrad, Appl. Phys. Lett. **11**, 12 (1967).
[14]R. C. Henderson, W. J. Polito, and J. Simpson, Appl. Phys. Lett. **16**, 15 (1970).
[15]R. C. Henderson, R. B. Marcus, and W. J. Polito, J. Appl. Phys. **42**, 1208 (1971).
[16]R. C. Henderson, J. Electrochem. Soc. **119**, 772 (1972).
[17]Y. Ishikawa, N. Ikeda, M. Kenmochi, and T. Ichinokawa, Surf. Sci. **159**, 256 (1985).
[18]R. M. Chrenko, L. J. Schowalter, E. L. Hall, and N. Lewis, Mater. Res. Soc. Symp. Proc. **56**, 27 (1986).
[19]R. M. Chrenko, E. L. Hall, N. Lewis, and G. A. Smith, Mater. Res. Soc. Symp. Proc. **82**, 373 (1987).
[20]HCl:HNO_3:H_2O(3:1:1), 20–25 °C, 10 min, followed by H_2SO_4 (added 0.5 vol. % H_2O_2 after each clean), 100 °C, 10 min, N_2 dry.
[21]P. Liaw and R. F. Davis, J. Electrochem. Soc. **132**, 642 (1985).

Al-Ga interdiffusion in heavily carbon-doped $Al_xGa_{1-x}As$-GaAs quantum well heterostructures

L. J. Guido, B. T. Cunningham, D. W. Nam,[a] K. C. Hsieh, W. E. Plano, J. S. Major, Jr., E. J. Vesely,[b] A. R. Sugg, N. Holonyak,Jr., and G. E. Stillman

Electrical Engineering Research Laboratory, Center for Compound Semiconductor Microelectronics, and Materials Research Laboratory, University of Illinois at Urbana-Champaign, Urbana, Illinois 61801

(Received 8 August 1989; accepted for publication 3 November 1989)

Impurity-induced layer disordering experiments on $Al_xGa_{1-x}As$-GaAs quantum well heterostructures (QWHs) that are doped heavily with carbon are described. The data show that carbon doping retards Al-Ga interdiffusion relative to an undoped crystal, and that interdiffusion in C-doped QWHs is not enhanced by a Ga-rich (versus As-rich) annealing ambient. The data are inconsistent with most Fermi-level-effect models for layer disordering that do not include chemical impurity dependence or sublattice dependence, and that do not consider the possibility of inhibited Al-Ga interdiffusion in extrinsic crystals.

Recent studies of impurity-induced layer disordering (IILD) on $Al_xGa_{1-x}As$-GaAs quantum well heterostructures (QWHs) have identified the importance of the crystal surface interaction with the ambient and the so-called Fermi-level effect.[1-3] Despite these encouraging results there is little agreement yet on a specific model for layer disordering. One important issue that remains to be resolved is to what extent the column III and column V sublattices couple during interdiffusion. We have investigated these issues further via annealing studies on $Al_xGa_{1-x}As$-GaAs QWHs that are doped with the As-sublattice acceptor carbon (C_{As}). The two salient features of this work are that C-doped *p-type* QWHs respond much differently to high-temperature annealing than more typical Mg-doped *p-type* QWHs, and that the C_{As} acceptor *inhibits* column-III sublattice layer disordering. These observations bring into question models for IILD that rely solely on the Fermi-level effect.

In order to determine the influence of the crystal surface stoichiometry on Al-Ga interdiffusion in a *p*-type crystal, a 40-period C-doped $Al_{0.6}Ga_{0.4}As$-GaAs superlattice ($L_B, L_z \sim 250$ Å) has been annealed under Ga-rich (+ Ga), As-rich (+ As), or equilibrium GaAs vapor pressure (+ 0) conditions. The superlattice crystal has been grown by metalorganic chemical vapor deposition (MOCVD) in an Emcore GS3000-DFM reactor using trimethylgallium, trimethylaluminum, and arsine (100%) precursors. The carbon doping level is controlled independently using a source of 500 ppm CCl_4 in ultrahigh purity

[a] Kodak Ph.D. fellow.
[b] National Science Foundation Ph.D. fellow.

0021-8979/90/042179-04$03.00

Journal of Electronic Materials, Vol. 19, No. 4, 1990

Carbon Tetrachloride Doped $Al_xGa_{1-x}As$ Grown by Metalorganic Chemical Vapor Deposition

B. T. CUNNINGHAM, J. E. BAKER and G. E. STILLMAN

Center for Compound Semiconductor Microelectronics,
Coordinated Science Laboratory, and Materials Research Laboratory
University of Illinois at Urbana-Champaign, Urbana, Illinois 61801

A dilute mixture of CCl_4 in H_2 has recently been shown to be a suitable carbon doping source for obtaining *p*-type GaAs grown by metalorganic chemical vapor deposition (MOCVD) with carbon acceptor concentrations in excess of $1 \times 10^{19}cm^{-3}$. To understand the effect of growth parameters on carbon incorporation in CCl_4 doped $Al_xGa_{1-x}As$ carbon acceptor concentration was studied as a function of Al composition, growth temperature, growth rate, and CCl_4 flow rate using electrochemical capacitance-voltage profiling. The carbon incorporation as a function of Al composition, growth temperature and CCl_4 flow rate was also measured by secondary ion mass spectroscopy (SIMS). All layers were grown by low pressure MOCVD using TMGa and TMAl as column III precursors, and 100% AsH_3 as the column V source. Increased Al composition reduced the dependence of carbon concentration on the growth temperature. Reduced growth rate, which resulted in substantially decreased carbon acceptor concentrations in GaAs, had an insignificant effect on the carrier concentration of $Al_{0.4}Ga_{0.6}As$. A linear relationship between hole concentration and CCl_4 flow rate in $Al_xGa_{1-x}As$ for $0.0 \leq x \leq 0.8$ was observed. These results are interpreted to indicate that adsorption and desorption of $CCl_y (y \leq 3)$ on the $Al_xGa_{1-x}As$ surface during crystal growth plays an important role in the carbon incorporation mechanism.

Key words: AlGaAs, MOCVD, carbon doping

Carbon is an attractive alternative to conventionally used *p*-type impurities in MOCVD, such as Mg and Zn due to its low diffusion coefficient.[1-7] Diffusion of *p*-type impurities is of particular concern in laser diode structures which are subjected to high temperature annealing for impurity diffusion in impurity induced layer disordering (IILD). Diffusion of *p*-type dopants into the active region of a quantum well heterostructure (QWH) laser or into the emitter of an npn heterojunction bipolar transistor (HBT) has been shown to result in degraded device performance.[8,9] Carbon incorporation from the methyl radicals associated with the column III growth precursors has been used to obtain carbon doping of diode laser structures grown by MOCVD.[5] However, carbon doping from a source separate from the growth precursors may be more desirable, as it allows greater flexibility in the choice of growth parameters.

A dilute mixture of CCl_4 in H_2 has been used successfully as a *p*-type dopant source for low pressure metalorganic chemical vapor deposition (MOCVD) growth of GaAs with carbon acceptor concentrations as high as 4×10^{19} cm^{-3}.[1,10] HBT structures grown by MOCVD with the thin *p*-type (<1000Å) base region heavily doped with CCl_4 ($p = 2 \times 10^{19}$ cm^{-3}) and a current gain cutoff frequency as high as $f_t = 26$ GHz have been reported.[11] *P*-type doping of $Al_xGa_{1-x}As$ in MOCVD grown heterojunction diode laser structures is another potentially important application of CCl_4 doping. CCl_4 doping may be used to obtain $Al_xGa_{1-x}As$ with higher carbon acceptor concentration than can be obtained solely with carbon incorporation from the growth precursors in MOCVD grown layers.

Because CCl_4 has not been extensively studied as a dopant source, little is understood about the gas phase and/or surface decomposition reactions which result in carbon incorporation. Thus, a knowledge of how Al composition affects carbon acceptor concentration under various growth conditions would be useful for understanding the CCl_4 decomposition mechanism, in addition to providing experimental data for the growth of device structures.

To determine the effect of growth parameters on carbon incorporation in CCl_4 doped $Al_xGa_{1-x}As$, carbon acceptor concentration was studied as a function of Al composition, growth temperature, growth rate, and CCl_4 flow rate through electrochemical capacitance-voltage profiling of the hole concentration. The carbon incorporation as a function of Al composition, growth temperature and CCl_4 flow rate was also measured by secondary ion mass spectroscopy (SIMS).

The SIMS ^{12}C concentration in CCl_4 doped $Al_xGa_{1-x}As$ was found to increase with decreasing growth temperature for all Al compositions considered. However, the rate of increase substantially declined as the Al composition increased. Reduced growth rate resulted in substantially decreased car-

(Received October 11, 1989; revised December 10, 1989)

0361-5235/1990/1401-331$5.00©90 AIME

Inst. Phys. Conf. Ser. No 106: Chapter 2
Paper presented at Int. Symp. GaAs and Related Compounds, Karuizawa, Japan, 1989

Carbon impurities in MOCVD InP

G.E. Stillman, B.T. Cunningham, S.A. Stockman, B. Lee, S.S. Bose*, I. Szafranek, and J.E. Baker

Center for Compound Semiconductor Microelectronics, Materials Research Laboratory, Coordinated Science Laboratory, University of Illinois, Urbana, Illinois 61801 USA

ABSTRACT: Intentional C doping of low pressure MOCVD-grown InP has been attempted. Using mixtures of 500 ppm and 1500 ppm CCl_4 in high-purity H_2 for the C dopant source, C acceptor concentrations as high as $4x10^{19}$ cm^{-3} have been achieved in GaAs. Under growth conditions similar to those used for heavy carbon incorporation in GaAs, injection of CCl_4 into the growth reactor during the growth of InP did not produce any measurable change in the carrier concentration of the InP epitaxial layers or result in any change in the ^{12}C concentration above the ^{12}C background level in secondary ion mass spectroscopy (SIMS) analysis. There is no evidence that the group IV impurity C is incorporated in InP grown with common epitaxial growth techniques.

1. INTRODUCTION AND BACKGROUND

Carbon is a very important residual acceptor in GaAs grown by various techniques, and in spite of early reports that C is a particularly effective scattering center in GaAs at room temperature (Stringfellow and Kunzel 1980), it is currently also of interest as an intentional p-type dopant in MOCVD and MBE epitaxial growth because of its low diffusion coefficient, compared with Group II p-type dopants which substitute on the Ga sublattice. Carbon is also interesting because, although it is from Group IV of the periodic table and thus is potentially amphoteric in GaAs, InP and other III-V compounds, it is only incorporated as an acceptor in GaAs; i.e., C is not incorporated on the Ga sublattice in GaAs. Carbon is particularly important for growth techniques based on metalorganic compounds since it is an intrinsic impurity in these source materials. In this paper, we review the evidence for identification of C acceptor impurities in InP using photoluminescence (PL) and discuss some potential experimental complications in PL identification of C acceptors in InP. Experiments in which we attempted intentional doping of low pressure MOCVD InP with CCl_4 under conditions similar to those which result in heavy carbon doping of GaAs are described. The results of these experiments support the conclusion that C is not incorporated in MOCVD InP.

2. IDENTIFICATION OF C ACCEPTOR LEVELS IN InP

Skromme, et al. (1984) have studied the identification of acceptor impurities in InP by measuring the acceptor luminescence in undoped InP grown by LPE, PH_3-VPE and LEC techniques and in intentionally doped material prepared by C, Be and Mg ion implantation into bulk crystals and epitaxial layers. The dominant residual acceptor in LPE InP was first reported by Hess, et al. (1974) and labelled A_1 by these authors. Although this acceptor has been widely assumed to be C, Skromme, et al. (1984) demonstrated that the energy of

*Present address: Penn State Univeristy, University Park, PA 16082 USA

Carbon-doped base GaAs/AlGaAs heterojunction bipolar transistor grown by metalorganic chemical vapor deposition using carbon tetrachloride as a dopant source

B. T. Cunningham[a)] and G. E. Stillman
Center for Compound Semiconductor Microelectronics, Coordinated Science Laboratory, and Materials Research Laboratory, University of Illinois at Urbana–Champaign, Urbana, Illinois 61801

G. S. Jackson
Raytheon Company, Research Division, Lexington, Massachusetts 02173

(Received 25 August 1989; accepted for publication 16 November 1989)

Carbon tetrachloride (CCl_4) has been used as a carbon doping source for the base region of a GaAs/AlGaAs *Npn* heterojunction bipolar transistor (HBT) grown by low-pressure metalorganic chemical vapor deposition (MOCVD). Transistors were fabricated and characterized for dc current gain, emitter-base junction ideality factor, base contact resistance, and external base resistance. Microwave characterization by *S*-parameter measurement was performed to determine the common emitter current gain and maximum available gain as a function of frequency. Transistors with the base contact area self-aligned to a $3\times 10\,\mu$m emitter finger had a dc current gain as high as 50, an emitter-base junction ideality factor of $n = 1.2$, and a current gain cutoff frequency of $f_t = 26$ GHz. Transistors of equal emitter area without self-alignment exhibited dc current gain as high as 86, $n = 1.2$, and $f_t = 20$ GHz. A base contact resistance of $R_c = 2.85\times 10^{-6}\ \Omega\ \text{cm}^2$ and an external base sheet resistance of $R_s = 533.4\ \Omega/\square$ were measured. These preliminary results indicate that carbon doping from CCl_4 may be an attractive substitute for Zn or Mg in GaAs/AlGaAs HBT structures grown by MOCVD.

In order to obtain GaAs/AlGaAs heterojunction bipolar transistors with high gain and high frequency response, a very thin (<1000 Å), very heavily doped ($p > 1\times 10^{19}$ cm^{-3}) *p*-type base layer is required.[1,2] For GaAs/AlGaAs HBT structures grown by metalorganic chemical vapor deposition (MOCVD), Mg and Zn are commonly used acceptor impurities for the base layer, while Be is typically used for heavy *p*-type doping of GaAs grown by molecular beam epitaxy (MBE). Unfortunately, the large diffusion coefficients associated with these impurities can lead to *p-n* junction redistribution during crystal growth or subsequent high-temperature processing.[3–5] *p*-type dopant diffusion has been shown to change the position of the base-emitter *p-n* junction relative to the position of the base-emitter GaAs/AlGaAs heterojunction, resulting in degraded HBT performance unless special set back doping layers are used.[5]

Carbon has been identified as an alternative acceptor to Mg, Zn, and Be.[6–10] Carbon incorporates primarily as a substitutional acceptor on the column V sublattice, and is expected to have a much smaller diffusion coefficient than Mg or Zn.[6,7,11,12] High carbon acceptor concentrations in GaAs have been obtained by MBE using carbon evaporated from a heated graphite source,[13] and by atomic layer epitaxy (ALE) using carbon incorporation from trimethylgallium.[14] To this date, the intentional addition of carbon to GaAs grown by MOCVD using a number of hydrocarbon sources has not been successful, or has led to films of low carbon content.[7,8] However, carbon acceptor concentrations in excess of 1×10^{19} cm^{-3} have been obtained in low-pressure MOCVD-grown GaAs using CCl_4 as a doping source.[10] Using CCl_4, very thin, heavily doped *p*-type layers have been grown with abrupt dopant turn-on and turn-off.[10,12]

In this work, CCl_4 has been used as a carbon doping source for the base region of a GaAs/AlGaAs *Npn* HBT grown by low-pressure MOCVD. Transistors with the base contact area either self-aligned of non-self-aligned to a 3×10 μm emitter finger were fabricated using wet chemical etching to expose the base and subcollector contact areas and liftoff techniques to pattern metallized areas. dc characterization was performed to determine the gain, base contact resistance, external base resistance, emitter-base ideality factor, and collector-base ideality factor of the transistors. Microwave *S*-parameter measurements were made to determine the common emitter current gain and the maximum available gain as a function of frequency.

The epitaxial structure was grown by low-pressure MOCVD in an Emcore GS3100 reactor on a 2° off (100) oriented undoped liquid-encapsulated Czochralski (LEC) GaAs substrate. The growth was carried out at a pressure of

TABLE I. Growth parameters for doping concentration, thickness, growth temperature, and Al composition of the HBT epitaxial structure. A growth temperature of 580 °C was used for the base layer to maximize carbon incorporation from the CCl_4. A 2 min growth pause under arsine was used to change the substrate temperature before and after the base layer.

Layer	Doping (cm^{-3})	Thickness (Å)	T_G (°C)	Material
Subcollector	$n = 1\times 10^{18}$	5000	600	GaAs
Collector	$n = 5\times 10^{16}$	5000	600	GaAs
Base	$p = 2\times 10^{19}$	1000	580	GaAs
Emitter grade	undoped	300	760	GaAs-$Al_xGa_{1-x}As$
Emitter	$N = 5\times 10^{17}$	1400	760	$Al_xGa_{1-x}As$
Cap grade	$n = 1\times 10^{18}$	300	760	$Al_xGa_{1-x}As$-GaAs
Cap	$n = 1\times 10^{18}$	1000	760	GaAs

a) ARO Fellow

 0003-6951/90/040361-03$02.00

Absence of ^{13}C incorporation in $^{13}CCl_4$-doped InP grown by metalorganic chemical vapor deposition

B. T. Cunningham, J. E. Baker, S. A. Stockman, and G. E. Stillman
Center for Compound Semiconductor Microelectronics, Materials Research Laboratory and Coordinated Science Laboratory, University of Illinois at Urbana–Champaign, Urbana, Illinois 61801

(Received 7 November 1989; accepted for publication 19 February 1990)

Intentional carbon doping of low-pressure metalorganic chemical vapor deposition (MOCVD) grown InP has been attempted with a 500 ppm mixture of $^{13}CCl_4$ in high-purity H_2, which has been used to obtain carbon-acceptor concentrations as high as 1×10^{19} cm^{-3} in GaAs. Under growth conditions similar to those used for heavy carbon incorporation in GaAs, injection of $^{13}CCl_4$ into the growth reactor during growth of InP did not produce any measurable change in the carrier concentration of the InP epitaxial layers or any change in the ^{13}C concentration above the ^{13}C background in secondary-ion mass spectroscopy analysis. These results support previous low-temperature photoluminescence measurements of high-purity InP in which no residual carbon acceptor is observed under many growth techniques and growth conditions, and hence support the hypothesis that carbon is not incorporated in InP grown by MOCVD.

Carbon has recently received a great deal of attention as an intentional *p*-type dopant for GaAs and AlGaAs grown by metalorganic chemical vapor deposition (MOCVD),[1–4] atomic layer epitaxy,[5] chemical beam epitaxy (CBE),[6] and molecular beam epitaxy[7] due to its low diffusion coefficient compared to group II *p*-type impurities.[8–10] Because carbon is an intrinsic impurity in metalorganic source materials, its behavior in III/V compounds grown with these precursors is particularly important. Although carbon is a group IV element and is potentially amphoteric in GaAs, InP, and other III/V compounds, in GaAs it is only incorporated as an acceptor on the As sublattice. Low-temperature photoluminescence (PL) measurements of high-purity epitaxial InP which had been subjected to low-dose ion implantation of carbon indicates that carbon can be incorporated as a shallow acceptor in InP.[11] However, the low-temperature PL spectra of high-purity InP grown by liquid phase epitaxy (LPE), liquid-encapsulated Czochralski (LEC), and hydride vapor phase epitaxy indicate that carbon was not incorporated as a residual acceptor for any of these growth techniques,[11] and in particular, low-temperature PL measurements of high-purity InP grown by low-pressure MOCVD demonstrate that no residual carbon is incorporated into the epitaxial layers regardless of the growth conditions.[12]

Although these results indicate that residual carbon impurities are not incorporated into InP grown by many techniques, the use of carbon as an intentional dopant in InP has not been previously investigated. In this work, experiments are described in which we attempted intentional doping of low-pressure MOCVD InP with CCl_4 under conditions which result in heavy carbon doping of GaAs. Injection of CCl_4 into the reactor during growth of InP did not produce any measurable change in the carrier concentration of the InP epitaxial layers or any change in the carbon concentration measured by secondary-ion mass spectroscopy (SIMS). The results of these experiments indicate that CCl_4 is not a viable *p*-type dopant source for MOCVD InP, and support the hypothesis that carbon is not incorporated in MOCVD InP.

The MOCVD reactor used in this work was an Emcore GS3100. All growths were carried out on 2° off (100) oriented towards the nearest (110) LEC GaAs or InP substrates with a reactor pressure of ~100 Torr, a total H_2 flow rate of ~9 slm, and a substrate rotation speed of ~1500 rpm. For GaAs growth, TMGa and 100% AsH_3 were the respective group III and V sources. TMIn and 100% PH_3 were the precursors for the growth of InP. The CCl_4 source was a 500 ppm mixture of $^{13}CCl_4$ in high-purity H_2. The ^{13}C isotope was used to obtain increased sensitivity for carbon detection during SIMS analysis.

SIMS analysis for carbon was performed with a Cameca IMS-3f instrument using a Cs^+ primary ion beam (160 nA, 13 keV) and negative secondary-ion detection to obtain maximum carbon atom yield and detection sensitivity. Low-resolution operation of this instrument results in a detection limit for ^{12}C of only $\sim3\times10^{16}$ cm^{-3}, below which no variation in the ^{12}C concentration can be measured. However, the detection limit for ^{13}C is $\sim2\times10^{14}$ cm^{-3} under these conditions.[2,13,14]

In order to demonstrate that injection of $^{13}CCl_4$ into the reactor during GaAs growth results in ^{13}C incorporation, a $^{13}CCl_4$-doped GaAs sample was grown with a constant growth temperature ($T_G = 640$ °C) and growth rate (R_G ~1000 Å/min), while the $^{13}CCl_4$-mixture flow rate was decreased in four steps of 150, 100, 50, and 25 sccm during the growth of ~0.6-μm-thick layers. Undoped GaAs grown under these conditions was *n* type with an electron concentration of $n\sim1\times10^{15}$ cm^{-3} as measured by capacitance-voltage (*C-V*) profiling.

To determine the effect of $^{13}CCl_4$ injection into the reactor during InP growth, two $^{13}CCl_4$-doped InP samples were grown in which the growth temperature ($T_G = 580$ °C, 630 °C) and growth rate ($R_G \sim 250$ Å/min) were held constant while the $^{13}CCl_4$ mixture flow rate was decreased in four steps of 150, 100, 50, and 25 sccm during the growth of ~0.25-μm-thick layers. Undoped InP samples grown under these conditions were *n* type with an electron concentration of $n\sim1.5\times10^{16}$ cm^{-3} as measured by electrochemical *C-V* profiling.

 0003-6951/90/181760-03$02.00

Growth-induced shallow acceptor defect and related luminescence effects in molecular beam epitaxial GaAs

I. Szafranek, M. A. Plano, M. J. McCollum, S. A. Stockman, S. L. Jackson, K. Y. Cheng, and G. E. Stillman

Center for Compound Semiconductor Microelectronics, Materials Research Laboratory and Coordinated Science Laboratory, University of Illinois at Urbana-Champaign, Urbana, Illinois 61801

(Received 20 November 1989; accepted for publication 11 April 1990)

We report a study of a defect responsible for the "g" bound exciton line at 1.511_2 eV that is frequently detected in photoluminescence spectra of GaAs grown by molecular beam epitaxy (MBE). A direct correlation has been observed between this line and a transition at 1.494_6 eV, which is shown to result from a conduction band-to-acceptor recombination involving a shallow, unidentified acceptorlike defect that is labeled "A." The activation energy of the defect is 24.8 ± 0.2 meV, about 1.7 meV lower than that of C_{As} acceptor. Upon hydrogenation the defect is passivated more extensively than any known shallow acceptor species in GaAs. This result is analyzed in terms of a passivation model, from which it can be inferred that the A defect is not due to a simple substitutional Group II impurity on a Ga site. Incorporation of the A defect strongly affects the luminescence properties of the material. An almost complete quenching of the donor-bound exciton lines, profound changes in the line shape and relative intensity of the free exciton recombination, and appearance of a sharp transition of unknown origin at 1.513_8 eV were observed with increasing defect concentration. Apparently "donorless" low temperature exciton recombination spectra are reported for defect-rich p-type MBE GaAs layers with donor concentrations as high as 7×10^{14} cm^{-3} and compensation ratios of ~ 0.3. The dependence of the defect incorporation on MBE growth parameters is discussed. The feasibility of MBE growth of high purity, nearly shallow defect-free p-type GaAs layers at marginally As-stabilized surface conditions over an about 1–5 μm/h range of deposition rates is demonstrated.

I. INTRODUCTION

Photoluminescence (PL) peaks have been frequently observed at energies in the vicinity of 1.495 and 1.491 eV in GaAs layers grown by molecular beam epitaxy (MBE).[1-9] Briones and Collins[1] were the first to report the transition at 1.491 eV among about nine broad luminescence peaks in the 1.471–1.491 eV spectral region. In their work they established an empirical relation, analogous to Haynes' rule,[10] between this low energy series of peaks, labeled d_n after Skromme *et al.*,[11] and the sharp PL lines in the range of 1.504–1.511 eV, denoted here as K-P lines, that were first observed by Künzel and Ploog[12] and attributed by them to recombination of defect-bound excitons. This relation between peak positions of the two families of lines relative to carbon-induced transitions led Briones and Collins to assign the low energy d_n peaks to "defect-complexes" involving the C_{As} acceptor and to suggest that those complexes may be responsible for the luminescence in both spectral domains.[1] These conclusions were supported by Skromme *et al.*[11] for the transitions d_1–d_4 in the 1.466–1.482 eV range, who also found that the temperature and excitation intensity dependence of these peaks is typical of donor-to-acceptor (D^0–A^0) and conduction band-to-acceptor (e–A^0) recombination processes. Selective excitation PL studies have confirmed the acceptor-bound exciton nature of the K-P lines, as well as compliance of the K-P and d_n series with Haynes' rule.[5,7,13]

A transition around 1.495 eV was initially detected by selective excitation of the K-P defect-bound exciton line at 1.511 eV, labeled "g," and was interpreted as its 1S-2S two-hole replica.[2-4] It was inferred that the g exciton is localized on a shallow acceptor whose activation energy is about 22.9 meV.[2-4] In addition, Contour *et al.*[2] observed a broad emission band at 1.497 eV which they, rather arbitrarily, attributed to the recombination from the conduction band to unidentified, neutral g acceptors, $g(e$–$A^0)$. However, these spectral features could not be reproduced.[13,14] Furthermore, Steiner *et al.*,[15] based on their time-resolved PL study, reinterpreted the two-hole replicas of the $g(d,X)$ peak, confirming its acceptor-bound exciton nature, but determining the binding energy of the corresponding acceptor species to be about 18.5 meV. Rao *et al.*[3] detected a transition at 1.496 ± 0.001 eV as a shoulder on the high energy side of the conduction band-to-carbon acceptor transition $C(e$–$A^0)$. The PL amplitude dependence of the former band on temperature and excitation intensity revealed behavior typical of the $(e$–$A^0)$ recombination process. Similar results were obtained by Skromme,[5] who labeled the peak at ~ 1.495 eV as d_0 $(e$–$A^0)$ and also detected the corresponding donor-to-acceptor $(D^0$–$A^0)$ band near 1.491 eV. In all of these cases[2-5,15] a tentative correlation between the $g(d,X)$ peak at 1.511 eV and the band at ~ 1.495 eV has been proposed. Although quantitatively inconsistent, these studies promoted the concept that the g peak is due to recombination of excitons bound to an acceptorlike center which, in contra-

 0021-8979/90/140741-14$03.00

ANOMALOUS LUMINESCENCE PROPERTIES OF GaAs GROWN BY MOLECULAR BEAM EPITAXY

I. SZAFRANEK, M.A. PLANO, M.J. McCOLLUM, S.L. JACKSON, S.A. STOCKMAN, K.Y. CHENG and G.E. STILLMAN
Center for Compound Semiconductor Microelectronics, Materials Research Laboratory and Coordinated Science Laboratory, University of Illinois at Urbana - Champaign, IL 61801.

ABSTRACT

A shallow acceptor-like defect labeled "A" is frequently incorporated in molecular beam epitaxial GaAs. We report here anomalous photoluminescence effects that are induced by this defect. With increasing concentration of the "A" defect: (1) neutral and ionized donor-bound exciton peaks disappear almost completely even for donor concentration as high as $7x10^{14}$ cm^{-3} and compensation ratio $N_D/N_A \approx 0.3$; (2) a new, sharp line emerges at 1.513_8 eV, and (3) the relative intensity and line shape of the free exciton transition change dramatically. These observations are discussed in the perspective of previous reports, where similar effects were, in our opinion, misinterpreted.

INTRODUCTION

GaAs layers grown by molecular beam epitaxy (MBE) often exhibit unique photoluminescence (PL) features associated with unidentified shallow defects. The best known are the series of lines in the 1.504-1.511 eV range due to defect-bound excitons (d,X), first reported by Künzel and Ploog[1] and denoted hereafter as K-P peaks. Recently, we have found that the g(d,X) peak at the high energy limit of the K-P series originates in an exciton bound to the shallowest known acceptor-like defect in GaAs, labeled "A".[2] The activation energy of this defect is ~24.8 meV, about 1.7 meV less than that of C_{As} acceptors.

In the present paper further investigation of the "A" defect is reported. We have characterized a set of MBE grown GaAs samples in which the relative PL intensities of the "A" defect-induced transitions, g(d,X) at 1.511_2 eV and the free electron-to-"A" defect A(e,A^0) at 1.494_6 eV, varied over a wide range, allowing for study of anomalous effects induced by this defect in the exciton recombination luminescence. Our observations are important, because they demonstrate that if some commonly used methods of semiquantitative assessment of semiconductors with PL spectroscopy are used indiscriminately, they may provide an entirely misleading indication of purity and compensation in GaAs grown by MBE.

EXPERIMENTAL

Nominally undoped, p-type layers were grown in Phi 430P MBE system using solid Ga and As sources. A Phi As cracker with a rhenium baffle was operated at a current of 4 A (no temperature calibration has been available). Approximately 10 μm thick layers were grown under the As-stabilized (2x4) surface reconstruction conditions on semi-insulating, undoped liquid-encapsulated Czochralski GaAs substrates oriented 2° off the (100) orientation.

The samples were characterized electrically with van der Pauw Hall-effect measurements at a magnetic field of 0.66 T. The ohmic contacts on these p-type samples were formed with alloyed In-Zn spheres. Concentrations of electrically active donor and acceptor impurities were determined by numerical curve fitting of Hall carrier concentration measured over the temperature range of 15-300 K.[3]

Residual acceptor impurities and shallow defects in the layers were assessed with low temperature PL. The samples were measured over the temperature range of 1.7-21 K, being immersed strain-free in either superfluid He^4 or flowing gaseous He. An unfocused 5145 Å line from an argon ion laser was used for the photoexcitation. The emitted radiation was spectrally resolved by an Instruments SA 1 m double spectrometer and detected by a thermoelectrically cooled GaAs photomultiplier tube, using the photon counting technique.

Mat. Res. Soc. Symp. Proc. Vol. 163. © 1990 Materials Research Society

REASSESSMENT OF ACCEPTOR PASSIVATION MODELS IN p-TYPE HYDROGENATED GaAs

I. SZAFRANEK AND G.E. STILLMAN
Center for Compound Semiconductor Microelectronics, Materials Research Laboratory and Coordinated Science Laboratory, University of Illinois at Urbana-Champaign, IL 61801

ABSTRACT

The existing microscopic models of acceptor passivation in p-type hydrogenated GaAs are reviewed in light of new experimental results concerning the relative thermodynamic stability of the passivating complexes. In particular, the present model for neutralization of Group II acceptors, Be, Mg and Zn, on Ga sites is shown to be inadequate to account for the observed trends, which imply existence of a strong interaction between the hydrogen and acceptor. It is proposed that a direct acceptor-hydrogen bond is formed due to attractive Coulomb interaction between the ionized species. The relative stability of the pair complex can be then explained based on electronegativity of the acceptor species. Passivation at intermediate pair separations up to about twice the Bohr radius of the nearest acceptor, is also discussed.

INTRODUCTION

It is a well established fact that the electrical and optical activity of shallow substitutional acceptors in p-type GaAs can be neutralized by exposure to hydrogen plasma.[1,2] By analogy with silicon it is assumed that interstitial hydrogen atoms form a deep donor level in GaAs.[2] Thus, in p-type material, in the extrinsic temperature regime compensation takes place, and this effect is sufficient to explain the observed reduction in carrier concentration upon hydrogenation. However, in order to account for phenomena such as mobility enhancement[3] or changes in photoluminescence (PL)[4] and infrared local vibrational mode (IR LVM)[5-8] spectra after hydrogenation, the concept of passivation is used to imply formation of neutral acceptor-hydrogen complexes (Acc-H).[9] In GaAs two types of acceptors are distinguished: Group II elements Be, Mg, Zn and Cd on Ga sites, and Group IV elements C, Si and Ge on As sites. Accordingly, models have been proposed for the two possible passivating configurations.[1,7] The underlying mechanism, invariant with the acceptor type, is assumed to be Coulomb-field enhanced diffusion of protons toward the ionized acceptor sites.

Any proposal for the microscopic structure of the passivating complexes should be consistent with the experimentally established relative extent and thermodynamic stability of passivation of different acceptor species. However, no such data has been available so far. Recently, we have reported the first results on this aspect of hydrogenation,[10] based on PL investigation of passivation efficiency and susceptibility to light-induced reactivation (LIR)[4] of different acceptors in high-purity p-type GaAs. The observed stability trends do not fully comply with predictions of the existing model for passivation of Group $[II]_{Ga}$ acceptors.[1] In this paper the experimental results are reviewed and the discrepancies with the model predictions analyzed. A modified passivation mechanism is then proposed, which is in general agreement with our measurements and is inherently compatible with the athermal, electronically stimulated acceptor reactivation effect previously reported.[4] Although PL does not provide a direct structural information, it allows for characterization of very high-purity materials (10^{13}-10^{15} cm^{-3}) compared to other techniques (SIMS, IR, Raman). We shall demonstrate that impurity concentration is an important factor to be considered, because it may affect the passivation process itself.

EXPERIMENTAL

Experimental procedures of hydrogenation, LIR and PL characterization are similar to those described in Ref. 4. High-purity epitaxial GaAs layers grown by molecular beam epitaxy (MBE), metal-organic chemical vapor deposition (MOCVD) and AsH_3-vapor phase epitaxy (VPE) were analyzed. They were either intentionally doped or nominally undoped, with total impurity concentrations of the order of 10^{14}-10^{15} cm^{-3}.

Mat. Res. Soc. Symp. Proc. Vol. 163. © 1990 Materials Research Society

Journal of Crystal Growth 105 (1990) 316–325
North-Holland

EFFECTS OF HIGH SOURCE FLOW AND HIGH PUMPING SPEED ON GAS SOURCE MOLECULAR BEAM EPITAXY / CHEMICAL BEAM EPITAXY

M.J. McCOLLUM *, S.L. JACKSON, I. SZAFRANEK and G.E. STILLMAN

Center for Compound Semiconductor Microelectronics, Coordinated Science Laboratory and Materials Research Laboratory, University of Illinois at Urbana-Champaign, Urbana, Illinois 61801, USA

We report the growth of GaAs by molecular beam epitaxy (MBE), gas source molecular beam epitaxy (GSMBE), and chemical beam epitaxy (CBE) in an epitaxial III–V reactor which features high pumping speed. The system is comprised of a modified Perkin-Elmer 430P molecular beam epitaxy system and a custom gas source panel from Emcore. The growth chamber is pumped with a 7000 l/s (He) diffusion pump (Varian VHS-10 with Monsanto Santovac 5 oil). The gas source panel includes pressure based flow controllers (MKS 1150) allowing triethylaluminum (TEA), triethylgallium (TEG), and trimethylindium (TMI) to be supplied without the use of hydrogen. All source lines, including arsine and phosphine, are maintained below atmospheric pressure. The high pumping speed allows total system flow rates as high as 100 SCCM and V/III ratios as high as 100. The purity of GaAs grown by MBE in this system increases with pumping speed. GaAs layers grown by GSMBE with arsine flows of 10 and 20 SCCM have electron concentrations of 1×10^{15} cm^{-3} (μ_{77} = 48,000 cm^2/V·s) and 2×10^{14} cm^{-3} (μ_{77} = 78,000 cm^2/V·s) respectively. Electron concentration varies with hydride injector temperature such that the minimum in electron concentration occurs for less than complete cracking. The effect of V/III ratio and the use of a metal eutectic bubbler on residual carrier concentration in GaAs grown by CBE is presented. Intentional Si and Be doping of CBE grown GaAs is demonstrated at a high growth rate of 5.4 μm/h.

1. Introduction

There has recently been a great interest in the conversion of molecular beam epitaxy (MBE) growth systems into chemical beam epitaxy (CBE), metalorganic molecular beam epitaxy (MOMBE), and gas source molecular beam epitaxy (GSMBE) systems. This conversion can be done in different ways which results in differing available growth parameter space.

The system used in this study has been designed and built specifically for growth by GSMBE/CBE and features high pumping speed, and high source gas flow capability. With this system we have grown GaAs by MBE, GSMBE, and CBE. Some effects of high flow and pumping speed on GaAs growth by these techniques are reported.

* Present address: NIST 724.02, 325 Broadway, Boulder, Colorado 80303, USA.

2. Growth system

2.1. Growth chamber

In this study, a standard Perkin-Elmer Phi 430P MBE system was modified. Along with the growth chamber, the vacuum system includes an introduction chamber and transfer chamber. The CBE system is shown schematically in fig. 1. The standard Phi growth chamber has an ion pump mounted below the chamber. To provide the pumping speed required for GSMBE/CBE, the ion pump was replaced with a twelve inch GNB (Hayward, CA) gate valve, a Varian circular chevron cryo-baffle, and Varian VHS-10 diffusion pump. The entire MBE system is mounted on a 28 inch high stand to allow adequate clearance from the floor for the gate valve, cryo-baffle, and diffusion pump.

The source flange on the growth chamber has ports for 8 separate sources. The eight source

0022-0248/90/$03.50

Species dependence of passivation and reactivation of acceptors in hydrogenated GaAs

I. Szafranek and G. E. Stillman
Center for Compound Semiconductor Microelectronics, Materials Research Laboratory and Coordinated Science Laboratory, University of Illinois at Urbana-Champaign, Illinois 61801

(Received 21 February 1990; accepted for publication 31 May 1990)

Effects of passivation and light-induced reactivation of acceptors in high-purity hydrogenated GaAs are investigated with low-temperature photoluminescence. The effectiveness of both processes has been found to be strongly dependent on the chemical identity of acceptor species, thus allowing a qualitative assessment of the relative stability of different acceptor-hydrogen passivating complexes in *p*-type hydrogenated GaAs. Efficient neutralization of acceptors in high-purity *n*-type hydrogenated GaAs is also reported, in contradiction with results of recent studies on heavily doped materials where passivation of minority dopants was not observed. The implications of these experimental data on theoretical models of the acceptor passivation mechanism are discussed.

I. INTRODUCTION

The ability of hydrogen to neutralize the electrical and optical activity of shallow substitutional impurities in GaAs after exposure to hydrogen plasma, proton implantation, etc., is well recognized.[1,2] The stability of the resulting passivated material is of great fundamental interest as well as of practical importance. This issue has been systematically studied in *n*-type hydrogenated GaAs (GaAs:H), where the activation energies for thermal reactivation of Si, Ge, Sn, S, Se, and Te donor species were determined ($E_T \simeq 2.1$ eV) in a series of isothermal and isochronal anneals in the 275–415 °C temperature range.[3] The information available on the reactivation of acceptors in *p*-type GaAs is more sporadic; the dissociation energy of the Zn_{Ga}—H passivating complex in the same temperature range was found to be $E_T \simeq 1.6$ eV.[4] C_{As} acceptors were reported to be reactivated after ~5 min annealing at 300 °C,[5] and we have recently observed that Mg_{Ga}, Be_{Ga}, and Si_{As} acceptors can be partially reactivated by a practically athermal, light-stimulated process.[6]

In this paper the relative passivation stability of different acceptor impurities in GaAs:H is qualitatively investigated with low-temperature photoluminescence (PL). A similar approach was previously employed by Weber *et al.*,[7] who demonstrated acceptor-specific nature of the neutralization process in GaAs. Although PL can neither provide direct structural information on the passivation mechanism nor allow straightforward quantitative evaluation of the hydrogenation effects, it has the advantage of being able to characterize very high-purity materials ($N_D + N_A \simeq 10^{13}$–10^{15} cm^{-3}), compared to other techniques, such as secondary-ion mass spectrometry and infrared or Raman spectroscopies. We shall demonstrate that impurity concentration is an important factor to consider, because it may affect the passivation process. Moreover, with PL the effects of passivation and reactivation can be easily studied simultaneously for all the acceptor species present in the material. This facilitates a direct, matrix-independent comparison of the relative affinity to hydrogen of various acceptor species and the resulting relative changes in concentrations of the optically active acceptors.

Our studies indicate that both the passivation efficiency and the susceptibility of different acceptors to light-induced reactivation (LIR)[6] are strongly dependent on the chemical identity of the acceptors involved. Assuming that the former process is directly related, whereas the latter is inversely related to the binding energy of an acceptor-hydrogen (Acc—H) neutralizing complex, a qualitative scale of the relative passivation stability of different acceptors in GaAs has been determined. The observed stability trends imply the existence of an interaction between H and the passivated acceptor and, therefore, do not fully agree with predictions of the currently accepted microscopic structure of the (Group [II]$_{Ga}$ acceptor)—H passivating complexes, in which the H atom is supposed to be covalently bound to an As host atom and to have no or a very weak interaction with the Group II acceptor species.[1,2,8–10] Characterization of *high-purity n-type* GaAs:H has revealed that minority acceptor impurities can be neutralized even under hydrogenation conditions which are known to be relatively ineffective for passivation of shallow donors. Since this observation disagrees with a recent conclusion by Pajot[10] that compensated minority impurities are not neutralized in heavily doped materials (~10^{18}–10^{19} cm^{-3}), it is plausible that the passivation mechanism of acceptors is dependent on the Fermi energy. All of these experimental results can be consistently accounted for if the interstitial hydrogen atoms form donor levels in GaAs,[9,37] thus compensating shallow acceptors in *p*-type material (or being partially compensated by minority shallow acceptors in *n*-type, depending on the energy of the Fermi level at the hydrogenation temperature). The passivation then results from the ionized donor-acceptor pairing that is promoted by Coulomb-field enhanced diffusion of protons toward the ionized acceptors.[1,2,9]

II. EXPERIMENT

High-purity GaAs layers grown by molecular beam epitaxy (MBE), metalorganic chemical vapor deposition

 0021-8979/90/193554-10$03.00

LOW - TEMPERATURE DEFECT - INDUCED AGING OF GaAs GROWN BY MOLECULAR BEAM EPITAXY

I. SZAFRANEK, S. A. STOCKMAN, M. SZAFRANEK, M. J. McCOLLUM, M. A. PLANO, W. R. MILLER AND G. E. STILLMAN
Center for Compound Semiconductor Microelectronics, Materials Research Laboratory and Coordinated Science Laboratory, University of Illinois at Urbana-Champaign, IL 61801

ABSTRACT

Degradation in optical and electrical properties has been observed for high-purity and high-mobility p-type GaAs layers which contain significant concentrations of an unidentified shallow acceptor-like defect, labeled "A", that is frequently incorporated in crystals grown by molecular beam epitaxy. Low-temperature photoluminescence and variable temperature Hall-effect measurements were employed to monitor the aging process in samples stored for about one year at room temperature. Profound changes in the exciton recombination spectra, indicative of increasing concentration of the "A" defect, have been accompanied by a decrease in hole mobility and an increase in carrier concentration. These results are discussed in the context of the acceptor-pair defect model, originally proposed by Eaves and Halliday [J. Phys. C: Solid State Phys. 17, L705 (1984)].

INTRODUCTION

Shallow acceptor-like defects of an unidentified microscopic nature are frequently incorporated in GaAs grown by molecular beam epitaxy (MBE).[1-3] One of these defects gives rise to an intense bound exciton photoluminescence (PL) peak at 1.511 eV, known as g(d,X)[4] or line 47.[5] We have recently reported that the "A" center responsible for the g(d,X) transition has an activation energy of 24.8 ± 0.2 meV, about 1.7 meV lower than that of the shallowest known substitutional acceptor in GaAs, C_{As}.[6] Furthermore, we have shown that large concentrations of the "A" defect cause anomalous quenching of donor-bound exciton transitions, appearance of a new, sharp line labeled P_0 at 1.513_8 eV, and variations in the line shape of the free exciton (FE) recombination in the low-temperature PL spectra.[6,7]

Continued investigation of high-purity and high-mobility p-type GaAs layers containing appreciable concentrations of the "A" defect have revealed that during storage for about a year at room temperature the PL spectra of near-band-edge exciton recombination have changed dramatically. A slight degradation in the electrical properties has been observed as well. The samples were characterized with low-temperature PL and with variable temperature Hall-effect techniques, and the results of these studies are reported in the present paper. Implications of our observations on a model explaining the origin of the acceptor-like defects, characteristic of GaAs grown by MBE, are also briefly discussed.

EXPERIMENTAL

The samples used in this study were all nominally undoped *p* type, grown in Phi 430P MBE system using solid Ga and As sources. The epitaxial layers were approximately 10 μm thick and grown under the As-stabilized (2×4) surface reconstruction conditions on semi-insulating, undoped liquid-encapsulated Czochralski GaAs substrates oriented 2° off the (100) orientation.

The samples were characterized electrically with Hall-effect measurements in van der Pauw configuration at a magnetic field of 0.66 T. The ohmic contacts on these p-type samples were formed with alloyed In-Zn spheres.

Residual acceptor impurities and shallow defects in the layers were assessed with low-temperature PL. The samples were immersed strain-free in superfluid ^{4}He at about 1.7 K. Unfocused 5145 Å radiation from an Ar^+ laser was used for the photoexcitation. The emitted radiation was spectrally resolved by an Instruments SA 1 m double spectrometer and detected by

Mat. Res. Soc. Symp. Proc. Vol. 184. © 1990 Materials Research Society

ELECTRONIC STIMULATION OF ACCEPTOR REACTIVATION IN p-TYPE HYDROGENATED GaAs

I. SZAFRANEK AND G. E. STILLMAN
Center for Compound Semiconductor Microelectronics, Materials Research Laboratory and Coordinated Science Laboratory, University of Illinois at Urbana-Champaign, IL 61801

ABSTRACT

The mechanism of light-induced reactivation (LIR) of shallow substitutional acceptors in high-purity p-type hydrogenated GaAs has been investigated. Photoluminescence was used to determine the dependence of the rate and extent of this effect on photon energy, illumination intensity, as well as on sample temperature and chemical composition. At a sample temperature of 1.7 K a sharp threshold in the photon energy, E_t, has been observed at about 7.5 meV below the bandgap energy of GaAs. This energy corresponds approximately to the onset of acceptor-bound exciton absorption in the material. For photon energy $E < E_t$, only a weak reactivation effect is observed. The efficiency of reactivation increases dramatically for $E > E_t$, and for sufficiently large values of (light intensity)·(illumination time) product the LIR process saturates. Both the extent of the subthreshold effect and the saturation level that is attainable with $E > E_t$ are independent of the photon energy, excitation power and exposure time in the investigated range of these quantities. For $E > E_t$ the initial LIR rate depends on the square of the light intensity, indicating a bimolecular reaction in terms of the photo-generated carrier densities. The observed strong dependence of the saturation level on the sample temperature during LIR is found to be consistent with the relative binding energies of different acceptor-hydrogen passivating complexes in GaAs. Based on these results, it is proposed that LIR of acceptors is electronically stimulated via recombination-enhanced vibrational excitation of acceptor-hydrogen complexes.

INTRODUCTION

We have recently reported that certain shallow substitutional acceptors in high-purity p-type hydrogenated GaAs undergo a reversible and, practically, athermal light-induced reactivation (LIR) at cryogenic temperatures.[1] The (LIR) process is strongly dependent on the chemical identity of the hydrogen-passivated acceptor species. An inverse correlation has been observed between the susceptibility to LIR and the binding energy of the different acceptor-hydrogen complexes (Acc-H) in GaAs.[2,3] Occurrence of LIR implies thermodynamic metastability of the hydrogenated GaAs. Since hydrogen-passivation is considered a promising processing technique in fabrication of semiconductor devices,[4] understanding of the LIR effect is important for prediction of the lifetime of devices based on this technology. Furthermore, the apparent similarity of the LIR phenomenon in GaAs to light-induced degradation in hydrogenated amorphous silicon (known as the Staebler-Wronski effect)[5] suggests, that the understanding of the former process may assist in the ongoing effort to establish the mechanism of the latter, which takes place in the much more complex amorphous material system.

In the present paper, results of a systematic experimental investigation of the LIR mechanism are presented. The LIR effect was monitored with low-temperature photoluminescence (PL) as a function of wavelength and power density of the excitation light, the sample temperature and the identity of acceptor impurities. The dependence of the rate and extent of LIR on these experimental parameters supports our previous tentative proposal[1] that the effect is brought about by a recombination-enhanced defect reaction (REDR) mechanism.[6,7]

EXPERIMENTAL

The high-purity epitaxial GaAs layers used in this work were grown by molecular beam epitaxy (MBE) and metalorganic chemical vapor deposition (MOCVD). The samples included intentionally doped and nominally undoped p-type crystals, with total impurity concentrations in the range of $N_A + N_D \leq 10^{15}$ cm^{-3}.

Mat. Res. Soc. Symp. Proc. Vol. 184. ©1990 Materials Research Society

Layer intermixing in heavily carbon-doped AlGaAs/GaAs superlattices

I. Szafranek, M. Szafranek, B. T. Cunningham,[a] L. J. Guido,[b] N. Holonyak, Jr., and G. E. Stillman

Center for Compound Semiconductor Microelectronics, Materials Research Laboratory and Coordinated Science Laboratory, University of Illinois at Urbana-Champaign, Illinois 61801

Interdiffusion of Al and Ga in heavily C-doped $Al_{0.3}Ga_{0.7}As$/GaAs superlattice (SL) structures has been investigated quantitatively for a variety of ambient and surface encapsulation conditions. High-resolution photoluminescence (PL) at $T = 1.7$ K was employed to evaluate the extent of layer intermixing after 24-h anneals at 825 °C. From the shifts to higher energies of the PL peaks due to $n = 1$ electron-to-heavy hole transitions in the quantum wells of the annealed SLs relative to the position of this peak in the as-grown crystal, approximate Al-Ga interdiffusion coefficients ($D_{Al\text{-}Ga}$) have been determined for different annealing conditions. For all encapsulants studied the interdiffusion in C-doped crystals is accelerated with increasing As_4 pressure in the annealing ampoule. This result disagrees with previously observed trends for Group II-doped p-type structures, which have led to the charged point-defect model (Fermi-level effect) of Al-Ga interdiffusion. The Si_3N_4 cap has provided the most effective surface sealing against ambient-stimulated layer interdiffusion, and yielded $D_{Al\text{-}Ga} \simeq 1.5 - 3.9 \times 10^{-19}$ cm^2/s. The most extensive layer intermixing has occurred for uncapped SL annealed under As-rich ambient ($D_{Al\text{-}Ga} \simeq 3.3 \times 10^{-18}$ cm^2/s). These values are up to ~40 times greater than those previously reported for nominally undoped $Al_xGa_{1-x}As$/GaAs SLs, implying that the C_{As} doping slightly enhances host-atom self-diffusion on the Group III sublattice, but significantly less than predicted by the Fermi-level effect. The discrepancies between the experimental observations and the model, are discussed.

I. INTRODUCTION

The dependence of Al-Ga interdiffusion in quantum-well heterostructures (QWHs) on anneal ambient and surface encapsulation conditions has been extensively investigated under both intrinsic and impurity-induced regimes for $Al_xGa_{1-x}As$/GaAs and related III/V material systems (for a recent review, see Ref. 1). Based on results of that work a consistent picture has evolved, whereby the self-diffusion of Group III host atoms, which causes the layer intermixing, is presumably mediated by the Group III vacancy (V_{III}) and interstitial (I_{III}) charged native point defects.[1-5] The concentrations of these defects depend on the Fermi-level position and crystal stoichiometry, and can be experimentally controlled by doping and/or the anneal ambient atmosphere.[1-5] Specifically, Al-Ga interdiffusion has been found to increase in n-type superlattice (SL) crystals with heavy doping of either Group IV (e.g., Si)[4] or Group VI (e.g., Se)[6] substitutional donors during anneals under As-rich ambient, both conditions enhancing solubility of the negatively charged V_{III}. On the other hand, when a SL is p-type with a heavy doping of Group II on Ga sublattice elements (e.g., Mg),[4] increased interface smearing has been observed after Ga-rich anneals, supposedly because of an excess concentration of positively charged I_{III} defects.[1-5]

Recent advances in heavy carbon doping of GaAs and $Al_xGa_{1-x}As$ grown by metalorganic chemical vapor deposition (MOCVD)[7-9] have allowed, for the first time, tests of the trends outlined above also for this Group IV on As sublattice acceptor species.[7] In that work[9] the extent of Al-Ga interdiffusion was found to be extremely small compared to other p-type dopants, and could not be detected with conventional microanalytical techniques such as cross-sectional two-beam transmission electron microscopy (TEM) or secondary-ion mass spectrometry (SIMS). This led to the conclusion that heavy C_{As} doping suppresses layer disordering in $Al_xGa_{1-x}As$/GaAs SLs relative to an undoped crystal. Also, using low-resolution photoluminescence (PL) at $T = 77$ K, lack of interdiffusion enhancement under Ga rich compared to As-rich annealing conditions was observed.[9] These recent results obviously disagree with previous data on impurity-induced layer disordering (IILD) in general, and the Fermi-level (or charged point-defect) interdiffusion model,[1-5] in particular.

Because of the central importance of the data on IILD in heavily C-doped SL crystals to the understanding of the Group III self-diffusion, we have performed a more complete, quantitative study of anneal ambient and surface encapsulation effects on this process. In this work low-temperature, weak-excitation PL has been employed for improved spectral resolution. The layer disordering-induced shifts to higher energies (ΔE) of the $n = 1$ electron-to-heavy hole ($e \rightarrow hh$) confined-particle transitions were analyzed to yield Al-Ga interdiffusion coefficients ($D_{Al\text{-}Ga}$) for different annealing conditions at $T = 825$ °C. This work confirms one of the major conclusions of the earlier study.[9] We have observed clear trends of enhanced interface smearing in SLs annealed under As rich relative to As-deficient ambients for all cases of crystal surface sealing. However, the calculated values of $D_{Al\text{-}Ga}$ (825 °C) fall in the range of

[a] Now at Sandia National Laboratories, Division 1141, Albuquerque, NM 87185

[b] Now at Yale University, Department of Electrical Engineering, Center for Microelectronic Materials and Structures, Box 2157 Yale Station, New Haven, CT 06520

 0021-8979/90/235615-06$03.00

Defect Control in Semiconductors
K. Sumino (ed.)

KINETIC EFFECTS AND IMPURITY INCORPORATION IN MBE GROWTH OF GALLIUM ARSENIDE

G.E. Stillman, B. Lee, I. Szafranek, M.A. Plano, M.J. McCollum, S.S. Bose* and M.H. Kim+

Center for Compound Semiconductor Microelectronics, Materials Research Laboratory, Coordinated Science Laboratory, University of Illinois, Urbana, Illinois 61801 USA

The incorporation of the Group IV impurities Si, Ge and C, as well as other defects, during MBE epitaxial growth of GaAs has been studied by photoluminescence, photothermal ionization spectroscopy, and variable temperature Hall effect measurements. Growth with constant Si doping flux but with different V/III flux ratios has shown that the sticking coefficient for Si under ordinary MBE growth conditions is not unity, but varies with the V/III flux ratio. The Si donor concentration increases substantially with increasing As_4/Ga flux ratio, while the Si acceptor concentration remains nearly constant at less than $10^{14}cm^{-3}$. Thus, the commonly observed variation of carrier concentration with V/III ratio during Si doping is not due to the amphoteric behavior of Si, but is due to the variation with V/III ratio of the non-unity sticking coefficient of Si. This variation is explained by the kinetic effects associated with the surface reaction processes involved in Si impurity incorporation. The orientation dependence of the amphoteric behavior of Si, Ge and C has also been studied, and can be explained by different kinetic effects on the different orientations. The simple arguments concerning single or double dangling bonds and site availability as often worked, cannot explain the observed orientation dependence.

1. INTRODUCTION

The Group IV elements are particularly interesting as dopants in GaAs because they have the potential of being incorporated on the Ga or As sublattices and thus being amphoteric, i.e. acting as either a donor or acceptor substitutional impurity, respectively. This amphoteric behavior is generally undesirable, since it results in compensation that degrades the transport properties of the semiconductor samples or devices. It has been pointed out that the amphoteric behavior or auto compensation of Group IV impurities in GaAs is influenced by the covalent radius of the impurity relative to the host atom, by the differences between the electronegativity of the impurity and the host atom it replaces, and by the relative availability of the two different lattice sites.[1,2]

These simple equilibrium considerations qualitatively explain some of the properties of the Group IV impurities. For example, it has been shown that Si incorporates primarily as a donor in VPE, MOCVD, and MBE growth of GaAs on (100) oriented substrates, but primarily as an acceptor in LPE growth on (100) substrates.[3] Recent studies of the orientation dependence of Si incorporation during simultaneous growth on multiple low index oriented substrates by MBE, however, have shown that kinetic effects are very important in the amphoteric behavior of Si in particular, and the Group IV dopants in general, in MBE growth of GaAs.[4-6] From spectroscopic and Hall effect measurements on lightly Si doped MBE samples grown simultaneously on 100, (311)A, and (311)B substrates,[7] it was found that for growth on the (100) substrate the epitaxial layer was n-type, and the Si amphoteric ratio, defined as the ratio of the concentration of Si acceptors to Si donors, $[Si_{AS}]/[Si_{Ga}]$, was only 0.08. For the sample grown on the (311)B substrate the layer was also n-type, but the amphoteric ratio for this sample was even smaller at 0.01. The sample grown simultaneously on the (311)A substrate was p-type and was relatively uncompensated, with an amphoteric ratio estimated to be greater than 4. (The amphoteric ratio of Si in the p-type sample could only be estimated since the relative concentration and identity of the donor species present could not be determined using photothermal ionization spectroscopy. The estimate above was obtained assuming that the total donor concentration was due to Si_{Ga}, and because of residual S donors the $[Si_{Ga}]$ is certainly much less that N_D.) The amphoteric ratio of

*Present address: Penn State University, 121 Electrical Engineering East, University Park, PA 16802
+Present address: Bandgap Technologies, 891A Interloken Parkway, Broomfield, CO 80020

Instability of partially disordered carbon-doped AlGaAs/GaAs superlattices

I. Szafranek, J. S. Major, Jr.,[a] B. T. Cunningham,[b] L. J. Guido,[c] N. Holonyak, Jr., and G. E. Stillman

Center for Compound Semiconductor Microelectronics, Materials Research Laboratory and Coordinated Science Laboratory, University of Illinois at Urbana-Champaign, Illinois 61801

(Received 20 July 1990; accepted for publication 1 October 1990)

Superlattices of $Al_{0.3}Ga_{0.7}As/GaAs$ grown by metalorganic chemical vapor deposition and heavily doped with carbon using CCl_4 were annealed for 24 h at 825 °C under a variety of ambient and surface encapsulation conditions. Pronounced changes in photoluminescence from the annealed superlattices with storage time at room temperature, as opposed to an excellent reproducibility of that from the as-grown, not annealed samples, are reported. These changes may be indicative of degraded thermal stability of the annealed superlattice crystals due to high-temperature-induced lattice defects. The systematic failure to fabricate buried-heterostructure quantum well lasers via impurity-induced layer disordering in similarly doped AlGaAs/GaAs crystals, which may be related to the same effect, is also discussed.

High-temperature annealings have long been used to stimulate diffusion processes in quantum well heterostructures (QWHs) and superlattices (SLs) in attempts to modify the structure and thus the optical properties of the crystals (for a recent review on this subject, see Ref. 1). This procedure has been applied to both nominally undoped and doped crystals, the latter case being referred to as the impurity-induced layer disordering (IILD),[2] and it provides an important additional degree of freedom in device fabrication.[1] The layer intermixing effect is promoted by native defects whose concentrations increase at elevated temperatures. An important aspect of the potential applicability of the high-temperature heat treatments is the influence that such processes may have on the long-term stability of the optical and electrical properties of the annealed crystals.

In this letter we present an evidence of significant changes in luminescence properties of C-doped $Al_xGa_{1-x}As/GaAs$ SL crystals during storage of several months at room temperature following annealing at 825 °C. This effect possibly indicates a structural instability of the annealed crystals due to high-temperature-induced lattice defects and, therefore, it may bear on performance of laser diodes and other electro-optical devices realized using IILD processing. Specifically, a systematic failure to fabricate buried-heterostructure QW lasers using IILD in similarly doped crystals is reported.

The crystals investigated here were grown by low-pressure metalorganic chemical vapor deposition (MOCVD) in an Emcore GS3100 reactor. The carbon doping source was a 500 ppm mixture of CCl_4 (Matheson) in high-purity H_2.[3,4] It provided an approximately uniform p-type doping level of $[C_{As}] \approx 8 \times 10^{18}$ cm^{-3} throughout the whole stack of GaAs and $Al_xGa_{1-x}As$ epitaxial layers, as determined by secondary-ion mass spectrometry (SIMS) and C-V electrochemical depth profiles. The growth conditions and the SL structure are described in detail elsewhere.[5]

The anneals were performed in evacuated quartz ampoules (volume ≈ 3 cm^3, $p \approx 10^{-6}$ Torr) at $T = 825$ °C for 24 h. Three sets of samples were annealed in separate ampoules with (i) an excess of elemental As $-(+\text{As})$, (ii) an excess of elemental Ga $-(+\text{Ga})$, and (iii) with neither Ga nor As added to the ampoule $-(+0)$. A set of three samples was loaded into each ampoule: two were encapsulated with a CVD-grown ~ 1000-Å-thick layer of either SiO_2 or Si_3Ni_4, and the third sample was uncapped.

The optical properties of all the samples were assessed with low-temperature photoluminescence (PL). The samples were mounted strain-free in superfluid ^{4}He at $T \approx 1.7$ K, and were excited with the 5145 Å line from an AR^+ laser, using low power density of ~ 36 mW/cm^2. The emitted radiation was dispersed by an Instruments SA 1 m double spectrometer and detected by a thermoelectrically cooled GaAs photomultiplier tube, using the photon counting technique. The PL measurements were initially taken several weeks after the SL crystals were grown and annealed. Subsequently, all the samples (including the as-grown) were repeatedly measured under identical experimental conditions several times during a period of more than a year, while being stored at room temperature. An unfocused beam of about 3 mm in diameter was used to probe almost the entire area of the samples, thus averaging over possible lateral inhomogeneities of the crystals.

In the as-grown sample the SL-related low-temperature PL consists of a single, symmetric peak at $h\nu \approx 1.5316$ eV with full width at half maximum (FWHM) of ~ 17.6 meV. This peak is attributed to $n = 1$ electron-to-heavy hole ($e \rightarrow$ hh) confined-particle recombination in GaAs QWs as discussed in detail elsewhere.[5] In the PL spectra of the annealed SLs this transition is accompanied

[a] Intel Doctoral Fellow.
[b] Now at Sandia National Laboratories, Division 1141, Albuquerque, NM 87185.
[c] Now at Yale University, Department of Electrical Engineering, Center for Microelectronic Materials and Structures, Box 2157 Yale Station, New Haven, CT 06520.

 0003-6951/90/532910-03$02.00

Hydrogenation of Si- and Be-doped InGaP

J. M. Dallesasse, I. Szafranek, J. N. Baillargeon, N. El-Zein, N. Holonyak, Jr., G. E. Stillman, and K. Y. Cheng
Electrical Engineering Research Laboratory, Center for Compound Semiconductor Microelectronics and Materials Research Laboratory, University of Illinois at Urbana-Champaign, Urbana, Illinois 61801

(Received 20 June 1990; accepted for publication 13 August 1990)

Data are presented on the hydrogenation of Be-doped (p-type) and Si-doped (n-type) $In_{1-x}Ga_xP$ epitaxial layers grown lattice matched to GaAs ($x \sim 0.5$). Low-temperature (1.7 K) photoluminescence, electrochemical carrier concentration profiling, and scanning electron microscopy are used to study the effects of hydrogenation on carrier recombination, carrier concentration, and surface morphology. Hydrogenation is found to passivate Si donors and Be acceptors and to improve photoluminescence efficiency, but causes mild surface damage. The carrier concentration following hydrogenation is found to be lowest in acceptor-doped material.

I. INTRODUCTION

Since the discovery that exposure of Ge to a hydrogen plasma alters the electronic properties of the surface,[1] it has been known that semiconductors more generally can be modified by exposure to atomic hydrogen. The study of semiconductors exposed to hydrogen plasmas received renewed interest when hydrogenation of amorphous and crystalline Si was found to result in improvement in the photoluminescence properties,[2] passivation of grain boundaries,[3] and reduction of carrier concentration.[4] More recently the exposure of compound semiconductors to hydrogen plasmas has received extensive study. In the $Al_xGa_{1-x}As$ system hydrogenation has been found to improve photoluminescence efficiency[5] and to provide some passivation of donors[6] and acceptors[7] to the depth hydrogen diffuses during the hydrogenation process. The fact that this effect is maskable has been utilized to fabricate single-stripe and high-power multistripe lasers in the $Al_xGa_{1-x}As$-GaAs[8,9] and $Al_yGa_{1-y}As$-GaAs-$In_xGa_{1-x}As$[10] systems.

An important III-V system for the construction of visible-spectrum lasers and light-emitting diodes is the quaternary $In_y(Al_xGa_{1-x})_{1-y}P$.[11-13] This system, a modification of the high-gap ternary $In_yGa_{1-y}P$,[14] has received renewed interest because of the advent of advanced growth techniques such as metalorganic chemical vapor deposition (MOCVD)[15] and gas-source molecular-beam epitaxy (GSMBE).[16] Room-temperature continuous-wave (cw) diode lasers at wavelengths as short as 6395 Å[17-19] and photopumped lasers at wavelengths as short as 6250 Å[20,21] have been produced in this system. Improvements in material quality and device structure should result in shorter wavelengths and better device performance. Examination of hydrogenation in this system is thus of some interest, because the improved current confinement and lower thermal impedance[8,9] of hydrogenated stripe-geometry lasers have the potential to yield devices with improved performance characteristics.[22]

In this paper hydrogenation of $In_{1-x}Ga_xP$ grown lattice matched to GaAs ($y \sim 0.5$) is examined via low-temperature photoluminescence, electrochemical carrier concentration profiling, and scanning electron microscopy. Hydrogen plasma exposure is found to increase the photoluminescence efficiency and to passivate dopants and impurities to the depth of the hydrogen diffusion. $In_{1-x}Ga_xP$ crystals that are doped p type are found to be compensated to a greater extent than crystals that are doped n type.

II. EXPERIMENTAL PROCEDURE

The $In_{1-x}Ga_xP$ crystals employed in these experiments are grown by gas-source MBE on (100) GaAs substrates. Gases for the Column V constituents (AsH_3 and PH_3) are handled using an Emcore GS3000 system. The Column III constituents In and Ga, as well as the p- and n-type dopants Be and Si, are provided by standard MBE effusion cells. Substrates are prepared for crystal growth by degreasing in trichloroethylene, followed by acetone, methanol, and deionized water rinses. Final sample preparation with HCl, H_2SO_4, and deionized water leaves the surface with a thin native oxide as a protective layer. The samples are grown at 500 °C with a growth rate of $\sim$ 1.6 μm/h.

Hydrogenation of the crystals takes place in a parallel-plate reactor (Texas Instruments Model A-24-D) originally designed for plasma-enhanced chemical vapor deposition (PECVD).[9] An rf generator operating at 13.6 MHz applies power to the top electrode. The lower electrode supports the sample and serves as ground. This electrode is equipped with a heater capable of operating to 400 °C. For this work samples are hydrogenated at temperatures ranging from 150 to 300 °C, pressures ranging from 375 to 1500 mT, and rf power densities ranging from 0.125 to 0.375 W/cm^2. In order to minimize diffusion of the hydrogen within the crystal following hydrogenation, samples are thermally quenched to room temperature by removal from the process chamber within $\sim$ 45 s of extinguishing the plasma.

The effect of hydrogenation on the carrier recombination is determined by comparing low-temperature (1.7 K) photoluminescence measurements on hydrogenated and as-grown crystals. These measurements employ an Ar$^+$ laser operating at 5145 Å. The sample luminescence is analyzed via a 1.0-m double grating spectrometer equipped

 0021-8979/90/235866-05$02.40

Mechanism of light-induced reactivation of acceptors in *p*-type hydrogenated gallium arsenide

I. Szafranek, M. Szafranek, and G. E. Stillman
Center for Compound Semiconductor Microelectronics, Materials Research Laboratory and Coordinated Science Laboratory, University of Illinois at Urbana-Champaign, Urbana, Illinois 61801
(Received 21 October 1991)

The mechanism of light-induced reactivation (LIR) of shallow substitutional acceptors in high-purity *p*-type hydrogenated GaAs has been investigated. Low-temperature photoluminescence was used to determine the dependence of the rate and extent of this effect on photon energy, illumination intensity, sample temperature, and chemical identity of the passivated acceptor impurities. The efficiency of LIR at $T=1.7$ K increases sharply for photon energies greater than a threshold value of $E_t \approx E_g - 7.5 \pm 0.5$ meV, where E_g is the band-gap energy of GaAs. This energy corresponds approximately to the onset of acceptor-bound exciton absorption in the material. For $h\nu > E_t$, the initial LIR rate depends on the square of the light intensity, indicating a bimolecular reaction involving the photogenerated carriers. For sufficiently large values of the product of the light intensity, and the illumination time, the LIR process saturates. Both the extent of the subthreshold effect for $h\nu < E_t$, and the saturation level that is attainable for $h\nu > E_t$ are independent of the photon energy, excitation power, and exposure time in the investigated ranges of these quantities. The LIR effect is practically athermal for very weakly neutralized acceptor species (e.g., Mg), but it is thermally assisted for Zn, Si, and Ge acceptors which form more stable complexes with hydrogen. From these results it is inferred, that the LIR of acceptors is electronically stimulated, possibly via a recombination-enhanced vibrational excitation of the acceptor-hydrogen complexes. A kinetic model of the LIR process, which accounts for the experimental results by assuming a reverse reaction of electronically stimulated relaxation of hydrogen toward an acceptor (light-induced passivation), is proposed.

I. INTRODUCTION

We have recently reported that certain shallow substitutional acceptors in high-purity *p*-type hydrogenated GaAs undergo a reversible and, essentially, athermal light-induced reactivation (LIR) at cryogenic temperatures.[1] The LIR process is strongly dependent on the chemical identity of the hydrogen-passivated acceptor species. An inverse correlation has been observed between the susceptibility to LIR and the binding energies of the different acceptor-hydrogen complexes (A-H) in GaAs.[2,3] The occurrence of LIR implies thermodynamic metastability of the hydrogenated GaAs (GaAs:H). Recently, Tavendale *et al.*[4] have confirmed instability of acceptor passivation in *p*-type GaAs:H under minority-carrier injection by illumination with above-band-gap light at room temperature. Since passivation of impurities and other defects via hydrogenation is considered a promising processing technique in fabrication of semiconductor devices,[5] an understanding of the LIR effect is important for the prediction of the long-term stability of devices based on this technology. Furthermore, the apparent similarity of the LIR phenomenon in GaAs to light-induced degradation in hydrogenated amorphous silicon (known as the Staebler-Wronski effect)[6] suggests that the understanding of the former process may assist in the ongoing effort to establish the mechanism of the latter, which takes place in the more complex amorphous material system. In this context the possibility of investigating hydrogen-related processes in GaAs under distinctly decoupled conditions of either pure electronic or optical stimulation, such as LIR at cryogenic temperatures, or pure thermal excitation [e.g., acceptor reactivation during high-temperature anneals at $T > 300$ °C (Refs. 7–9)], is particularly interesting.

In the present paper results of a systematic experimental investigation of the LIR mechanism are presented. The LIR effect was monitored as a function of photon energy and power density of the excitation light, as well as the sample temperature and the chemical identity of acceptor impurities using low-temperature photoluminescence (PL). The dependence of the rate and extent of LIR on these experimental parameters confirms our previous tentative proposal[1] that the effect is electronically stimulated, possibly via the recombination-enhanced defect reaction (REDR) mechanism.[10,11] An important aspect of LIR at $T=1.7$ K is the fact that for large enough values of the product of the light intensity and the illumination time the reactivation process saturates at a level which is independent of the photon energy and light intensity, and is significantly lower than a complete recovery of the original acceptor concentration in the as-grown crystal. We discuss possible mechanisms that can cause the saturation effect and suggest that it is due to chemical equilibrium between LIR and the reverse process of light-induced passivation (LIP) of acceptors by hydrogen. A kinetic model, which agrees quantitatively with the experimental data and which supports the equilibrium concept, is presented.

Minority carrier transport in carbon doped gallium arsenide

C. M. Colomb, S. A. Stockman, S. Varadarajan, and G. E. Stillman
Center for Compound Semiconductor Microelectronics, University of Illinois at Urbana-Champaign, Illinois 61801

(Received 26 August 1991; accepted for publication 28 October 1991)

Minority carrier electron mobilities and diffusion lengths in *p*-type C-doped GaAs have been measured at room temperature and 77 K using the zero field time of flight (ZFTOF) technique on p^+–n structures with p^+ carrier concentrations of 1.1×10^{19}, 6.0×10^{18}, 1.8×10^{18} cm^{-3}, which were grown by low-pressure metalorganic chemical vapor deposition (MOCVD) using CCl_4 as the dopant. The electron mobilities obtained are higher than those reported for Be-doped MBE GaAs but lower than those reported for Ge-doped, LPE GaAs, while the diffusion lengths are similar to those found in similar concentration Be-doped samples.

Minority carrier transport in heavily doped *p*-type GaAs is important for both electrical and optical devices. Recently, there has been considerable interest in carbon as a dopant for these applications because of its low diffusivity and high solubility. In this letter, we report the first results from zero field time of flight (ZFTOF) measurement of minority carrier electron mobilities and diffusion lengths in *p*-type C-doped GaAs at 300 and 77 K. The structures used for this measurement simulate the base transport in *npn* heterojunction bipolar transistors (HBT). The ZFTOF technique[1-3] consists of measuring the transient photovoltage, which occurs when electrons which are generated optically near the surface of a p^+–n diode diffuse to the edge of the depletion region and are collected. ZFTOF has previously been used to study Be-doped structures at room temperature at much lower doping densities than considered in this paper by Ahrenkiel *et al.*,[2] and by Lovejoy *et al.*,[3] at comparable doping levels.

The structures, p^+–n GaAs diodes, studied had a thin p^- AlGaAs cap layer at the surface to reduce the surface recombination velocity (SRV). Three p^+–n structures with p^+ carrier concentrations of 1.1×10^{19}, 6×10^{18}, and 1.8×10^{18} cm^{-3} were grown in an Emcore low-pressure metalorganic chemical vapor deposition (MOCVD) GS3000 reactor, using a gaseous mixture of 1500 ppm CCl_4 in high-purity hydrogen gas as the *p*-type dopant source. High hole concentrations can readily be obtained using CCl_4 which also allows controlled doping at lower levels under a variety of growth conditions.[4] The p^- layer thicknesses for these three structures measured here were 1.0, 1.85, and 1.9 μm, respectively. Due to the short minority carrier lifetime in heavily doped material, the sample must be thin enough so that photon recycling[5] does not influence the results. The doping levels and thicknesses were verified by Hall effect and scanning electron microscopy (SEM) measurements, respectively.

Mesa diodes, 450 μm in diameter, were fabricated with Au–Zn, *p*-type contacts and Au-Sn *n*-type contacts. The devices were then cleaved and mounted on a high-speed test fixture consisting of Wiltron *K* connectors and a 50 Ω coplanar microstrip line designed to minimize package parasitics.

Figure 1 is a diagram of the experimental arrangement. A Spectra-Physics Tsunami mode-locked, titanium-doped, sapphire laser system is used to generate the carriers, with a 1.6 ps pulse. The laser is tunable from 720 to 840 nm. A Tektronix 11801 sampling oscilloscope, with an SD26, 18 ps, sampling head is used to measure the transient voltage pulse and also calculate its time derivative, which is proportional to the transient photocurrent. To extract the lifetime and diffusion coefficient from the data, an analytical solution to the minority carrier diffusion equation is found, and the voltage and the time derivative of the voltage are calculated using the short circuit photocurrent and an equivalent circuit model. The calculated curves are then fit to the experimental data by adjusting the carrier lifetime and diffusion coefficient.

To model the transient photovoltage generated by the light pulse, an equivalent circuit is used which includes the photocurrent source, the device depletion capacitance, the inductance of the lead wires, and the 50 Ω load of the sampling oscilloscope. The circuit is shown in the inset of Fig. 1. If all of the light is absorbed in the undepleted p^+ layer, the photogenerated current is a diffusion current and is given by

$$i(t)=qD_n\left.\frac{\partial n(x,t)}{\partial x}\right|_{x=d}, \tag{1}$$

where $n(x,t)$ is the time dependent spatial variation of the excess carrier concentration and d is the boundary between the p^+ region and the n region. The small extension of the depletion region into the p^- layer is ignored. The excess carrier concentration is given by the solution to the conti-

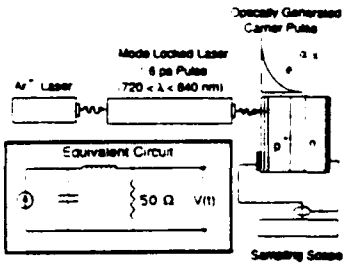

FIG. 1. Schematic of the experimental setup for ZFTOF measurements. The inset shows the equivalent circuit used to calculate voltage transient.

 0003-6951/92/010065-03$03.00

PUBLICATIONS

N. Holonyak, Jr.

Stability of AlAs in $Al_xGa_{1-x}As$-AlAs-GaAs quantum well heterostructures

J. M. Dallesasse, P. Gavrilovic,[a] N. Holonyak, Jr., R. W. Kaliski,[b] D. W. Nam,[c] and E. J. Vesely[d]

Electrical Engineering Research Laboratory, Center for Compound Semiconductor Microelectronics, and Materials Research Laboratory, University of Illinois at Urbana–Champaign, Urbana, Illinois 61801

R. D. Burnham

Amoco Technology Company, Amoco Research Center, Naperville, Illinois 60566

(Received 12 January 1990; accepted for publication 3 April 1990)

Data are presented on the long-term ($\gtrsim 8$ yr) degradation of $Al_xGa_{1-x}As$-AlAs-GaAs quantum well heterostructure material because of the instability of underlying (internal) AlAs layers. Material containing thicker ($>0.4\ \mu m$) AlAs "buried" layers (confining layers) is found to be much less stable than material containing thinner (≤ 200 Å) AlAs layers. Hydrolysis of the AlAs layers because of cleaved edges and pinholes in the cap layers leads to the deterioration.

Since the introduction of AlAs barrier layers in $Al_xGa_{1-x}As$-GaAs quantum well heterostructures (QWHs) to suppress the effects of alloy clustering,[1] the use of AlAs layers in QWHs has become quite common in lasers and other devices. It is of interest that almost from the beginning of extensive study of III-V compounds the binary Al-bearing III-V's have been listed as unstable.[2] In early work on high-performance $Al_xGa_{1-x}As$-GaAs solar cells, AlAs layers employed as window layers have been found to be unstable when exposed to air.[3,4] In order to circumvent this problem, AlAs layers have either been passivated using anodization,[3] or have been replaced by high-composition ($x \sim 0.8$) $Al_xGa_{1-x}As$ layers.[4] In QWHs they are, of course, "buried" in the layered structure. As is well known[2] the instability of AlAs is due to the extremely reactive nature of the Al, particularly in a moist environment. Because of this behavior, an important consideration for the reliable operation of QWH lasers, as well as other QWH devices, is the stability of the AlAs layers if they are employed in the QWH. In this letter data are presented on the degradation of AlAs in $Al_xGa_{1-x}As$-AlAs-GaAs QWHs and superlattices (SLs). Thicker ($>0.4\ \mu m$) AlAs layers that are exposed to the environment through "pinholes" in encapsulating layers or at cleaved edges are found to decompose, resulting in a slow destruction of the QWH material. Thinner AlAs layers (~ 200 Å) contained within a SL structure are found to have increased stability.

The crystals used in this experiment are grown by metalorganic chemical vapor deposition (MOCVD) on (100) *n*-type GaAs substrates.[5] In Fig. 1(b) a scanning electron microscope (SEM) photomicrograph of the cross section of the primary QWH material used in this experiment is shown. Growth begins with a thick *n*-type GaAs buffer layer and then an $Al_{0.7}Ga_{0.3}As$ layer ($\sim 0.8\ \mu m$). This is followed by a ~ 0.4-μm-thick *n*-type AlAs lower confining layer. Next is the symmetrical active region of the QWH which consists of a ~ 150 Å GaAs quantum well (QW) between two ~ 600 Å $Al_{0.3}Ga_{0.7}As$ waveguide (WG) layers. Then a thick ($\sim 0.5\ \mu m$) AlAs *p*-type upper confining layer is grown, followed by the growth of a $\sim 0.4\ \mu m$ *p*-type $Al_{0.7}Ga_{0.3}As$ layer. The entire structure is capped by a heavily doped *p*-type GaAs cap layer ($\sim 0.6\ \mu m$). The 40-period comparison SL sample is grown similarly by MOCVD but with 150 Å AlAs barriers and 45 Å GaAs wells.

The *p-n* QWH crystal of main issue here dates back to April, 1982. At the time of its growth unmounted probe tested laser diodes exhibited (300 K) pulsed threshold current densities of 3000 A/cm^2. This indicates fair quality crystal. The as-grown crystal was observed (by optical microscopy) to be free of any obvious defects. The wafer was then maintained under normal room environmental conditions. With the passage of time, atmospheric water vapor reacts with the buried AlAs layers, possibly forming Al_2O_3, $Al_2O_3 \cdot H_2O$, $Al_2O_3 \cdot 3H_2O$, $AlAs \cdot 8H_2O$, AlO(OH), or $Al(OH)_3$. This occurs via crystal edges and pinholes in the GaAs-$Al_xGa_{1-x}As$ encapsulating layers, thus leading to slow decomposition of the QWH material. Two examples of the destructive reactions that can occur are

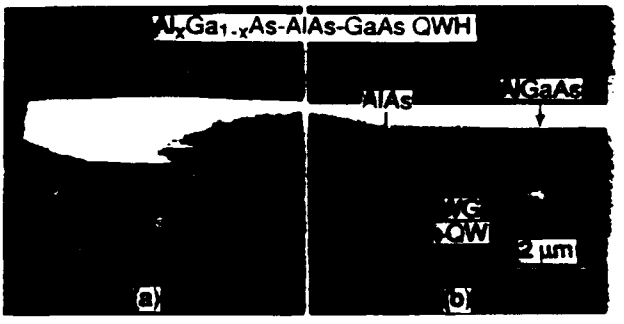

FIG. 1. Scanning electron microscope (SEM) photomicrograph of the cross section of an $Al_xGa_{1-x}As$-AlAs-GaAs QWH grown in 1982 that, because of thick ($\sim 0.4\ \mu m$) "buried" AlAs confining layers and cleaved edges and pinholes, hydrolyzes and deteriorates. The arrow in (a) marks the boundary between hydrolyzed AlAs and AlAs that is unreacted. Panel (b) shows the layer structure of the as-grown QWH material in an area unaffected by the hydrolysis.

[a] Now at Polaroid. Polaroid Corp., 21 Osborn St., Cambridge, MA 02139.

[b] Now at Amoco. Amoco Research Center, Naperville, Illinois 60566.

[c] Kodak Doctoral Fellow.

[d] National Science Foundation Doctoral Fellow.

 0003-6951/90/242436-03$02.00

Environmental degradation of $Al_xGa_{1-x}As$-GaAs quantum-well heterostructures

J. M. Dallesasse, N. El-Zein, N. Holonyak, Jr., and K. C. Hsieh
Electrical Engineering Research Laboratory, Center for Compound Semiconductor Microelectronics, and Materials Research Laboratory, University of Illinois at Urbana-Champaign, Urbana, Illinois 61801

R. D. Burnham
Amoco Research and Development, Naperville, Illinois 60566

R. D. Dupuis
University of Texas at Austin, Austin, Texas 78712

(Received 5 April 1990; accepted for publication 14 May 1990)

Data describing the deterioration of $Al_xGa_{1-x}As$-GaAs heterostructures in long-term exposure (2–12 years) to normal room environmental conditions ($\sim$20–25 °C, varying humidity) are presented. Optical microscopy, scanning electron microscopy, transmission electron microscopy, and electron dispersion x-ray spectroscopy are used to examine $Al_xGa_{1-x}As$-GaAs quantum-well heterostructure material that has hydrolyzed at cleaved edges, cracks, and fissures, and at pinholes in cap layers. The hydrolysis is found to be significant for thicker ($>0.1\ \mu m$) $Al_xGa_{1-x}As$ layers of higher composition ($x>0.85$).

I. INTRODUCTION

An important question in the long-term stability, and thus reliability, of $Al_xGa_{1-x}As$-GaAs quantum-well heterostructure (QWH) devices is that of the material stability when exposed to normal environmental conditions. This is especially true for double-heterostructure and QWH lasers, where cleaved facets are generally used to define the optical cavities and high-composition $Al_xGa_{1-x}As$ confining layers are often used to provide optical and charge confinement.[1] Because of the extreme reactivity of Al and its tendency to form various oxygen-rich compounds [Al_2O_3, $Al_2O_3{\cdot}H_2O$, $Al_2O_3{\cdot}3H_2O$, $AlAsO_4{\cdot}8H_2O$, AlO(OH), $Al(OH)_3$], $Al_xGa_{1-x}As$ layers are expected to become more unstable with increasing Al content. This is confirmed by early work on $Al_xGa_{1-x}As$-GaAs solar cells where AlAs layers used as low absorption windows decomposed over time when exposed to room air.[2,3] More recently thick ($>0.4\ \mu m$) AlAs buried layers in $Al_xGa_{1-x}As$-AlAs-GaAs QWHs have been found to cause decomposition of the QWH material.[4]

In the present work a more complete account is given of the degradation that occurs in $Al_xGa_{1-x}As$-GaAs QWHs with high-composition ($x\gtrsim0.85$) $Al_xGa_{1-x}As$ confining layers. Optical microscopy is used first to identify QWH crystals that have, as described by a colleague,[5] "rusted" (deteriorated and discolored because of hydrolization). Then, scanning electron microscopy is used to examine the crystal surfaces and cleaved edges of representative samples. This shows the extent of the degradation, and reveals the layers that are involved in the deterioration process. Next, transmission electron microscopy (TEM) is employed to study the interface between the region of hydrolyzed and intact crystal. Finally, electron dispersion x-ray spectroscopy (EDS) is used to probe these regions to give insight into the deterioration mechanism.

II. DEGRADATION OF $Al_xGa_{1-x}As$ QWH MATERIAL

A. Experimental procedure

The crystals studied in the present work have been grown by metalorganic chemical vapor deposition (MOCVD) on (100) *n*-type GaAs substrates. The first sample of interest dates back to 1978. As usual, for the QWH crystal growth the various sources are trimethylgallium (TMGa), trimethylaluminum (TMAl), and arsine (AsH_3).[6] Typically the crystal growth begins with a GaAs buffer layer $\sim$1.0 μm thick. Next, a $\sim$1.0-μm-thick $Al_xGa_{1-x}As$ ($x\gtrsim0.9$) lower confining layer is grown. The active region of one of the QWHs of interest here consists of four GaAs wells ($L_z\sim50$ Å) separated by three $Al_xGa_{1-x}As$ ($x\gtrsim0.5$) barriers ($L_B\sim50$ Å). The wafer is capped by a $\sim$3000-Å-thick $Al_xGa_{1-x}As$ ($x\gtrsim0.9$) layer. All of the layers are undoped. For this particular sample the exact composition of the Al-containing layers is not known because of a minor difficulty (at the time of the crystal growth, 1978) with the calibration of the Al mass-flow controller. At the time of the QWH growth x-ray diffraction measurements were not performed to determine exact Al compositions. Despite this difficulty, the sample was found (1978) to be of excellent quality as determined by its capability to operate as a photopumped continuous 300-K laser (e.g., see Ref. 7).

The second crystal of concern here dates back to 1982. The sources for the Al, Ga, and As are once again TMAl, TMGa, and AsH_3. The donor and acceptor dopants, Se, Si, and Zn, are provided by H_2Se, SiH_4, and diethylzinc (DEZn). The crystal growth begins with a thick *n*-type GaAs buffer layer and then an $Al_{0.7}Ga_{0.3}As$ layer ($\sim$0.75 μm). This is followed by a thick ($\sim$0.4 μm) AlAs lower-confining layer and then the symmetrical active region of the QWH, which consists of a $\sim$150-Å GaAs quantum well

 0021-8979/90/172235-04$03.00

Hydrogenation of Si- and Be-doped InGaP

J. M. Dallesasse, I. Szafranek, J. N. Baillargeon, N. El-Zein, N. Holonyak, Jr., G. E. Stillman, and K. Y. Cheng
Electrical Engineering Research Laboratory, Center for Compound Semiconductor Microelectronics and Materials Research Laboratory, University of Illinois at Urbana-Champaign, Urbana, Illinois 61801

(Received 20 June 1990; accepted for publication 13 August 1990)

Data are presented on the hydrogenation of Be-doped (p-type) and Si-doped (n-type) $In_{1-x}Ga_xP$ epitaxial layers grown lattice matched to GaAs ($x \sim 0.5$). Low-temperature (1.7 K) photoluminescence, electrochemical carrier concentration profiling, and scanning electron microscopy are used to study the effects of hydrogenation on carrier recombination, carrier concentration, and surface morphology. Hydrogenation is found to passivate Si donors and Be acceptors and to improve photoluminescence efficiency, but causes mild surface damage. The carrier concentration following hydrogenation is found to be lowest in acceptor-doped material.

I. INTRODUCTION

Since the discovery that exposure of Ge to a hydrogen plasma alters the electronic properties of the surface,[1] it has been known that semiconductors more generally can be modified by exposure to atomic hydrogen. The study of semiconductors exposed to hydrogen plasmas received renewed interest when hydrogenation of amorphous and crystalline Si was found to result in improvement in the photoluminescence properties,[2] passivation of grain boundaries,[3] and reduction of carrier concentration.[4] More recently the exposure of compound semiconductors to hydrogen plasmas has received extensive study. In the $Al_xGa_{1-x}As$ system hydrogenation has been found to improve photoluminescence efficiency[5] and to provide some passivation of donors[6] and acceptors[7] to the depth hydrogen diffuses during the hydrogenation process. The fact that this effect is maskable has been utilized to fabricate single-stripe and high-power multistripe lasers in the $Al_xGa_{1-x}As$-GaAs[8,9] and $Al_yGa_{1-y}As$-GaAs-$In_xGa_{1-x}As$[10] systems.

An important III-V system for the construction of visible-spectrum lasers and light-emitting diodes is the quaternary $In_y(Al_xGa_{1-x})_{1-y}P$.[11-13] This system, a modification of the high-gap ternary $In_yGa_{1-y}P$,[14] has received renewed interest because of the advent of advanced growth techniques such as metalorganic chemical vapor deposition (MOCVD)[15] and gas-source molecular-beam epitaxy (GSMBE).[16] Room-temperature continuous-wave (cw) diode lasers at wavelengths as short as 6395 Å [17-19] and photopumped lasers at wavelengths as short as 6250 Å[20,21] have been produced in this system. Improvements in material quality and device structure should result in shorter wavelengths and better device performance. Examination of hydrogenation in this system is thus of some interest, because the improved current confinement and lower thermal impedance[8,9] of hydrogenated stripe-geometry lasers have the potential to yield devices with improved performance characteristics.[22]

In this paper hydrogenation of $In_{1-x}Ga_xP$ grown lattice matched to GaAs ($y \sim 0.5$) is examined via low-temperature photoluminescence, electrochemical carrier concentration profiling, and scanning electron microscopy. Hydrogen plasma exposure is found to increase the photoluminescence efficiency and to passivate dopants and impurities to the depth of the hydrogen diffusion. $In_{1-x}Ga_xP$ crystals that are doped p type are found to be compensated to a greater extent than crystals that are doped n type.

II. EXPERIMENTAL PROCEDURE

The $In_{1-x}Ga_xP$ crystals employed in these experiments are grown by gas-source MBE on (100) GaAs substrates. Gases for the Column V constituents (AsH_3 and PH_3) are handled using an Emcore GS3000 system. The Column III constituents In and Ga, as well as the p- and n-type dopants Be and Si, are provided by standard MBE effusion cells. Substrates are prepared for crystal growth by degreasing in trichloroethylene, followed by acetone, methanol, and deionized water rinses. Final sample preparation with HCl, H_2SO_4, and deionized water leaves the surface with a thin native oxide as a protective layer. The samples are grown at 500 °C with a growth rate of ~ 1.6 μm/h.

Hydrogenation of the crystals takes place in a parallel-plate reactor (Texas Instruments Model A-24-D) originally designed for plasma-enhanced chemical vapor deposition (PECVD).[9] An rf generator operating at 13.6 MHz applies power to the top electrode. The lower electrode supports the sample and serves as ground. This electrode is equipped with a heater capable of operating to 400 °C. For this work samples are hydrogenated at temperatures ranging from 150 to 300 °C, pressures ranging from 375 to 1500 mT, and rf power densities ranging from 0.125 to 0.375 W/cm^2. In order to minimize diffusion of the hydrogen within the crystal following hydrogenation, samples are thermally quenched to room temperature by removal from the process chamber within $\sim$ 45 s of extinguishing the plasma.

The effect of hydrogenation on the carrier recombination is determined by comparing low-temperature (1.7 K) photoluminescence measurements on hydrogenated and as-grown crystals. These measurements employ an Ar^+ laser operating at 5145 Å. The sample luminescence is analyzed via a 1.0-m double grating spectrometer equipped

 0021-8979/90/235866-05$02.40

Low-threshold disorder-defined buried-heterostructure $Al_xGa_{1-x}As$-GaAs quantum well lasers by open-tube rapid thermal annealing

T. A. Richard, J. S. Major, Jr.,[a] F. A. Kish,[b] and N. Holonyak, Jr.
Electrical Engineering Research Laboratory, Center for Compound Semiconductor Microelectronics, and Materials Research Laboratory, University of Illinois at Urbana–Champaign, Urbana, Illinois 61801

S. C. Smith and R. D. Burnham
Amoco Technology Company, Amoco Research Center, Naperville, Illinois 60566

(Received 1 October 1990; accepted for publication 31 October 1990)

$Al_xGa_{1-x}As$-GaAs single stripe quantum well heterostructure (QWH) lasers fabricated via Si impurity-induced layer disordering (IILD) in an As-free open tube rapid thermal annealing furnace are reported. The Si IILD, with good surface morphology, is obtained using a Si/Si_3N_4 source layer with the QWH wafer in face-to-face contact with a GaAs substrate during the anneal (13 min, 1000 °C). Continuous wave (cw) 300 K operation of the lasers with uncoated facets has produced output powers as high as 25 mW/facet with threshold currents as low as 7 mA. The devices operate single mode at a wavelength of 812 nm and have high differential quantum efficiencies of ~44%, with some as high as 57%.

The observation that the heterobarriers of an AlAs-GaAs superlattice are unstable against Zn diffusion[1] led directly to the discovery of impurity-induced layer disordering (IILD),[2] which now is a relatively large area of study. It was realized immediately that IILD could be employed to selectively shift the quantum well gap of, say, an $Al_xGa_{1-x}As$-GaAs quantum well heterostructure (QWH) to a higher bulk-crystal energy gap and thus to a lower index of refraction.[3] This makes possible, via a planar diffusion technology (IILD), simultaneous carrier and optical confinement in a QWH. For example, these properties of IILD have made possible planar fabrication of various forms of sophisticated QWH lasers.[2,4] Continuing improvements in layer disordering techniques (IILD) have led to low-threshold stripe-geometry buried-heterostructure quantum well lasers in the $Al_xGa_{1-x}As$-GaAs,[5] $Al_xGa_{1-x}As$-GaAs-$In_yGa_{1-y}As$,[6] and $In_{0.5}(Al_xGa_{1-x})_{0.5}P$-InGaP[7] systems. In general, the fabrication of these and other layer-disordered devices relies on closed tube thermal annealing of the QWH crystal for times and temperatures much lower than those required for ordinary thermal interdiffusion of the heterolayers. These techniques require relatively long annealing times and limit the throughput of devices. An open tube rapid thermal annealing (RTA) process is desirable in that it requires much shorter diffusion times and provides for increased throughput and potential safety because of the absence of free As. In this letter we demonstrate low threshold operation of $Al_xGa_{1-x}As$-GaAs QW heterostructure lasers fabricated in an open tube RTA furnace with a flowing H_2/N_2 ambient.

The QWH crystal used for this device has been grown by metalorganic chemical vapor deposition (MOCVD)[8] in an Emcore reactor. All layers are grown at 870 °C except the GaAs cap which is grown at 800 °C. The dopants for the epitaxial layers are Se (n type) or Mg (p type). The QWH layers are grown as follows: (1) a 0.5 μm n-type GaAs buffer layer, (2) a 1.0 μm n-type $Al_{0.23}Ga_{0.77}As$ buffer layer, (3) a 1.1 μm n-type $Al_{0.55}Ga_{0.45}As$ lower confining layer, (4) a 0.2 μm undoped $Al_{0.23}Ga_{0.77}As$ waveguide layer with a single 200 Å $Al_{0.08}Ga_{0.92}As$ QW at its center, (5) a 0.9 μm p-type $Al_{0.57}Ga_{0.43}As$ upper confining layer, and finally (6) an 800 Å p-type GaAs cap (contact layer).

The first step in fabrication of the laser diodes is to pattern 6-μm-wide photoresist stripes on the QWH crystal. These stripes are then used as a mask in the selective removal of the GaAs cap with a $H_2SO_4:H_2O_2:H_2O$ (1:8:80) etch. A 200 Å Si layer is electron beam evaporated onto the exposed high-gap $Al_{0.57}Ga_{0.43}As$ upper confining layer, which is then followed by a lift-off procedure to rid the GaAs-contact stripe regions of the Si and photoresist. Next, the entire crystal is capped by the chemical vapor deposition (CVD) of ~1000 Å of Si_3N_4. The sample is annealed for 13 min at 1000 °C in an open tube RTA furnace with a flowing H_2/N_2 (~1:1) ambient to induce IILD. During the anneal, the sample is in face-to-face contact with a clean GaAs substrate wafer to reduce the evaporation of As from the QWH crystal surface.[9]

After the RTA cycle, the encapsulants are removed and a 45 min broad-area Zn diffusion at 540 °C is performed in order to improve the contact to the p-type stripes. Then 6 μm photoresist stripes are again patterned on the crystal aligned with the QW laser stripes, and are used as a mask for a 150 keV H_2^+ proton isolation (5×10^{14} cm^{-2} dose) to minimize edge leakage current near the crystal surface. The photoresist is removed and the crystal is lapped and polished from the substrate side to a thickness of ~125 μm. The sample is metallized with Ti-Pt-Au as the p contact and with Ge-Au-Ni-Au as the n contact. Finally, the crystal is cleaved into dies that are then mounted with In onto copper heat sinks for testing.

The high-temperature RTA cycle induces Si-IILD

[a] Now at Spectra Diode Labs, San Jose, CA 95134.
[b] AT&T Doctoral Fellow.

 0003-6951/90/532904-03$02.00

Environmental degradation of $Al_xGa_{1-x}As$-GaAs quantum-well heterostructures

J. M. Dallesasse, N. El-Zein, N. Holonyak, Jr., and K. C. Hsieh
Electrical Engineering Research Laboratory, Center for Compound Semiconductor Microelectronics, and Materials Research Laboratory, University of Illinois at Urbana-Champaign, Urbana, Illinois 61801

R. D. Burnham
Amoco Research and Development, Naperville, Illinois 60566

R. D. Dupuis
University of Texas at Austin, Austin, Texas 78712

(Received 5 April 1990; accepted for publication 14 May 1990)

Data describing the deterioration of $Al_xGa_{1-x}As$-GaAs heterostructures in long-term exposure (2–12 years) to normal room environmental conditions ($\sim$20–25 °C, varying humidity) are presented. Optical microscopy, scanning electron microscopy, transmission electron microscopy, and electron dispersion x-ray spectroscopy are used to examine $Al_xGa_{1-x}As$-GaAs quantum-well heterostructure material that has hydrolyzed at cleaved edges, cracks, and fissures, and at pinholes in cap layers. The hydrolysis is found to be significant for thicker ($>0.1\ \mu m$) $Al_xGa_{1-x}As$ layers of higher composition ($x>0.85$).

I. INTRODUCTION

An important question in the long-term stability, and thus reliability, of $Al_xGa_{1-x}As$-GaAs quantum-well heterostructure (QWH) devices is that of the material stability when exposed to normal environmental conditions. This is especially true for double-heterostructure and QWH lasers, where cleaved facets are generally used to define the optical cavities and high-composition $Al_xGa_{1-x}As$ confining layers are often used to provide optical and charge confinement.[1] Because of the extreme reactivity of Al and its tendency to form various oxygen-rich compounds [Al_2O_3, $Al_2O_3{\cdot}H_2O$, $Al_2O_3{\cdot}3H_2O$, $AlAsO_4{\cdot}8H_2O$, AlO(OH), $Al(OH)_3$], $Al_xGa_{1-x}As$ layers are expected to become more unstable with increasing Al content. This is confirmed by early work on $Al_xGa_{1-x}As$-GaAs solar cells where AlAs layers used as low absorption windows decomposed over time when exposed to room air.[2,3] More recently thick ($>0.4\ \mu m$) AlAs buried layers in $Al_xGa_{1-x}As$-AlAs-GaAs QWHs have been found to cause decomposition of the QWH material.[4]

In the present work a more complete account is given of the degradation that occurs in $Al_xGa_{1-x}As$-GaAs QWHs with high-composition ($x\gtrsim0.85$) $Al_xGa_{1-x}As$ confining layers. Optical microscopy is used first to identify QWH crystals that have, as described by a colleague,[5] "rusted" (deteriorated and discolored because of hydrolization). Then, scanning electron microscopy is used to examine the crystal surfaces and cleaved edges of representative samples. This shows the extent of the degradation, and reveals the layers that are involved in the deterioration process. Next, transmission electron microscopy (TEM) is employed to study the interface between the region of hydrolyzed and intact crystal. Finally, electron dispersion x-ray spectroscopy (EDS) is used to probe these regions to give insight into the deterioration mechanism.

II. DEGRADATION OF $Al_xGa_{1-x}As$ QWH MATERIAL

A. Experimental procedure

The crystals studied in the present work have been grown by metalorganic chemical vapor deposition (MOCVD) on (100) *n*-type GaAs substrates. The first sample of interest dates back to 1978. As usual, for the QWH crystal growth the various sources are trimethylgallium (TMGa), trimethylaluminum (TMA1), and arsine (AsH_3).[6] Typically the crystal growth beings with a GaAs buffer layer $\sim1.0\ \mu m$ thick. Next, a ~1.0-μm-thick $Al_xGa_{1-x}As$ ($x\geq0.9$) lower confining layer is grown. The active region of one of the QWHs of interest here consists of four GaAs wells ($L_z\sim50$ Å) separated by three $Al_xGa_{1-x}As$ ($x\geq0.5$) barriers ($L_B\geq50$ Å). The wafer is capped by a $\sim$3000-Å-thick $Al_xGa_{1-x}As$ ($x\geq0.9$) layer. All of the layers are undoped. For this particular sample the exact composition of the Al-containing layers is not known because of a minor difficulty (at the time of the crystal growth, 1978) with the calibration of the Al mass-flow controller. At the time of the QWH growth x-ray diffraction measurements were not performed to determine exact Al compositions. Despite this difficulty, the sample was found (1978) to be of excellent quality as determined by its capability to operate as a photopumped continuous 300-K laser (e.g., see Ref. 7).

The second crystal of concern here dates back to 1982. The sources for the Al, Ga, and As are once again TMA1, TMGa, and AsH_3. The donor and acceptor dopants, Se, Si, and Zn, are provided by H_2Se, SiH_4, and diethylzinc (DEZn). The crystal growth begins with a thick *n*-type GaAs buffer layer and then an $Al_{0.75}Ga_{0.25}As$ layer ($\sim0.75\ \mu m$). This is followed by a thick ($\sim0.4\ \mu m$) AlAs lower-confining layer and then the symmetrical active region of the QWH, which consists of a $\sim$150-Å GaAs quantum well

 0021-8979/90/172235-04$03.00

Hydrolyzation oxidation of $Al_xGa_{1-x}As$-AlAs-GaAs quantum well heterostructures and superlattices

J. M. Dallesasse, N. Holonyak, Jr., A. R. Sugg, T. A. Richard, and N. El-Zein

Electrical Engineering Research Laboratory, Center for Compound Semiconductor Microelectronics, and Materials Research Laboratory, University of Illinois at Urbana–Champaign, Urbana, Illinois 61801

(Received 3 October 1990; accepted for publication 23 October 1990)

Data are presented on the conversion (selective conversion) of high-composition $(AlAs)_x(GaAs)_{1-x}$ layers, e.g., in $Al_xGa_{1-x}As$-AlAs-GaAs quantum well heterostructures and superlattices (SLs), into dense transparent native oxide by reaction with H_2O vapor (N_2 carrier gas) at elevated temperatures (400 °C). Hydrolyzation oxidation of a fine-scale AlAs(L_B)-GaAs(L_z) SL ($L_B - L_z \lesssim 100$ Å), or random alloy $Al_xGa_{1-x}As$ ($x \gtrsim 0.7$), is observed to proceed more slowly and uniformly than a coarse-scale "alloy" such as an AlAs-GaAs superlattice with $L_B - L_z \gtrsim 200$ Å.

Ordinarily the $Al_xGa_{1-x}As$-AlAs-GaAs heterosystem, and its various quantum well heterostructure (QWH) and superlattice (SL) extensions, is viewed as stable against atmospheric deterioration, e.g., hydrolyzation. Recently we have shown that this is not necessarily correct[1,2] and, depending upon $Al_xGa_{1-x}As$ composition ($x \gtrsim 0.7$) and layer thickness ($\gtrsim 0.1$ μm), atmospheric hydrolyzation of $Al_xGa_{1-x}As$-AlAs-GaAs QWHs over long time periods (2–10 yr) can be severe. It is, of course, a nuisance to wait, say, ten years, or even one year, to observe this process. For study purposes obviously we wish to accelerate it. A likely way to attempt this is to raise the QWH crystal temperature and pass water vapor over it, the classic method (after Frosch, 1955) to oxidize and mask Si[3] but thus far not recognized as particularly useful for III-V semiconductors. In this letter we show that instead of destructive hydrolyzation, this procedure results in the formation of smooth dense natural oxides on $(AlAs)_x(GaAs)_{1-x}$. A fine scale uniform alloy, $Al_xGa_{1-x}As$, oxidizes more slowly, and a coarser "alloy", for example, as represented by a superlattice (SL), oxidizes "faster" and more completely. In this letter we show that we can render (selectively) a red gap ($E_z \sim 1.6$ eV) AlAs-GaAs SL into yellow-gap (2.1 eV) $Al_xGa_{1-x}As$ ($x \sim 0.8$) by impurity-induced layer disordering (IILD),[4] and then change the remaining red-gap SL, where desired, to transparent native oxide by hydrolyzation oxidation.

The experiments we describe here are performed on AlAs-GaAs SLs grown by metalorganic chemical vapor deposition as has been described extensively elsewhere.[5] Several (~ 1 μm thick) SLs are employed, one (SL1) with AlAs barriers of size $L_B \sim 150$ Å and GaAs wells of width $L_z \sim 45$ Å and the second (SL2) with L_B(AlAs) ~ 70 Å and L_z(GaAs) ~ 30 Å. Although SLs have a special character (size quantization), they can be regarded also as relatively "coarse" (nonstochastic) $Al_xGa_{1-x}As$ alloys, with in the present case SL1 roughly two times coarser than SL2. We can render these simply into random (or fine scale) alloys, in a patterned form, by IILD.[4,6] For both SLs of interest here with (100) surfaces this has been done by Zn diffusion from $ZnAs_2$ at 575 °C (1/2 h).[4,6] The SLs have been masked with ~ 37-μm-diam SiO_2 disks deposited by chemical vapor deposition and patterned (by standard photolithography) in a rectangular array on ~ 76 μm centers. After the Zn diffusion and removal of the masking SiO_2, as well as the crystal substrates (by the usual mechanical lapping and wet chemical etching), we obtain completely smooth yellow-gap $Al_xGa_{1-x}As$ platelets (thickness ~ 1 μm) with red-gap SL disks (37 μm diameter) distributed in a uniform array. We thus have fine scale (yellow) and "coarse" scale (red) alloy in one sample, which can then be oxidized (by "hydrolyzation") at 400 °C in a furnace supplied with a N_2 carrier gas bubbled through H_2O at a temperature of 95 °C.

Instead of the stained cracked form of destructive atmospheric hydrolyzation shown, for example, by Fig. 1 of Ref. 2, we obtain smooth samples with remarkably shiny surfaces, much shinier than before oxidation. This is the first substantial sign of the formation of a "hard" or useful form of oxide on the samples. A cleaved section of SL1 after heating (400 °C) for 3 h is shown in Fig. 1. The top cleaved edge cutting through the 37-μm-diam SL disks has been arranged to expose the edge of the SL samples (disks) to the heat treatment and oxidation process. The bottom row of disks is exposed to the $N_2 - H_2O$ vapor only via the surface (front and back). As Fig. 1 shows, 24 μm of each of the upper row of SL disks has converted (edgewise) to oxide, while only some slight delineation or attack is evident on the periphery of the bottom row of disks and, of course, some surface oxide is present. In other words, the upper row of disks is solid and almost totally clear across each disk, while the surrounding IILD $Al_xGa_{1-x}As$ ($x \sim 0.8$) remains yellow in appearance and the bottom row of discs red (SL1 with oxide surface).

By reducing the time of the oxidation process to 1 h, we reduce the edge oxide conversion of a SL1 disk to ~ 3 μm as shown in Fig. 2. A more striking case is shown in Fig. 3 where we have exposed SL2 ($L_B - L_z \sim 100$ Å) to 400 °C heating in a $N_2 - H_2O$ vapor for 4 h, significantly longer than the case of Fig. 1. Edge oxidation of a SL2 disk penetrates only 2–3 μm in spite of the lengthy oxidation. The surrounding yellow-gap $Al_xGa_{1-x}As$ ($x \sim 0.7$) IILD alloy obviously oxidizes also, but not nearly as extensively, in fact, hardly noticeable at all except for the shiny surface.

 0003-6951/90/522844-03$02.00

Native oxide stabilization of AlAs-GaAs heterostructures

A. R. Sugg, N. Holonyak,Jr., J. E. Baker, F. A. Kish,[a] and J. M. Dallesasse[b]
Electrical Engineering Research Laboratory, Center for Compound Semiconductor Microelectronics, and Materials Research Laboratory, University of Illinois at Urbana–Champaign, Urbana, Illinois 61801

(Received 18 December 1990; accepted for publication 14 January 1991)

Data are presented on the stabilization of AlAs-GaAs heterostructures against atmospheric (destructive) hydrolysis using the native oxide that can be formed ($N_2 + H_2O$, 400 °C, 3 h) on the AlAs layer. The ~0.1-μm-thick native oxide formed from the AlAs layer is shown to be stable with aging (~100 days), while unoxidized samples degrade through the AlAs (0.1 μm) down into the GaAs as deep as ~1 μm. Relative to oxides formed (~25 °C) on AlAs (or $Al_xGa_{1-x}As$, $x \gtrsim 0.7$) under atmospheric conditions (hydrolysis), oxides formed (via $N_2 + H_2O$) at higher temperatures ($\gtrsim$400 °C) are much more stable and seal the underlying crystal (e.g., GaAs).

The environmental degradation (hydrolysis) of high Al composition $Al_xGa_{1-x}As$ ($x \gtrsim 0.7$) in AlGaAs-GaAs quantum well heterostructures (QWHs) can be the basis for serious reliability problems.[1,2] Recently device-quality native oxide formed on QWHs from $Al_xGa_{1-x}As$ ($x \gtrsim 0.8$) via an elevated-temperature ($\gtrsim$400 °C) water vapor process has been demonstrated[3,4] and changes the nature of this problem. In a rich water vapor ambient at higher temperatures ($\gtrsim$400 °C) more stable oxides form than those created in atmospheric conditions at room temperature.[5] In this letter we demonstrate the stabilizing nature of this native oxide on AlAs-GaAs heterostructures, which is in sharp contrast to the destructive hydrolyzation of atmospheric processes. An AlAs-GaAs heterostructure is oxidized and compared to the same structure that is allowed to hydrolyze naturally. The oxidized crystal, once sealed, is unaffected by the destructive character of atmospheric hydrolysis. In contrast, atmospheric hydrolysis (80–100 days) of AlAs-GaAs is shown to affect the AlAs layer (~0.1 μm) itself, as well as ~1 μm of the underlying GaAs.

The crystals used in this experiment are grown by metalorganic chemical vapor deposition (MOCVD) on {100} *n*-type GaAs substrates[6] in an EMCORE GS 3000 DFM reactor at 760 °C. The crystal growth pressure, V/III ratio, and growth rate are 100 Torr, 60, and ~1000 Å/min, respectively. An undoped ~0.5 μm GaAs layer is grown first, followed by a ~0.1-μm-thick nominally undoped AlAs layer. The crystal is then cleaved in two, half of which is then exposed to atmospheric conditions at room temperature. The other half is oxidized at 400 °C (3 h) in an H_2O vapor atmosphere obtained by passing N_2 carrier gas (~1.5 scfh) through an H_2O bubbler maintained at 95 °C.[3,4]

The two types of samples, (a) and (b), are then exposed to identical atmospheric conditions. Within hours unoxidized crystals begin to degrade in color to a yellowish brown, while oxidized wafers maintain a uniform blue appearance. Figure 1 shows (Nomarski image) the surface of an (a) crystal and that of a (b) crystal after, in both cases, atmospheric exposure for 100 days. Obviously the figure does not show the yellow-brown stained color of the hydrolyzed (a) sample, nor the blue color of the oxidized (b) sample. The surface of (a) is clearly "rougher" than that of (b), which agrees with the even more extreme case of Fig. 1 of Ref. 2. The oxidized surface is smoother than the hydrolyzed surface and the cleaved edge is intact, whereas the edge of the hydrolyzed sample shows sign of destructive attack (roughening).

Figure 2 is a scanning electron microscope (SEM) image of the edges of the (a) and (b) samples of Fig. 1. The sample edges are unstained cleaved cross sections that are aged 100 days. The atmospherically hydrolyzed (a) sample shows ~ 1 μm of chemical attack into the crystal (indicated by the vertical arrows), which is well beyond the ~0.1 μm AlAs top layer of the as-grown crystal. In contrast, the cross section of the oxidized (b) sample exhibits a ~0.1 μm oxide layer (shown between the vertical arrows), agreeing more or less with the initial AlAs thickness, and with no perceptible degradation. The cross section of the hydrolyzed sample appears to be nonuniformly etched. This is remarkable considering that the sample is not stained to highlight this layer.

The results of secondary-ion mass spectrometer (SIMS) analysis on (a) and (b) samples after 80 days are

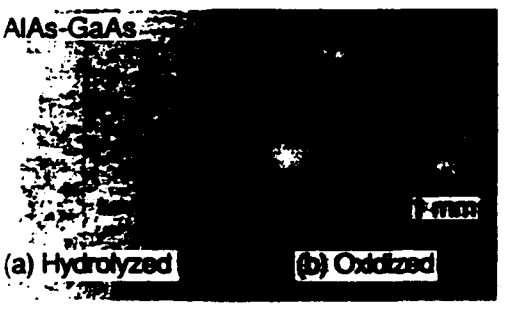

FIG. 1. Photograph (Nomarski image) after 100 days of (a) an atmospherically hydrolyzed and (b) an oxidized ($N_2 + H_2O$, 400 °C, 3 h) AlAs-GaAs heterostructure. The unoxidized sample (a) shows the characteristic roughening of atmospheric hydrolysis, while the oxidized sample (b), which is covered with a smooth "blue" oxide, is unaffected by the aging process.

[a] AT&T Doctoral Fellow.
[b] Now at Amoco Technology Company, Amoco Research Center, Naperville, IL 60566.

 0003-6951/91/111199-03$02.00

Native-oxide stripe-geometry $Al_xGa_{1-x}As$-GaAs quantum well heterostructure lasers

J. M. Dallesasse and N. Holonyak, Jr.
Electrical Engineering Research Laboratory, Center for Compound Semiconductor Microelectronics, and Materials Research Laboratory, University of Illinois at Urbana–Champaign, Urbana, Illinois 61801

(Received 11 October 1990; accepted for publication 16 November 1990)

Data are presented on the room-temperature continuous (cw) operation of native-oxide single-stripe $Al_xGa_{1-x}As$-GaAs quantum well heterostructure (QWH) lasers. The device quality native oxide is produced by the conversion of high Al composition $Al_xGa_{1-x}As$ ($x \sim 0.8$) confining layers via H_2O vapor oxidation (400 °C) in a N_2 carrier gas. The 10-μm-wide cw 300 K QWH lasers, which are fabricated by simplified processing, have excellent spectral quality and have been operated to powers in excess of 100 mW per facet.

It has long been known in Si technology that the formation of a high quality native oxide (SiO_2) is possible by exposing the crystal to H_2O vapor (steam) in a carrier gas.[1] In fact, Si integrated circuit technology is due largely to the existence of the high quality SiO_2 native oxide. One difficulty with GaAs and most other III-V compound semiconductors is that they lack a stable native oxide. This difficulty has been overcome to some degree by using other methods such as sputtering, chemical vapor deposition (CVD), and plasma-assisted chemical vapor deposition to apply non-native oxides (or other dielectrics) onto the crystal surface. Recently we have examined the stability of high composition $Al_xGa_{1-x}As$ ($x \gtrsim 0.7$) layers in $Al_xGa_{1-x}As$-GaAs quantum well heterostructures (QWHs) and have studied the slow atmospheric deterioration of the QWH material by hydrolysis.[2,3] To speed the process of $Al_xGa_{1-x}As$ ($x \gtrsim 0.7$) hydrolysis we have resorted to heating of the QWH crystal in H_2O vapor (N_2 carrier gas) and have discovered that native oxides of sufficient quality for device use can be formed on the $Al_xGa_{1-x}As$ crystal.[4] In fact, AlAs-GaAs superlattices, a "coarser" form of $(AlAs)_x(GaAs)_{1-x}$ alloy, can be transformed completely to transparent oxide.[4] In this letter the use of this native oxide in the fabrication of gain-guided oxide-stripe QWH lasers is demonstrated. These devices, which are formed by simplified processing, are found to have outstanding performance characteristics.

The epitaxial layers for these laser structures are grown on n-type (100) GaAs substrates by metalorganic chemical vapor deposition (MOCVD) as described extensively elsewhere.[5] An $Al_{0.8}Ga_{0.2}As$ lower confining layer is grown after first a GaAs buffer layer. The active region of the QWH is grown next and consists of symmetrical ~ 1000 Å $Al_{0.25}Ga_{0.75}As$ waveguide layers (undoped) on either side of a ~ 400 Å GaAs QW. Finally at the top of the QWH a p-type $Al_{0.8}Ga_{0.2}As$ confining layer is grown ~ 9000 Å thick. The entire QWH is capped by a heavily doped p-type GaAs contact layer (~ 800 Å thick).

Diodes are constructed by first depositing ~ 1000 Å of CVD SiO_2 on the crystal surface. Using standard photolithography and plasma etching, we define 10-μm-wide SiO_2 stripes on the wafer surface for masking purposes. The crystal is then etched in H_2SO_4:H_2O_2:H_2O (1:8:80) to remove the GaAs contact layer in areas not protected by the SiO_2 masking stripes. Except in the 10-μm-wide stripe regions, this exposes the high composition ($x \sim 0.8$) $Al_xGa_{1-x}As$ upper confining layer. A native oxide is formed from ~ 1500 Å of the exposed $Al_xGa_{1-x}As$ ($x \sim 0.8$) layer by heating the QWH crystal at ~ 400 °C for 3 h in a H_2O vapor atmosphere produced by passing a N_2 carrier gas (~ 1.4 scfh) through a H_2O bubbler maintained at ~ 95 °C. The oxide that is produced has a thickness of 1000–1500 Å and a uniform blue color. Following oxidation of the $Al_xGa_{1-x}As$, the SiO_2 masking layer is removed by plasma etching (CF_4 + 4% O_2). The native oxide is unaffected by plasma removal of the SiO_2 layer, which is employed merely to help in processing.

Figure 1 shows a cross section of the crystal before removal of the SiO_2 masking layer. The vertical arrows in Fig. 1(a) indicate as labeled the thickness of the SiO_2 layer (left side) and the native oxide layer (to the right). Figure 1(b) shows a cross section in which the native oxide (right side) has been removed by etching in a KOH-$K_3Fe(CN)_6$ mixture. The pair of vertical arrows [Fig. 1(b)] indicates the location of the oxide prior to removal. An important property of the oxidation process is the possibility that it is sensitive to crystal orientation. For example, where the oxide undercuts the SiO_2 masking stripe and the GaAs contact layer, a tendency exists to develop a crystallographic step on the $Al_xGa_{1-x}As$ ($x \sim 0.8$) confining layer. This is shown by the small slanted arrow in Fig. 1(b).

After the SiO_2 masking stripes are removed, the crystal is sealed in an ampoule for shallow Zn diffusion ($ZnAs_2$ source, 540 °C, 25 min) to increase the GaAs stripe contact doping. Then the crystal is metallized (Ti-Pt-Au) across the native oxide onto the exposed GaAs contact stripe. We note that the metallization adheres onto the native oxide much better than on the usual deposited dielectrics, on which frequently the metallization peels. After the p-type side metallization the crystal is thinned (100 μm) from the substrate side and is metallized on the n-type side (Ge-Au-Ni-Au). The wafer is cleaved into Fabry–Perot bars, and saw-cut stripe-contact sections are attached to Cu heat sinks with In for continuous (cw) 300 K laser operation. Similar saw-cut sections with no contact stripe regions are prepared to check the blocking behavior of the oxide. Figure 2(a) shows the I-V characteristic of a diode prepared on the QWH crystal in the GaAs contact stripe region, and

 0003-6951/91/040394-03$02.00

Native-oxide-defined coupled-stripe $Al_xGa_{1-x}As$-GaAs quantum well heterostructure lasers

J. M. Dallesasse, N. Holonyak, Jr., D. C. Hall, N. El-Zein, and A. R. Sugg
Electrical Engineering Research Laboratory, Center for Compound Semiconductor Microelectronics, and Materials Research Laboratory, University of Illinois at Urbana–Champaign, Urbana, Illinois 61801

S. C. Smith and R. D. Burnham
Amoco Technology Center, Amoco Research Center, Naperville, Illinois 60566

(Received 26 October 1990; accepted for publication 26 November 1990)

Data are presented on the continuous-wave (cw) room-temperature (300 K) operation of multiple stripe $Al_xGa_{1-x}As$-GaAs quantum well heterostructure (QWH) laser arrays defined with native oxide contact masking. Use of the native $Al_xGa_{1-x}As(x \gtrsim 0.7)$ oxide allows the fabrication of high-performance devices without depositing foreign oxide or dielectric layers (SiO_2 or Si_3N_4). Arrays of ten 5-μm-wide emitters on 7 μm centers are coupled and operate at powers as high as 300 mW per facet, or at wider stripe spacing (5 μm emitters on 10 μm centers) as high as 400 mW per facet. These data indicate that current blocking layers of native oxide, formed from $Al_xGa_{1-x}As$ with H_2O vapor in N_2 carrier gas (400 °C, 3 h), can be used in the construction of high-power multiple stripe QWH arrays with excellent performance characteristics.

We have shown recently that instead of the usual destructive atmospheric hydrolyzation of higher composition $(AlAs)_x(GaAs)_{1-x}(x \gtrsim 0.7)$,[1,2] the alloy can be converted to native oxide by higher temperature heating ($\gtrsim 400$ °C) in H_2O vapor (N_2 carrier gas).[3] This has been demonstrated on fine scale (random) alloy and simultaneously, for comparison, on coarse scale alloy as represented by a superlattice ($x \gtrsim 0.7$).[3] Moreover, the native oxide is of sufficient quality so as to be useful in device fabrication,[4] which is of special interest in the present work. One of the more notable features of the native $Al_xGa_{1-x}As$ ($x \gtrsim 0.7$) oxide is how well it can be metallized, and thus can be employed in device heat sinking. Also, via ordinary photolithographic processes, the natural oxide permits delineation of device geometries without the need to deposit foreign and thus potentially mismatched dielectric materials (e.g., SiO_2 or Si_3N_4). We show in the present work these features of the natural $Al_xGa_{1-x}As$ ($x \gtrsim 0.7$) oxide by constructing, with simplified processing, high-performance ten-stripe $Al_xGa_{1-x}As$-GaAs quantum well heterostructure (QWH) lasers. We show directly the considerable difference in the oxidation behavior of $Al_xGa_{1-x}As$ ($x \gtrsim 0.7$) as compared to GaAs, which, relative to oxide formation, is much weaker and readily permits current-contact metallization.

The epitaxial layers for these coupled-stripe QWH lasers are grown on n-type (100)GaAs substrates by metalorganic chemical vapor deposition (MOCVD) as described extensively elsewhere.[5] A GaAs buffer layer is grown first, followed by an n-type $Al_{0.8}Ga_{0.2}As$ lower confining layer. The active region of the QWH is grown next and consists of a ~ 400 Å GaAs QW with ~ 1000 Å $Al_{0.25}Ga_{0.75}As$ waveguide layers (undoped) on either side. Finally, a p-type $Al_{0.8}Ga_{0.2}As$ confining layer (~ 9000 Å) is grown on top of the active region. The entire QWH is capped by a heavily doped p-type GaAs contact layer (~ 800 Å thick).

The GaAs contact layer is removed where desired to provide access to the upper confining layer for formation of the native oxide.[3] As we show here, the GaAs layer does not oxidize readily, and consequently can be used directly as a mask (and then contact layer) in forming the native oxide on the upper confining layer. Standard photolithography is used to mask sets of ten 5-μm-wide GaAs stripes that are located 2 μm apart (7 μm center-to-center spacing). The GaAs between the stripes (2 μm width), as well as the GaAs between sets of stripes, is removed with H_2SO_4:H_2O_2:H_2O (1:8:80). This exposes the high composition $Al_xGa_{1-x}As$ ($x \sim 0.8$) upper confining layer for oxidation after removal of the photoresist. The $Al_xGa_{1-x}As$ oxidation is accomplished by heating the QWH at 400 °C (3 h) in a H_2O vapor atmosphere obtained by passing N_2 carrier gas (~ 1.4 scfh) through a H_2O bubbler maintained at 95 °C.[3,4]

The QWH crystal after oxidation is shown in Fig. 1(a). The 5 μm GaAs contact stripes remain shiny (silvery) and basically unaffected by the oxidation. The rest of the crystal, including the 2 μm regions between the GaAs stripes, is covered with a uniform oxide that appears blue in color and, as is shown elsewhere,[4] is 1000–1500 Å thick. Besides the significant difference in contacting behavior (conducting versus insulating), this is direct evidence [Fig. 1(a)] of the different oxidation behavior of $Al_xGa_{1-x}As$ at one extreme $x = 0$ (GaAs) and at the other, $x \sim 1$ (AlAs).

After the QWH is metallized (Ti-Pt-Au) across its entire surface it appears as shown in Fig. 1(b). Before metallization the crystal is Zn diffused ($ZnAs_2$, 540 °C, 25 min) to a shallow depth to improve the contact on the GaAs stripes. This procedure obviously does not require any special masking. The crystal is thinned to ~ 100 μm and is metallized on the substrate side (Ge-Au-Ni-Au), and is cleaved into Fabry–Perot resonator strips that are then saw-cut into separate ten-stripe dies. These are attached to Cu with In on the stripe side for heat sinking and

 0003-6951/91/080834-03$02.00

Native-oxide masked impurity-induced layer disordering of $Al_xGa_{1-x}As$ quantum well heterostructures

J. M. Dallesasse,[a] N. Holonyak, Jr., N. El-Zein, T. A. Richard, F. A. Kish, and A. R. Sugg
Electrical Engineering Research Laboratory, Center for Compound Semiconductor Microelectronics, and Materials Research Laboratory, University of Illinois at Urbana-Champaign, Urbana, Illinois 61801

R. D. Burnham and S. C. Smith
Amoco Technology Company, Amoco Research Center, Naperville, Illinois 60566

(Received 21 November 1990; accepted for publication 4 January 1991)

Data are presented showing that the native oxide that can be formed on high Al composition $Al_xGa_{1-x}As$ ($x \gtrsim 0.7$) confining layers on $Al_yGa_{1-y}As$-$Al_zGa_{1-z}As$ ($y > z$) superlattices or quantum well heterostructures serves as an effective mask against impurity diffusion (Zn or Si), and thus against impurity-induced layer disordering. The high quality native oxide is produced by the conversion of high Al composition $Al_xGa_{1-x}As$ ($x \gtrsim 0.7$) confining layers, which can be grown on a variety of heterostructures, via H_2O vapor oxidation ($\gtrsim 400$ °C) in an N_2 carrier gas.

Ordinarily high Al composition $Al_xGa_{1-x}As$ ($x \gtrsim 0.7$) is susceptible to destructive (atmospheric) hydrolization[1,2] but not if heated at high enough temperature ($\gtrsim 400$ °C) in a rich H_2O-vapor ambient.[3] At higher temperatures and high H_2O vapor pressure, more stable phases of the oxide form,[3,4] which indeed are useful in device applications.[5,6] For even greater usefulness an important question is that of the masking capability of the natural oxide that can be formed on $Al_xGa_{1-x}As$ ($x > 0.7$). In this letter we demonstrate this behavior via Zn diffusion and impurity-induced layer disordering (IILD),[7-10] i.e., layer disordering of a bare $Al_xGa_{1-x}As$-GaAs superlattice (SL) or quantum well heterostructure (QWH) crystal in contrast to masking of the SL or QWH by the natural oxide. In the latter case (oxide masking) the quantum well (QW) and superlattice (SL) layers are preserved.

The SL and QWH crystals used in these experiments are grown on (100)GaAs substrates by metalorganic chemical vapor deposition (MOCVD) as described extensively elsewhere.[11] In the case of the SL crystal (crystal No. 1), a GaAs buffer layer is grown first and next an undoped $Al_{0.8}Ga_{0.2}As$ lower confining layer (~ 0.1 μm). Then the SL consisting of 40 GaAs wells ($L_z \sim 110$ Å) and 41 $Al_{0.4}Ga_{0.6}As$ barriers ($L_B \sim 150$ Å) is grown. The total SL thickness is $\sim$ 1.05 μm (see Fig. 1). Finally a 1000 Å $Al_{0.8}Ga_{0.2}As$ confining layer is grown on top of the SL. The structure is capped with a 3000 Å GaAs layer. The first part of the MOCVD QWH (crystal No. 2) is an n-type GaAs buffer layer (~ 0.5 μm), which is followed by an n-type $Al_{0.25}Ga_{0.75}As$ intermediate layer. An n-type $Al_{0.8}Ga_{0.2}As$ lower confining layer is grown next. This is followed by the QWH active region, which is a $\sim$ 200 Å $Al_{0.06}Ga_{0.94}As$ QW sandwiched by two undoped $\sim$ 1000 Å $Al_{0.25}Ga_{0.75}As$ waveguide (WG) layers. Finally a p-type $Al_{0.8}Ga_{0.2}As$ confining layer (~ 9000 Å) is grown on top of the active region. The entire QWH, which is useful in laser diode construction, is capped by a heavily doped p-type GaAs contact layer (~ 800 Å).

The GaAs cap layer on either the SL or the QWH is removed to allow the upper AlGaAs confining layer ($x \sim 0.8$) to be oxidized.[3] The presence of Ga in the oxidized layer and at the oxide-semiconductor interface does not adversely affect the structure of the oxide since the Ga-O and Al-O compounds form structural isomorphs, and Al_2O_3 and Ga_2O_3 form a solid solution over the entire compositional range.[4] The $Al_xGa_{1-x}As$ oxidation is accomplished by heating the samples at 400 °C (3 h) in an H_2O vapor atmosphere obtained by passing N_2 carrier gas (~ 1.5 scfh) through an H_2O bubbler maintained at 95 °C.[3,4] Lower temperatures are not used so as not to form poorer oxides.[4]

In order to effect selective Zn diffusion and layer disordering of the SL sample (crystal No. 1),[7-10] a photoresist stripe pattern (20 μm stripes on 50 μm centers) is defined on top of the oxide. Using a NH_4F:HF (7:1) buffered HF

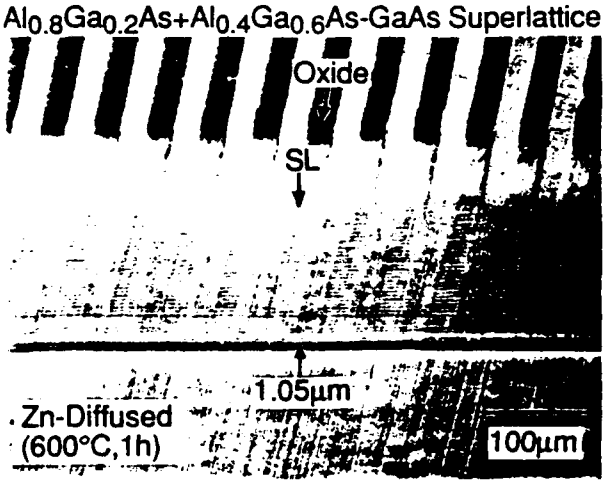

FIG. 1. Shallow-angle beveled cross section of a 1.05 μm $Al_xGa_{1-x}As$-GaAs SL ($L_z \sim 110$ Å, $L_B \sim 150$ Å) following Zn diffusion with 20 μm natural-oxide masking stripes (top) on the crystal surface. The lower part of the slant cross section shows regions where the superlattice is disordered (regions not masked by the oxide) alternating with regions where the superlattice is intact (regions masked by the oxide).

[a] Now at Amoco Technology Company, Amoco Research Center, Naperville, IL 60566.

 0003-6951/91/090974-03$02.00

Low-threshold disorder-defined native-oxide delineated buried-heterostructure $Al_xGa_{1-x}As$-GaAs quantum well lasers

F. A. Kish,[a] S. J. Caracci, N. Holonyak, Jr., J. M. Dallesasse,[b] and G. E. Höfler
Electrical Engineering Research Laboratory, Center for Compound Semiconductor Microelectronics, and Materials Research Laboratory, University of Illinois at Urbana–Champaign, Urbana, Illinois 61801

R. D. Burnham and S. C. Smith
Amoco Technology Company, Amoco Research Center, Naperville, Illinois 60566

(Received 3 December 1990; accepted for publication 13 February 1991)

Impurity-induced layer disordering (IILD) along with oxidation (native oxide) of high-gap $Al_xGa_{1-x}As$ confining layers is employed to fabricate low-threshold stripe-geometry buried-heterostructure $Al_xGa_{1-x}As$-GaAs quantum well heterostructure (QWH) lasers. Silicon IILD is used to intermix the quantum well and waveguide regions with the surrounding confining layers (beyond the laser stripe) to provide optical and current confinement in the QW region of the stripe. The high-gap $Al_xGa_{1-x}As$ upper confining layer is oxidized in a self-aligned configuration defined by the contact stripe and reduces IILD leakage currents at the crystal surface and diffused shunt junctions. $Al_xGa_{1-x}As$-GaAs QWH lasers fabricated by this method have continuous 300 K threshold currents as low as 5 mA and powers > 31 mW/facet for ~ 3-μm-wide active regions.

By means of relatively simple processing, impurity-induced layer disordering (IILD)[1,2] has been employed to produce very high performance planar buried-heterostructure (BH) quantum well heterostructure (QWH) lasers.[3] Various dopants and diffusion techniques have been employed to fabricate disorder-defined BH lasers, including (1) Si solid-source diffusion,[4] (2) Si implantation and annealing,[5] (3) Ge diffusion from the vapor,[6] (4) Zn diffusion from the vapor,[7] (5) Si-O diffusion from Al-reduced SiO_2,[8] (6) Si diffusion from Al-reduced Si/Si_3N_4 via rapid thermal annealing,[9] and (7) Si diffusion from laser-melted Si_3N_4.[10] Many of these have the disadvantage that they form a very highly conducting layer at the crystal surface. This conducting layer is a source of leakage, and thus increases laser threshold currents. Under some conditions the alloying is so severe that a relatively deep proton implant is required to passivate the leakage regions to insure low-threshold laser operation.[9,11] In this letter a self-aligned process is reported in which these surfaces are converted to current blocking native oxide. The oxide passivates the surface, reducing surface and shunt junction leakage currents, and thus yielding an improved form of low-threshold disorder-defined BH $Al_xGa_{1-x}As$-GaAs quantum well heterostructure laser.

The QWH laser crystal employed in this work is grown by metalorganic chemical vapor deposition (MOCVD)[12] on an n-type substrate. The growth begins with n-type buffer layers of GaAs (~ 0.5 μm) and $Al_{0.25}Ga_{0.75}As$ (~ 1 μm). This is followed by the growth of a ~ 1.1 μm $Al_{0.77}Ga_{0.23}As$ n-type lower confining layer, a ~ 2000 Å $Al_{0.25}Ga_{0.75}As$ undoped waveguide region, a ~ 1.1 μm $Al_{0.8}Ga_{0.2}As$ p-type upper confining layer, and a ~ 0.1 μm p-type GaAs cap. In the center of the waveguide is a ~ 200 Å $Al_{0.06}Ga_{0.94}As$ quantum well (undoped).

The laser diode fabrication process begins with a shallow Zn diffusion over the entire surface in an evacuated quartz ampoule (540 °C, 30 min). The shallow p^+ layer formed by the diffusion helps control lateral Si diffusion at the crystal surface under the masked regions in later processing steps.[6] After Zn diffusion, the crystal is encapsulated with ~ 1000 Å of Si_3N_4 deposited by chemical vapor deposition (CVD) at 720 °C. The Si_3N_4 is patterned with photoresist and etched with a CF_4 plasma into two choices of stripe width, 4 and 6 μm. The photoresist is removed, and the remaining Si_3N_4 stripes serve as masks for chemical etching (H_2SO_4:H_2O_2:H_2O, 1:8:80) of the GaAs contact layer, thus leaving the high-gap $Al_{0.8}Ga_{0.2}As$ upper confining layer exposed. Following stripe delineation, CVD is used to deposit a ~ 300 Å Si layer (550 °C) and a ~ 1700 Å SiO_2 cap layer (400 °C). The crystal is then sealed in an evacuated quartz ampoule and annealed with excess As at 850° C for 6.5 h. The high-temperature anneal results in Si diffusion and IILD outside of the GaAs contact stripes. All encapsulants are then removed by etching with a CF_4 plasma, and the crystal is placed in an open tube furnace (supplied with a N_2 carrier gas bubbled through H_2O at 95 °C) at 400 °C for 3 h. This process results in oxidation of ~ 2000 Å of the exposed high-gap upper confining layers at the edge and beyond the GaAs contact stripe regions.[13] No oxide is formed on the GaAs contact stripes due to the selectivity of the oxidation process.[14] Native oxides are only formed in areas of high Al composition, resulting in self-aligned contact stripes. Following the oxidation process, the wafer is sealed in an ampoule with a $ZnAs_2$ source, and is annealed at 540 °C for 30 min to form a shallow, heavily doped p-type region only in the contact area. (We note that the native oxide provides an effective mask for the Zn diffusion.)[15] Samples are

[a] AT&T Doctoral Fellow.
[b] Now at Amoco Technology Company, Amoco Research Center, Naperville, Illinois 60566.

 0003-6951/91/161765-03$02.00

Native-oxide stripe-geometry $Al_xGa_{1-x}As$-GaAs quantum well heterostructure lasers

J. M. Dallesasse and N. Holonyak, Jr.
Electrical Engineering Research Laboratory, Center for Compound Semiconductor Microelectronics, and Materials Research Laboratory, University of Illinois at Urbana–Champaign, Urbana, Illinois 61801

(Received 11 October 1990; accepted for publication 16 November 1990)

Data are presented on the room-temperature continuous (cw) operation of native-oxide single-stripe $Al_xGa_{1-x}As$-GaAs quantum well heterostructure (QWH) lasers. The device quality native oxide is produced by the conversion of high Al composition $Al_xGa_{1-x}As$ ($x \sim 0.8$) confining layers via H_2O vapor oxidation (400 °C) in a N_2 carrier gas. The 10-μm-wide cw 300 K QWH lasers, which are fabricated by simplified processing, have excellent spectral quality and have been operated to powers in excess of 100 mW per facet.

It has long been known in Si technology that the formation of a high quality native oxide (SiO_2) is possible by exposing the crystal to H_2O vapor (steam) in a carrier gas.[1] In fact, Si integrated circuit technology is due largely to the existence of the high quality SiO_2 native oxide. One difficulty with GaAs and most other III-V compound semiconductors is that they lack a stable native oxide. This difficulty has been overcome to some degree by using other methods such as sputtering, chemical vapor deposition (CVD), and plasma-assisted chemical vapor deposition to apply non-native oxides (or other dielectrics) onto the crystal surface. Recently we have examined the stability of high composition $Al_xGa_{1-x}As$ ($x \gtrsim 0.7$) layers in $Al_xGa_{1-x}As$-GaAs quantum well heterostructures (QWHs) and have studied the slow atmospheric deterioration of the QWH material by hydrolysis.[2,3] To speed the process of $Al_xGa_{1-x}As$ ($x \gtrsim 0.7$) hydrolysis we have resorted to heating of the QWH crystal in H_2O vapor (N_2 carrier gas) and have discovered that native oxides of sufficient quality for device use can be formed on the $Al_xGa_{1-x}As$ crystal.[4] In fact, AlAs-GaAs superlattices, a "coarser" form of $(AlAs)_x(GaAs)_{1-x}$ alloy, can be transformed completely to transparent oxide.[4] In this letter the use of this native oxide in the fabrication of gain-guided oxide-stripe QWH lasers is demonstrated. These devices, which are formed by simplified processing, are found to have outstanding performance characteristics.

The epitaxial layers for these laser structures are grown on *n*-type (100) GaAs substrates by metalorganic chemical vapor deposition (MOCVD) as described extensively elsewhere.[5] An $Al_{0.8}Ga_{0.2}As$ lower confining layer is grown after first a GaAs buffer layer. The active region of the QWH is grown next and consists of symmetrical ~ 1000 Å $Al_{0.25}Ga_{0.75}As$ waveguide layers (undoped) on either side of a ~ 400 Å GaAs QW. Finally at the top of the QWH a *p*-type $Al_{0.8}Ga_{0.2}As$ confining layer is grown ~ 9000 Å thick. The entire QWH is capped by a heavily doped *p*-type GaAs contact layer (~ 800 Å thick).

Diodes are constructed by first depositing ~ 1000 Å of CVD SiO_2 on the crystal surface. Using standard photolithography and plasma etching, we define 10-μm-wide SiO_2 stripes on the wafer surface for masking purposes. The crystal is then etched in H_2SO_4:H_2O_2:H_2O (1:8:80) to remove the GaAs contact layer in areas not protected by the SiO_2 masking stripes. Except in the 10-μm-wide stripe regions, this exposes the high composition ($x \sim 0.8$) $Al_xGa_{1-x}As$ upper confining layer. A native oxide is formed from ~ 1500 Å of the exposed $Al_xGa_{1-x}As$ ($x \sim 0.8$) layer by heating the QWH crystal at ~ 400 °C for 3 h in a H_2O vapor atmosphere produced by passing a N_2 carrier gas (~ 1.4 scfh) through a H_2O bubbler maintained at ~ 95 °C. The oxide that is produced has a thickness of 1000–1500 Å and a uniform blue color. Following oxidation of the $Al_xGa_{1-x}As$, the SiO_2 masking layer is removed by plasma etching (CF_4 + 4% O_2). The native oxide is unaffected by plasma removal of the SiO_2 layer, which is employed merely to help in processing.

Figure 1 shows a cross section of the crystal before removal of the SiO_2 masking layer. The vertical arrows in Fig. 1(a) indicate as labeled the thickness of the SiO_2 layer (left side) and the native oxide layer (to the right). Figure 1(b) shows a cross section in which the native oxide (right side) has been removed by etching in a KOH-$K_3Fe(CN)_6$ mixture. The pair of vertical arrows [Fig. 1(b)] indicates the location of the oxide prior to removal. An important property of the oxidation process is the possibility that it is sensitive to crystal orientation. For example, where the oxide undercuts the SiO_2 masking stripe and the GaAs contact layer, a tendency exists to develop a crystallographic step on the $Al_xGa_{1-x}As$ ($x \sim 0.8$) confining layer. This is shown by the small slanted arrow in Fig. 1(b).

After the SiO_2 masking stripes are removed, the crystal is sealed in an ampoule for shallow Zn diffusion ($ZnAs_2$ source, 540 °C, 25 min) to increase the GaAs stripe contact doping. Then the crystal is metallized (Ti-Pt-Au) across the native oxide onto the exposed GaAs contact stripe. We note that the metallization adheres onto the native oxide much better than on the usual deposited dielectrics, on which frequently the metallization peels. After the *p*-type side metallization the crystal is thinned (100 μm) from the substrate side and is metallized on the *n*-type side (Ge-Au-Ni-Au). The wafer is cleaved into Fabry–Perot bars, and saw-cut stripe-contact sections are attached to Cu heat sinks with In for continuous (cw) 300 K laser operation. Similar saw-cut sections with no contact stripe regions are prepared to check the blocking behavior of the oxide. Figure 2(a) shows the *I-V* characteristic of a diode prepared on the QWH crystal in the GaAs contact stripe region, and

 0003-6951/91/040394-03$02.00

Native-oxide-defined coupled-stripe $Al_xGa_{1-x}As$-GaAs quantum well heterostructure lasers

J. M. Dallesasse, N. Holonyak, Jr., D. C. Hall, N. El-Zein, and A. R. Sugg
Electrical Engineering Research Laboratory, Center for Compound Semiconductor Microelectronics, and Materials Research Laboratory, University of Illinois at Urbana–Champaign, Urbana, Illinois 61801

S. C. Smith and R. D. Burnham
Amoco Technology Center, Amoco Research Center, Naperville, Illinois 60566

(Received 26 October 1990; accepted for publication 26 November 1990)

Data are presented on the continuous-wave (cw) room-temperature (300 K) operation of multiple stripe $Al_xGa_{1-x}As$-GaAs quantum well heterostructure (QWH) laser arrays defined with native oxide contact masking. Use of the native $Al_xGa_{1-x}As(x \gtrsim 0.7)$ oxide allows the fabrication of high-performance devices without depositing foreign oxide or dielectric layers (SiO_2 or Si_3N_4). Arrays of ten 5-μm-wide emitters on 7 μm centers are coupled and operate at powers as high as 300 mW per facet, or at wider stripe spacing (5 μm emitters on 10 μm centers) as high as 400 mW per facet. These data indicate that current blocking layers of native oxide, formed from $Al_xGa_{1-x}As$ with H_2O vapor in N_2 carrier gas (400 °C, 3 h), can be used in the construction of high-power multiple stripe QWH arrays with excellent performance characteristics.

We have shown recently that instead of the usual destructive atmospheric hydrolyzation of higher composition $(AlAs)_x(GaAs)_{1-x}(x \gtrsim 0.7)$,[1,2] the alloy can be converted to native oxide by higher temperature heating ($\gtrsim 400$ °C) in H_2O vapor (N_2 carrier gas).[3] This has been demonstrated on fine scale (random) alloy and simultaneously, for comparison, on coarse scale alloy as represented by a superlattice ($x \gtrsim 0.7$).[3] Moreover, the native oxide is of sufficient quality so as to be useful in device fabrication,[4] which is of special interest in the present work. One of the more notable features of the native $Al_xGa_{1-x}As$ ($x \gtrsim 0.7$) oxide is how well it can be metallized, and thus can be employed in device heat sinking. Also, via ordinary photolithographic processes, the natural oxide permits delineation of device geometries without the need to deposit foreign and thus potentially mismatched dielectric materials (e.g., SiO_2 or Si_3N_4). We show in the present work these features of the natural $Al_xGa_{1-x}As$ ($x \gtrsim 0.7$) oxide by constructing, with simplified processing, high-performance ten-stripe $Al_xGa_{1-x}As$-GaAs quantum well heterostructure (QWH) lasers. We show directly the considerable difference in the oxidation behavior of $Al_xGa_{1-x}As$ ($x \gtrsim 0.7$) as compared to GaAs, which, relative to oxide formation, is much weaker and readily permits current-contact metallization.

The epitaxial layers for these coupled-stripe QWH lasers are grown on n-type (100)GaAs substrates by metalorganic chemical vapor deposition (MOCVD) as described extensively elsewhere.[5] A GaAs buffer layer is grown first, followed by an n-type $Al_{0.8}Ga_{0.2}As$ lower confining layer. The active region of the QWH is grown next and consists of a $\sim$400 Å GaAs QW with $\sim$1000 Å $Al_{0.25}Ga_{0.75}As$ waveguide layers (undoped) on either side. Finally, a p-type $Al_{0.8}Ga_{0.2}As$ confining layer ($\sim$9000 Å) is grown on top of the active region. The entire QWH is capped by a heavily doped p-type GaAs contact layer ($\sim$800 Å thick).

The GaAs contact layer is removed where desired to provide access to the upper confining layer for formation of the native oxide.[3] As we show here, the GaAs layer does not oxidize readily, and consequently can be used directly as a mask (and then contact layer) in forming the native oxide on the upper confining layer. Standard photolithography is used to mask sets of ten 5-μm-wide GaAs stripes that are located 2 μm apart (7 μm center-to-center spacing). The GaAs between the stripes (2 μm width), as well as the GaAs between sets of stripes, is removed with H_2SO_4:H_2O_2:H_2O (1:8:80). This exposes the high composition $Al_xGa_{1-x}As$ ($x \sim 0.8$) upper confining layer for oxidation after removal of the photoresist. The $Al_xGa_{1-x}As$ oxidation is accomplished by heating the QWH at 400 °C (3 h) in a H_2O vapor atmosphere obtained by passing N_2 carrier gas ($\sim$1.4 scfh) through a H_2O bubbler maintained at 95 °C.[3,4]

The QWH crystal after oxidation is shown in Fig. 1(a). The 5 μm GaAs contact stripes remain shiny (silvery) and basically unaffected by the oxidation. The rest of the crystal, including the 2 μm regions between the GaAs stripes, is covered with a uniform oxide that appears blue in color and, as is shown elsewhere,[4] is 1000–1500 Å thick. Besides the significant difference in contacting behavior (conducting versus insulating), this is direct evidence [Fig. 1(a)] of the different oxidation behavior of $Al_xGa_{1-x}As$ at one extreme $x = 0$ (GaAs) and at the other, $x \sim 1$ (AlAs).

After the QWH is metallized (Ti-Pt-Au) across its entire surface it appears as shown in Fig. 1(b). Before metallization the crystal is Zn diffused ($ZnAs_2$, 540 °C, 25 min) to a shallow depth to improve the contact on the GaAs stripes. This procedure obviously does not require any special masking. The crystal is thinned to $\sim$100 μm and is metallized on the substrate side (Ge-Au-Ni-Au), and is cleaved into Fabry–Perot resonator strips that are then saw-cut into separate ten-stripe dies. These are attached to Cu with In on the stripe side for heat sinking and

 0003-6951/91/080834-03$02.00

Native-oxide masked impurity-induced layer disordering of $Al_xGa_{1-x}As$ quantum well heterostructures

J. M. Dallesasse,[a] N. Holonyak, Jr., N. El-Zein, T. A. Richard, F. A. Kish, and A. R. Sugg
Electrical Engineering Research Laboratory, Center for Compound Semiconductor Microelectronics, and Materials Research Laboratory, University of Illinois at Urbana-Champaign, Urbana, Illinois 61801

R. D. Burnham and S. C. Smith
Amoco Technology Company, Amoco Research Center, Naperville, Illinois 60566

(Received 21 November 1990; accepted for publication 4 January 1991)

Data are presented showing that the native oxide that can be formed on high Al composition $Al_xGa_{1-x}As$ ($x \gtrsim 0.7$) confining layers on $Al_yGa_{1-y}As$-$Al_zGa_{1-z}As$ ($y > z$) superlattices or quantum well heterostructures serves as an effective mask against impurity diffusion (Zn or Si), and thus against impurity-induced layer disordering. The high quality native oxide is produced by the conversion of high Al composition $Al_xGa_{1-x}As$ ($x \gtrsim 0.7$) confining layers, which can be grown on a variety of heterostructures, via H_2O vapor oxidation ($\gtrsim 400$ °C) in an N_2 carrier gas.

Ordinarily high Al composition $Al_xGa_{1-x}As$ ($x \gtrsim 0.7$) is susceptible to destructive (atmospheric) hydrolization[1,2] but not if heated at high enough temperature ($\gtrsim 400$ °C) in a rich H_2O-vapor ambient.[3] At higher temperatures and high H_2O vapor pressure, more stable phases of the oxide form,[3,4] which indeed are useful in device applications.[5,6] For even greater usefulness an important question is that of the masking capability of the natural oxide that can be formed on $Al_xGa_{1-x}As$ ($x > 0.7$). In this letter we demonstrate this behavior via Zn diffusion and impurity-induced layer disordering (IILD),[7-10] i.e., layer disordering of a bare $Al_xGa_{1-x}As$-GaAs superlattice (SL) or quantum well heterostructure (QWH) crystal in contrast to masking of the SL or QWH by the natural oxide. In the latter case (oxide masking) the quantum well (QW) and superlattice (SL) layers are preserved.

The SL and QWH crystals used in these experiments are grown on (100)GaAs substrates by metalorganic chemical vapor deposition (MOCVD) as described extensively elsewhere.[11] In the case of the SL crystal (crystal No. 1), a GaAs buffer layer is grown first and next an undoped $Al_{0.8}Ga_{0.2}As$ lower confining layer (~ 0.1 μm). Then the SL consisting of 40 GaAs wells ($L_z \sim 110$ Å) and 41 $Al_{0.4}Ga_{0.6}As$ barriers ($L_B \sim 150$ Å) is grown. The total SL thickness is $\sim$ 1.05 μm (see Fig. 1). Finally a 1000 Å $Al_{0.8}Ga_{0.2}As$ confining layer is grown on top of the SL. The structure is capped with a 3000 Å GaAs layer. The first part of the MOCVD QWH (crystal No. 2) is an *n*-type GaAs buffer layer (~ 0.5 μm), which is followed by an *n*-type $Al_{0.25}Ga_{0.75}As$ intermediate layer. An *n*-type $Al_{0.8}Ga_{0.2}As$ lower confining layer is grown next. This is followed by the QWH active region, which is a $\sim$ 200 Å $Al_{0.06}Ga_{0.94}As$ QW sandwiched by two undoped $\sim$ 1000 Å $Al_{0.25}Ga_{0.75}As$ waveguide (WG) layers. Finally a *p*-type $Al_{0.8}Ga_{0.2}As$ confining layer (~ 9000 Å) is grown on top of the active region. The entire QWH, which is useful in laser diode construction, is capped by a heavily doped *p*-type GaAs contact layer (~ 800 Å).

The GaAs cap layer on either the SL or the QWH is removed to allow the upper AlGaAs confining layer ($x \sim 0.8$) to be oxidized.[3] The presence of Ga in the oxidized layer and at the oxide-semiconductor interface does not adversely affect the structure of the oxide since the Ga-O and Al-O compounds form structural isomorphs, and Al_2O_3 and Ga_2O_3 form a solid solution over the entire compositional range.[4] The $Al_xGa_{1-x}As$ oxidation is accomplished by heating the samples at 400 °C (3 h) in an H_2O vapor atmosphere obtained by passing N_2 carrier gas (~ 1.5 scfh) through an H_2O bubbler maintained at 95 °C.[3,4] Lower temperatures are not used so as not to form poorer oxides.[4]

In order to effect selective Zn diffusion and layer disordering of the SL sample (crystal No. 1),[7-10] a photoresist stripe pattern (20 μm stripes on 50 μm centers) is defined on top of the oxide. Using a NH_4F:HF (7:1) buffered HF

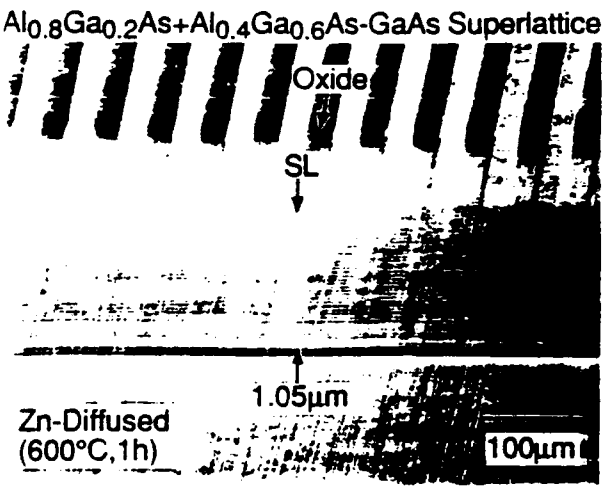

FIG. 1. Shallow-angle beveled cross section of a 1.05 μm $Al_xGa_{1-x}As$-GaAs SL ($L_z \sim 110$ Å, $L_B \sim 150$ Å) following Zn diffusion with 20 μm natural-oxide masking stripes (top) on the crystal surface. The lower part of the slant cross section shows regions where the superlattice is disordered (regions not masked by the oxide) alternating with regions where the superlattice is intact (regions masked by the oxide).

[a] Now at Amoco Technology Company, Amoco Research Center, Naperville, IL 60566.

 0003-6951/91/090974-03$02.00

Native-oxide stripe-geometry $In_{0.5}(Al_xGa_{1-x})_{0.5}P$-$In_{0.5}Ga_{0.5}P$ heterostructure laser diodes

F. A. Kish,[a] S. J. Caracci,[b] N. Holonyak, Jr., J. M. Dallesasse,[c] and A. R. Sugg
Electrical Engineering Research Laboratory, Center for Compound Semiconductor Microelectronics, and Materials Research Laboratory, University of Illinois at Urbana–Champaign, Urbana, Illinois 61801

R. M. Fletcher, C. P. Kuo, T. D. Osentowski, and M. G. Craford
Hewlett–Packard Company, Optoelectronics Division, San Jose, California 95131

(Received 26 April 1991; accepted for publication 15 May 1991)

Data are presented demonstrating the formation of stable, device-quality native oxides from high Al composition $In_{0.5}(Al_xGa_{1-x})_{0.5}P$ ($x \sim 0.9$) via reaction with H_2O vapor (in N_2 carrier gas) at elevated temperatures (>500 °C). The oxide exhibits excellent current-blocking characteristics and is employed to fabricate continuous room-temperature stripe-geometry $In_{0.5}(Al_xGa_{1-x})_{0.5}P$-$In_{0.5}Ga_{0.5}P$ double-heterostructure laser diodes.

The study of the problem of degradation of high composition $Al_xGa_{1-x}As$ ($x>0.7$) on $Al_xGa_{1-x}As$-$Al_yGa_{1-y}As$-GaAs quantum well heterostructures[1,2] has led to the discovery that device-quality native oxides can be formed from high-gap $Al_xGa_{1-x}As$ under proper conditions,[3] e.g., at temperatures $\gtrsim$ 400 °C by reaction with H_2O vapor in a N_2 carrier gas. The $Al_xGa_{1-x}As$ native oxide, with excellent insulating properties,[4] has already proven to be quite useful in such applications as impurity masking,[5] stripe-geometry laser diode fabrication,[4,6] AlAs layer stabilization,[7] reduction of parasitic leakage currents,[8] and formation of optical waveguides.[9] These desirable qualities are attributable to the formation of aluminum oxide and hydroxide compounds during the "wet" oxidation process.[7] These results suggest other III-V semiconductor materials containing an appreciable amount of Al are candidates for conversion to various forms of native oxides. In this letter we extend the "wet" oxidation procedure employed successfully on $Al_xGa_{1-x}As$ to other III-V systems. Specifically, we demonstrate formation of stable, device-quality native oxides in the $In_{0.5}(Al_xGa_{1-x})_{0.5}P$ system. The oxide is of sufficient quality to be employed in fabrication of continuous (cw) room-temperature (23 °C) $In_{0.5}(Al_xGa_{1-x})_{0.5}P$-$In_{0.5}Ga_{0.5}P$ double-heterostructure (DH) laser diodes.

The crystal employed in this work is grown on an *n*-type GaAs substrate by metalorganic chemical vapor deposition (MOCVD) as described extensively elsewhere.[10] The epitaxial layers of interest consist of an $\sim$0.8 μm *n*-type $In_{0.5}(Al_{0.9}Ga_{0.1})_{0.5}P$ lower confining layer, a $\sim$1000 Å $In_{0.5}Ga_{0.5}P$ active region (undoped), an $\sim$ 0.8 μm *p*-type $In_{0.5}(Al_{0.9}Ga_{0.1})_{0.5}P$ upper confining layer, and a low-gap *p*-type contact layer.

The device fabrication begins with deposition of $\sim$ 1000 Å of Si_3N_4 by chemical vapor deposition at 720 °C which is then patterned into 10 μm stripes. The Si_3N_4 serves as a mask for the chemical etching of the contact layer using 0.1% Br-methanol, leaving the high-gap $In_{0.5}(Al_{0.9}Ga_{0.1})_{0.5}P$ upper confining layer exposed outside of the laser stripe. The Si_3N_4 also prevents any subsequent oxidation of the contact layer. The sample is next placed in an open tube furnace (supplied with a N_2 carrier gas bubbled through H_2O at 95 °C) at 500 °C for 4 h. This process results in the oxidation of $\sim$ 1000 Å of the exposed $In_{0.5}(Al_{0.9}Ga_{0.1})_{0.5}P$ upper confining layer. The oxide formed is smooth and shiny with a uniform dark blue color, and is free of any observable pinholes. The Si_3N_4 masking stripes are then removed in a CF_4 plasma. The native oxide is unaffected by this treatment. The samples are next lapped to a thickness of $\sim$ 125 μm, polished, metallized with Au-Zn-Au for contact to the *p*-type side and with Ge-Ni-Au for the *n*-type side, alloyed, cleaved into bars $\sim$ 375 μm in length, and are sawed into individual devices. We note that the metallization adheres well to the native oxide, allowing the saw cuts to be made directly on the metallized oxide. This is in contrast to deposited films which require the metals to be photolithographically lifted off in the areas to be sawed to prevent peeling during the sawing process. The excellent adhesion of the metallization suggests less stress is present in the oxide films and permits better heat sinking than with deposited dielectrics.

Figure 1 shows a scanning electron microscope (SEM) image of a stained cross section of the crystal before removal of the Si_3N_4 masking stripe. The oxide [Fig. 1(b)] is $\sim$1000 Å thick and is uniform across the wafer surface. Additionally, the oxide grows up to the edge of and slightly undercuts the contact stripe [Fig. 1(a)], resulting in complete isolation of the noncontacted areas.

The insulating properties of the oxide are demonstrated in the current-voltage (*I-V*) characteristics of Fig. 2. The *I-V* characteristic of a diode prepared in the contact region [corresponding to the (a) region of Fig. 1] is shown in Fig. 2(a). The diode exhibits typical characteristics with "turn-on" of conduction at $\sim$ 1.6 V and a forward resistance of $\sim$ 5 Ω. To check the current-blocking characteristics of the oxide, devices are also sawed with no contact stripe regions present. These devices [corresponding to

[a] AT & T Doctoral Fellow.
[b] Supported by Wright Laboratory/Material Directorate.
[c] Now at Amoco Technology Company, Amoco Research Center, Naperville, Illinois 60566.

 0003-6951/91/280354-03$02.00

Native-oxide-masked Si impurity-induced layer disordering of $Al_xGa_{1-x}As$-$Al_yGa_{1-y}As$-$Al_zGa_{1-z}As$ quantum-well heterostructures

N. El-Zein, N. Holonyak, Jr., F. A. Kish,[a] A. R. Sugg, T. A. Richard, and J. M. Dallesasse[b]
Electrical Engineering Research Laboratory, Center for Compound Semiconductor Microelectronics, and Materials Research Laboratory, University of Illinois at Urbana-Champaign, Urbana, Illinois 61801

S. C. Smith and R. D. Burnham
Amoco Technology Company, Amoco Research Center, Naperville, Illinois 60566

(Received 18 April 1991; accepted for publication 17 May 1991)

Data are presented showing that the native oxide that can be formed on high Al composition $Al_xGa_{1-x}As$ ($x \gtrsim 0.7$) confining layers commonly employed on $Al_xGa_{1-x}As$-$Al_yGa_{1-y}As$-$Al_zGa_{1-z}As$ ($y > z$) superlattices or quantum-well heterostructures serves as an effective mask against Si diffusion, and thus impurity-induced layer disordering. The high-quality native oxide is produced by the conversion of high-composition $Al_xGa_{1-x}As$ ($x \gtrsim 0.7$) confining layers via H_2O vapor oxidation ($\gtrsim 400$ °C) in N_2 carrier gas.

I. INTRODUCTION

High-composition $Al_xGa_{1-x}As$ ($x \gtrsim 0.7$) layers may be unstable in normal room environmental conditions (20–25 °C, varying humidity) because of destructive hydrolyzation.[1,2] This is more of a problem for thicker layers ($\gtrsim 0.1$ μm) of higher alloy composition ($x \gtrsim 0.7$) and less of a problem for thinner layers ($\lesssim 100$ Å), even at high compositions. This instability is of major concern for various device applications employing high-gap $Al_xGa_{1-x}As$, e.g., higher-composition thick confining layers on quantum-well heterostructures (QWHs) or on superlattices (SLs). Recently, in an attempt to accelerate the destructive hydrolyzation process for further study, we have formed stable native oxides from high-composition $Al_xGa_{1-x}As$ (Ref. 3) by reaction with H_2O vapor (in an N_2 carrier gas) at elevated temperatures ($\gtrsim 400$ °C). We mention that higher-temperature oxidation is important for the formation of stable, device-quality Al-bearing oxides (compared to generally poorer suboxides formed at lower temperatures).[4] Native oxides formed on $Al_xGa_{1-x}As$ can serve as excellent insulators and have proved to be useful in device applications.[5,6] Development of more sophisticated devices utilizing the native $Al_xGa_{1-x}As$ oxide require the oxide to mask impurity diffusion, e.g., for definable or patterned impurity-induced layer disordering (IILD).[7] The masking capability of the native $Al_xGa_{1-x}As$ oxide for IILD Zn diffusion (Zn vapor, ~ 600 °C) has been previously demonstrated.[8] In many cases, it is more important to be able to perform donor diffusion (Si) and realize IILD in a patterned (maskable) form. This generally requires higher temperatures (~ 800 °C) and frequently solid sources, as well as sometimes vapor sources. In this paper we demonstrate the capability of the native $Al_xGa_{1-x}As$ oxide to mask diffusion and IILD from a Si solid source. Scanning electron microscopy (SEM), shallow-angle beveled cross sections, and photoluminescence measurements are used to demonstrate the oxide masking of Si diffusion (solid-source diffusion), and thus patterned IILD.

II. EXPERIMENTAL PROCEDURE

Both superlattice (SL) and single-quantum-well-heterostructure (QWH) crystals are employed in the present work. The SLs and QWHs are grown on (100) GaAs substrates by metalorganic chemical vapor deposition (MOCVD) as described extensively elsewhere.[9] One SL (designated SL1) consists of 20 GaAs wells ($L_z \sim 500$ Å) and 21 $Al_{0.5}Ga_{0.5}As$ barriers ($L_B \sim 500$ Å) that are confined on the upper and lower sides with ~ 1000 Å of $Al_{0.8}Ga_{0.2}As$. Another SL (designated SL2) consists of 15 GaAs wells ($L_z \sim 335$ Å) and 16 $Al_{0.5}Ga_{0.5}As$ barriers ($L_B \sim 335$ Å) confined with ~ 1000 Å of $Al_{0.6}Ga_{0.4}As$ on both sides. On top of the upper confining layer of SL2 is a 500-Å $Al_xGa_{1-x}As$ linearly graded region (from $x = 0$ to 0.85) followed by a $Al_{0.85}Ga_{0.15}As$ cap layer (0.1 μm). Both SL crystals are undoped. The QWH crystal employed here (which is useful for QWH lasers) consists of an n-type GaAs buffer layer, followed by a ~ 1-μm n-type $Al_{0.8}Ga_{0.2}As$ lower confining layer, an undoped ~ 2000-Å $Al_{0.25}Ga_{0.75}As$ waveguide region, a ~ 0.9-μm p-type $Al_{0.8}Ga_{0.2}As$ upper confining layer, and a heavily doped p-type GaAs cap (~ 800 Å) layer on top. In the center of the waveguide region is an undoped 200-Å $Al_{0.06}Ga_{0.94}As$ quantum well.

Oxidation of the wafers is performed at 400 °C in a "wet" atmosphere ($N_2 + H_2O$ vapor) in an open-tube furnace. The "wet" atmosphere is provided by flowing an N_2 carrier gas (1.5 scfh) through an H_2O bubbler maintained at 95 °C.[3] Since both SL samples are not capped, they are immediately subjected to oxidation after the crystal growth to prevent destructive atmospheric hydrolyzation.[4] Superlattice 1 (SL1) is oxidized for 3 h, and SL2 for only 1 h.

[a] AT&T Doctoral Fellow
[b] Current address: Amoco Technology Company, Amoco Research Center, Naperville, Illinois 60566.

 0021-8979/91/042031-04$03.00

Diffusion of manganese in GaAs and its effect on layer disordering in $Al_xGa_{1-x}As$-GaAs superlattices

C. H. Wu, K. C. Hsieh, G. E. Höfler, N. EL-Zein, and N. Holonyak, Jr.
Center for Compound Semiconductor Microelectronics, Department of Electrical and Computer Engineering and Materials Research Laboratory, University of Illinois at Urbana-Champaign, Illinois 61801

(Received 8 April 1991; accepted for publication 10 June 1991)

Several diffusion runs of Mn in GaAs are performed in sealed quartz ampoules with four different Mn-containing sources: (a) solid crystal granules of Mn, (b) Mn_3As, (c) MnAs, and (d) Mn thin films coated on GaAs substrates. Among these, only MnAs results in a smooth GaAs surface and uniform doping distributions. For the others interactions between the source materials and GaAs substrates give rise to poor surface morphologies and inhomogeneous distributions of new-phase (Mn,Ga) crystals. For diffusion at 800 °C, surface p-type carrier concentrations as high as $10^{20}/cm^3$ are obtained. Diffusion profiles determined by C-V techniques resemble those obtained for Zn diffusions. A substitutional-interstitial mechanism is suggested as the primary diffusion mechanism for Mn in GaAs. Data are also presented showing that layer disordering in AlGaAs-GaAs superlattices can be induced by Mn impurities.

Various impurities have long been incorporated into bulk semiconductors or epitaxial layers during crystal growth or processing for various device applications. Zn, Be, and Mg are commonly used for p-type doping in GaAs- and/or InP-based compound semiconductors grown by metalorganic chemical vapor deposition (MOCVD) or molecular beam epitaxy (MBE), but Cd and Mn are rarely used. With Cd and Mn, it is difficult to dope above $1\times10^{18}/cm^3$.[1-3] Additional concern with Mn doping is the poor surface morphology. Ripple-like features parallel to $[1\bar{1}0]$ are observed in MBE-grown GaAs with Mn doping higher than $1\times10^{17}/cm^3$. The origin of the ripple structure has been suggested to be associated with the surface segregation of the doping species during crystal growth.[2] Very limited data on Mn diffusion are available in the literature, and a surface concentration of only $2\times10^{18}/cm^3$ has been reported by Seltzer.[4] In the present work we report that very high carrier concentrations ($\sim10^{20}/cm^3$) from Mn diffusion can be realized with smooth surface morphology. Our results indicate that using different Mn-containing sources for the diffusion of Mn in GaAs can have a profound influence on the ultimate surface carrier concentration, surface morphology, and as a result, on the effectiveness of impurity induced layer disordering (IILD) in AlGaAs-GaAs superlattices.[5]

Four different Mn-containing sources have been used to introduce Mn into GaAs, including separate solid sources of Mn, MnAs, or Mn_3As (granules) enclosed in the quartz diffusion ampoules, as well as thin Mn films that are deposited directly onto the substrates by electron beam evaporation. The substrates for Mn diffusion are semi-insulating GaAs. The undoped AlGaAs-GaAs superlattices investigated here for IILD have been grown by low-pressure metalorganic chemical vapor deposition in an Emcore GS 3100 reactor. The sources for the growth of column III and V materials are trimethylaluminum (TMAl), trimethylgallium (TMGa), and 100% AsH_3, respectively. Crystal growth temperatures have been varied from 600 °C for GaAs layers to 740 °C for AlGaAs layers. The superlattice structure consists of 20 periods of $Al_xGa_{1-x}As$ ($x\sim0.4$) and GaAs, with both wells and barriers approximately 180 Å thick. These layers are confined on top (1000 Å) and on the substrate side (1000 Å) by two $Al_yGa_{1-y}As$ ($y=0.85$) layers. As usual a GaAs buffer layer is grown first, and a GaAs cap layer is grown on top.

Sample preparation for Mn diffusion consists of the usual surface cleaning procedures of degreasing with solvents, followed by an NH_4OH etch for 1 min. The samples are then loaded into degreased and etched quartz ampoules with the Mn sources, and are evacuated to $\sim2\times10^{-6}$ Torr and sealed. The diffusions are performed at 800 °C for times less than 12 h. Nomarski optical microscopy and transmission electron microscopy (TEM) are used to investigate the surface morphology and annealing surface reactions. Mn diffusion profiles were obtained by either secondary ion mass spectroscopy (SIMS) or capacitance-voltage (C-V) electrochemical etch profiler.

The surface morphologies of the samples after Mn-diffusion at 800 °C (2 h) using different Mn-containing sources are shown in Fig. 1. Different degrees of surface degradation of the GaAs surfaces have occurred depending on the choice of Mn sources. Poor surface morphologies result from chemical reactions between the vapor of the Mn-containing sources and GaAs substrates are clearly observed except when MnAs is used as the diffusion source. As a result of these reactions, inhomogeneous new-phase crystals of (Ga, Mn) form across the surface and to various depths as identified by cross-section transmission electron microscopy and energy dispersive x-ray spectroscopy. These numerous minute crystals, having probably a cubic structure, are generally smaller than 500 Å. In addition to the phase transformation near the surface, dislocations and dislocation loops of various densities are observed at different depths in the substrate depending on the diffusion conditions. Detailed data will be presented elsewhere. SIMS profiles obtained at different positions on the Mn-

 0003-6951/91/351224-03$02.00

Planar native-oxide index-guided $Al_xGa_{1-x}As$-GaAs quantum well heterostructure lasers

F. A. Kish,[a] S. J. Caracci,[b] N. Holonyak, Jr., J. M. Dallesasse,[c] K. C. Hsieh, and M. J. Ries
Electrical Engineering Research Laboratory, Center for Compound Semiconductor Microelectronics, and Materials Research Laboratory, University of Illinois at Urbana-Champaign, Urbana, Illinois 61801

S. C. Smith and R. D. Burnham
Amoco Technology Company, Amoco Research Center, Naperville, Illinois 60566

(Received 19 April 1991; accepted for publication 11 July 1991)

A new form of planar index-guided laser diode is demonstrated with a relatively thick ($\sim$0.4 μm) native oxide employed to define the lateral optical waveguide (transverse to the laser stripe). Oxidation of high-gap $Al_xGa_{1-x}As$ in a "wet" ambient results in the transformation of most of the upper confining layer to a lower-index current-blocking native oxide outside of the active stripe. Planar quantum well heterostructure (QWH) $Al_xGa_{1-x}As$-GaAs laser diodes fabricated by this process exhibit both optical and current confinement. Continuous 300 K threshold currents as low as 10 mA (uncoated facets) and kink-free single-longitudinal-mode operation are demonstrated for $\sim$2-μm-wide active region devices.

The fabrication of high-performance laser diodes requires a means of providing both optical and current confinement in order to limit current spreading, define current paths, and form optical waveguides.[1] Recently a new technique has been demonstrated to fabricate stripe-geometry gain-guided laser diodes by the formation of a thin ($\sim$1000 Å) current-blocking high-gap $Al_xGa_{1-x}As$ native oxide outside of the laser stripe.[2,3] In this letter oxidation of most of the high-gap $Al_xGa_{1-x}As$[2] upper confining layer of an $Al_xGa_{1-x}As$-GaAs quantum well heterostructure (QWH) laser diode (outside of the active stripe) is employed to form a low-index current-blocking native oxide. The resulting planar index-guided devices exhibit both optical and current confinement as well as kink-free single-longitudinal-mode operation. Additionally, these lasers (fabricated on moderately low-threshold QWH crystals) have 300 K continuous (cw) thresholds as low as 10 mA for a $\sim$2-μm-wide active stripe.

The QWH crystal employed in this work is grown (on n-type GaAs) by metalorganic chemical vapor deposition (MOCVD).[4] The epitaxial layers of interest are a $\sim$1 μm $Al_{0.77}Ga_{0.23}As$ n-type lower confining layer, a $\sim$1400 Å undoped $Al_{0.3}Ga_{0.7}As$ waveguide region, a $\sim$0.5 μm $Al_{0.8}Ga_{0.2}As$ p-type upper confining layer, and a $\sim$800 Å heavily doped p-type GaAs cap. A $\sim$100 Å GaAs quantum well (undoped) is grown in the center of the waveguide layer.

The laser fabrication begins with the deposition on the crystal of $\sim$1000 Å Si_3N_4, which is patterned with photoresist into two choices of stripe width (2 and 8 μm). These stripes serve as a mask for chemical etching of the GaAs contact layer, leaving the high-gap $Al_{0.8}Ga_{0.2}As$ upper confining layer exposed outside of the laser stripe. The crystal is then placed in an open-tube furnace (supplied with a N_2 carrier gas bubbled through H_2O at 95 °C) at 450 °C for $\sim$30 min. This process results in the transformation of almost the entire exposed confining layer to a native oxide. Next the Si_3N_4 covering the contact stripe is removed, and the samples are Zn-diffused at 540 °C for 30 min to improve the contacts. The crystals are then lapped and polished, metallized with Ti-Au for p-type contacts and Ge-Ni-Au for n-type contacts, cleaved into $\sim$250-μm-wide bars, diced, and mounted on In-coated copper heat sinks.

Figure 1(a) shows a scanning electron microscope (SEM) image of a stained cross section of a $\sim$2-μm-wide laser structure after oxidation (except for the active region) of almost the entire thickness ($\sim$0.4 μm) of the upper confining layer. The native oxide extends downward almost to the waveguide region (WG in Fig. 2). The oxidation process obviously undercuts the GaAs cap "masking" layer, thus, resulting in $\sim$1.7-μm-wide active stripe embedded in native oxide. The native oxide exhibits excellent current-blocking properties and confines the current to the stripe region.[4,5] Additionally, the native oxide exhibits a much lower index of refraction (ellipsometer measurements, $n = 1.50$–1.60)[5] than the original upper confining layer ($n \sim 3.1$). Thus, the index step ($3.1 \rightarrow 1.6$), over a significant thickness of the QWH, forms an optical waveguide in the lateral direction.

The effect of the optical waveguide is shown by the near-field (NF) pattern in the inset (b) of the $\sim$2-μm-wide device of Fig. 1(a). The full width at half-maximum (FWHM) of the optical field (fundamental transverse mode) is 1.7 μm at a cw 300 K current of 20 mA ($I \sim 1.25\ I_{th}$) and remains fixed over the entire operating range investigated ($I \lesssim 3\ I_{th}$). The NF FWHM agrees well with the active stripe width defined by the native oxide [Fig. 1(a)], and indicates that the lower refractive index of the native oxide in the upper confining layer is sufficient to

[a] AT&T Doctoral Fellow.
[b] Supported by Wright Laboratory/Materials Directorate.
[c] Present address: Amoco Technology Company, Amoco Research Center, Naperville, Illinois 60566.

 0003-6951/91/391755-03$02.00

Native-oxide coupled-cavity $Al_xGa_{1-x}As$-GaAs quantum well heterostructure laser diodes

N. El-Zein, F. A. Kish,[a] N. Holonyak, Jr., A. R. Sugg, and M. J. Ries
Electrical Engineering Research Laboratory, Center for Compound Semiconductor Microelectronics, and Materials Research Laboratory, University of Illinois at Urbana–Champaign, Urbana, Illinois 61801

S. C. Smith, J. M. Dallesasse, and R. D. Burnham
Amoco Technology Company, Amoco Research Center, Naperville, Illinois 60566

(Received 9 August 1991; accepted for publication 23 September 1991)

Data are presented demonstrating $Al_xGa_{1-x}As$-GaAs quantum well heterostructure laser diodes consisting of an array of coupled cavities (19 μm long on 22 μm centers, $\sim$250 μm total length) arranged lengthwise in single 10-μm-wide laser stripes. The cavities are defined by a native oxide formed from a significant portion of the high-gap $Al_xGa_{1-x}As$ upper confining layer. The native oxide (grown at 425 °C in H_2O vapor + N_2 carrier gas) confines the injected carriers and optical field within the cavities, resulting in reflection and optical feedback distributed periodically along the laser stripe. These diodes exhibit single-longitudinal-mode operation over an extended range (relative to similar diodes fabricated without multiple cavities). At high current injection levels, longitudinal-mode spectra demonstrate unambiguously oscillation from the internal coupled cavities.

The high gain required for oscillation in semiconductor lasers results in a large optical bandwidth in which laser operation is possible. This large bandwidth generally results in multiple-longitudinal-mode operation. For many applications, single-longitudinal-mode operation is required. Consequently, sophisticated structures such as the distributed feedback (DFB) laser[1] and the cleaved-coupled-cavity (C^3) laser[2] have been developed to insure single-mode operation. These devices operate by reflecting the electromagnetic wave within the laser stripe to lock the laser mode. The DFB laser employs a fine-scale periodic corrugation of relatively small index steps to interact with the electromagnetic wave. The C^3 laser relies on several large-scale nonperiodic monolithic cavities for feedback and mode selection. In this letter, we describe $Al_xGa_{1-x}As$-GaAs quantum well heterostructure (QWH) laser diodes utilizing large periodic index steps to couple multiple cavities (19 μm long on 22 μm centers, $\sim$250 μm total length) arranged lengthwise along a single 10-μm-wide laser stripe. The index step is provided by "wet" oxidation (H_2O vapor + N_2 carrier gas, 425 °C) of the high-gap $Al_xGa_{1-x}As$ (Ref. 3) upper confining layer outside of the laser cavities. This native oxide possesses a low refractive index ($n = 1.60$) (Ref. 4) and excellent insulating characteristics,[5] thus confining the injected carriers and making possible reflections between the multiple cavities. The coupling of the optical wave between cavities results in an increased range of single-longitudinal-mode operation ($\sim I_{th}$ to $\sim 4I_{th}$, I_{th} = threshold current). At higher injection currents the longitudinal-mode spacing corresponds to laser operation from a 38 μm internal cavity (2×19 μm), indicating that the native oxide provides sufficient reflection of the optical wave for laser oscillation.

The QWH laser crystal employed in this work is grown on an n-type GaAs substrate by metalorganic chemical vapor deposition (MOCVD).[6] The growth begins with n-type buffer layers of GaAs ($\sim$0.5 μm) and $Al_{0.23}Ga_{0.77}As$ ($\sim$1.0 μm). These are followed by a $\sim$1.5 μm n-type $Al_{0.5}Ga_{0.5}As$ lower confining layer, a $\sim$2100 Å undoped $Al_{0.23}Ga_{0.77}As$ waveguide region, a $\sim$3500 Å p-type $Al_{0.8}Ga_{0.2}As$ upper confining layer, and a $\sim$800 Å heavily doped p-type GaAs contact layer. A $\sim$100 Å undoped GaAs quantum well (QW) is grown inside of the waveguide region $\sim$700 Å from the lower confining layer. The position of the QW is displaced from the center of the waveguide for more effective overlap of the high-gain region with the optical mode, which is displaced towards the substrate due to the asymmetric confining layers. This asymmetry is purposely introduced to minimize the effects of the surface of the laser crystal (located $\sim$3500 Å from the waveguide) by shifting the optical field toward the substrate. The shallow upper confining layer is desirable in order to minimize current spreading, allow finer pattern definition, and improved heat dissipation with the crystal mounted p side "down" and thus the active region closer to the heat sink.

The laser diode fabrication begins with deposition of $\sim$1000 Å of Si_3N_4 on the crystal surface which is then patterned into repeated (masked) rectangular cavities (19 μm long on 22 μm centers, 10 μm wide) arranged lengthwise in stripes. The Si_3N_4 masks the GaAs contact layer from chemical etching (H_2SO_4:H_2O_2:H_2O, 1:8:80), leaving the $Al_{0.8}Ga_{0.2}As$ upper confining layer exposed outside of the patterned cavities. The sample is next placed in an open tube furnace, supplied with H_2O vapor in an N_2 carrier gas, at 425 °C for 20 min. This process results in the transformation of $\sim$1300 Å of the $Al_{0.8}Ga_{0.2}As$ upper confining layer to native oxide outside of the repeated cavities. The Si_3N_4 is subsequently removed in a CF_4 plasma. Figure 1

[a]AT&T Doctoral Fellow.

 0003-6951/91/472838-03$02.00

Visible spectrum native-oxide coupled-stripe $In_{0.5}(Al_xGa_{1-x})_{0.5}P$–$In_{0.5}Ga_{0.5}P$ quantum well heterostructure laser arrays

F. A. Kish,[a] S. J. Caracci, N. Holonyak, Jr. and S. A. Maranowski
Electrical Engineering Research Laboratory, Center for Compound Semiconductor Microelectronics, and Materials Research Laboratory, University of Illinois at Urbana-Champaign, Urbana, Illinois 61801

J. M. Dallesasse, R. D. Burnham, and S. C. Smith
Amoco Technology Company, Amoco Research Center, Naperville, Illinois 60566

(Received 26 August 1991; accepted for publication 23 September 1991)

Data are presented demonstrating the continuous (cw) operation (10–50 °C) of coupled-stripe $In_{0.5}(Al_xGa_{1-x})_{0.5}P$–$In_{0.5}Ga_{0.5}P$ multiple quantum well heterostructure (QWH) visible ($\lambda \sim 655$ nm) laser arrays. The ten stripe QWH arrays (3 μm emitters on 4 μm centers) are defined by "wet" oxidation (H_2O vapor in N_2 carrier gas, 550 °C) of the high gap $In_{0.5}(Al_xGa_{1-x})_{0.5}P$ upper confining layer outside of the active stripes. The gain-guided arrays exhibit relatively low cw 20 °C threshold current densities (~ 1.6 kA/cm^2, ~ 450 μm cavity) and high output powers of 25 mW per uncoated facet (cw, 20 °C). Optical coupling between stripes results in a near diffraction-limited single-lobe far-field pattern indicative of oscillation in the lowest order supermode of the array (in-phase operation).

The observation of stimulated emission in $GaAs_{1-x}P_x$ diodes,[1] followed by $Al_xGa_{1-x}As$[2,3] and then $In_yGa_{1-y}P$,[4,5] demonstrated quite early the feasibility of visible spectrum semiconductor lasers. The capacity of substituting Al for Ga to form higher gap lattice-matched heterostructures via metalorganic chemical vapor deposition (MOCVD)[6] has led, in the $In_yGa_{1-y}P$ system, to the further capability of producing high-quality visible-wavelength $In_y(Al_xGa_{1-x})_yP$ quantum well heterostructure laser material lattice-matched ($y \sim 0.5$) to GaAs. These developments have resulted in short wavelength,[7,8] high-power,[9,10] and high reliability[11] visible spectrum laser diodes. However, little work has been concentrated on visible spectrum coupled-stripe arrays, which provide the advantage of delivering high output powers in a narrow beam. In this letter we present data demonstrating high power [25 mW per uncoated facet, 20 °C, continuous wave (cw)] coupled-stripe $In_{0.5}(Al_xGa_{1-x})_{0.5}P$–$In_{0.5}Ga_{0.5}P$ multiple quantum well heterostructure (QWH) laser arrays operating in the visible spectrum, $\lambda \sim 655$ nm. The ten stripe arrays are defined by conversion of the high-gap $In_{0.5}(Al_xGa_{1-x})_{0.5}P$ upper confining layer outside of the active stripes to native oxide (formed at 550 °C in H_2O vapor + N_2 carrier gas).[12,13]

The quantum well heterostructure (QWH) crystal employed in this work is grown by MOCVD on an n-type GaAs:Si substrate. The $In_{0.5}(Al_xGa_{1-x})_{0.5}P$ epitaxial layers consist of a ~ 1.0 μm n-type lower confining layer ($x \sim 0.9$), a multiple quantum well active region confined by ~ 750 Å linearly graded ($x \sim 0.9 \leftrightarrow x \sim 0.3$) regions, a ~ 1.0 μm p-type upper confining layer ($x \sim 0.9$), a p-type ($x \sim 0$) cap layer, and a heavily Zn-doped GaAs contact layer. The active region consists of four 100 Å quantum wells ($x \sim 0$) separated by three 200 Å barriers ($x \sim 0.3$). A four well structure is employed since previous work has shown that a similar design provides relatively high-performance short-wavelength operation.[7]

Laser diode fabrication begins by patterning 1000-Å thick Si_3N_4 into arrays of ten 3-μm wide stripes (on 4 μm centers) and, for comparison, 10-μm wide single stripes on the samples. These stripes serve as a mask for the chemical etching (Br-methanol, 0.1%) of the capping layers, leaving the high-gap $In_{0.5}(Al_{0.9}Ga_{0.1})_{0.5}P$ exposed outside of the active stripes. The Si_3N_4 also serves to prevent degradation of the contact layer during the oxidation process. The crystals are then placed in an open tube furnace (550 °C, 1 h) supplied with H_2O vapor in a N_2 carrier gas. This procedure results in the conversion of the exposed high-gap $In_{0.5}(Al_{0.9}Ga_{0.1})_{0.5}P$ to ~ 1000 Å of a current-blocking native oxide.[13] The Si_3N_4 (on the active stripes) is next removed in a CF_4 plasma, and the samples are lapped and polished to a thickness of ~ 125 μm. The crystals are metallized with Au–Zn–Au for the p-type contacts and Ge–Ni–Au for n-type contact, and then are cleaved, diced, and mounted p-side down on In-coated copper heat sinks.

In order to assess the quality of the QWH material, 10-μm wide native-oxide single-stripe lasers have been fabricated for comparison. Typical cw 20 °C performance of a 10 μm single stripe laser diode is shown in Fig. 1. The light versus current (L–I) curve shows a threshold current of 96 mA (uncoated facets, 305 μm cavity), corresponding to a current density of 3.1 kA/cm^2 (uncorrected for current spreading). The total external differential quantum efficiency (η) is 42% up to 1.5 mW, and the maximum output power is thermally limited to 5 mW per facet. The diode lases with multiple longitudinal modes, with the primary mode at $\lambda \simeq 6523$ Å (inset Fig. 1). We attribute the multimode operation to the weakly coupled four-well form of the QWH crystal, which makes each well in essence a separate laser. Despite the relatively high threshold current density, these lasers show no signs of degradation after hours of testing.

Continuous operation of a ten stripe coupled array (3 μm emitters on 4 μm centers) stabilized (on a thermoelec-

[a] AT&T Doctoral Fellow.

 0003-6951/91/472883-03$02.00

PUBLICATIONS

J.J. Coleman

High-power nonplanar quantum well heterostructure periodic laser arrays

M. E. Givens, C. A. Zmudzinski, R. P. Bryan, and J. J. Coleman
Department of Electrical and Computer Engineering and NSF Engineering Research Center for Compound Semiconductor Microelectronics, University of Illinois at Urbana–Champaign, 1406 West Green Street, Urbana, Illinois 61801

(Received 3 June 1988; accepted for publication 18 July 1988)

Optical pulsed powers of 8 W from a single uncoated facet and low (<200 A/cm^2) threshold current densities have been obtained from 3.1-mm-wide (cavity length = 483 μm) nonplanar periodic quantum well heterostructure laser diode arrays grown by metalorganic chemical vapor deposition over a selectively etched corrugated substrate. The resulting nonplanar lateral active layer profile provides index guiding and suppresses lateral lasing regardless of device width.

Multiple stripe semiconductor laser diode arrays are a very promising source of high-power emission, suitable for such applications as pumping solid-state Nd:YAG lasers.[1] The maximum output power before catastrophic optical damage[2] occurs is determined primarily by the effective aperture width, which is normally limited to a value less than the cavity length unless lateral lasing and amplified spontaneous emission processes are suppressed. In order to fabricate diodes having a width greater than the laser cavity length, thereby allowing higher total output powers to be obtained, it is necessary to provide some type of structural change to inhibit lateral lasing. Previously reported[3–5] methods of inhibiting lateral lasing and amplified spontaneous emission require extra processing steps in addition to the processing required to form the actual array elements, and also result in a portion of the array width which does not contribute to the laser output. In this letter, we report high-power operation of a simple nonplanar index-guided quantum well heterostructure periodic laser array structure in which lateral lasing is prevented in a manner that still allows for uniform and continuous front facet light emission. Growth over a corrugated substrate[6,7] is utilized for index guiding and definition of the individual elements, and the resulting nonplanar active region structure effectively suppresses lateral lasing and amplified spontaneous emission for the entire array.[8] No additional processing steps after growth, such as proton bombardment, chemical etching, diffusion, epitaxial regrowth, or insulator deposition, which may result in accelerated degradation due to the introduction of material defects, are required. Data are presented on the high-power light-current characteristics and optical near-field measurements for uncoated laser bars with an aperture width of up to 3.1 mm, showing output powers of 8 W per uncoated facet for periodic laser arrays with threshold current densities of 120–240 A/cm^2.

Prior to epitaxial growth, a periodic array of narrow mesa stripes was defined over the surface of a (100) GaAs:*n* (Si-doped) substrate using standard photolithographic and wet chemical etching techniques. The $Al_xGa_{1-x}As$/GaAs graded barrier quantum well heterostructure (GBQWH)[9,10] laser structure utilized in this study was grown in an atmospheric pressure metalorganic chemical vapor deposition (MOCVD) reactor[11] at a temperature of 800 °C. High composition ($x = 0.85$) $Al_xGa_{1-x}As$ confining layers surround the GBQWH active layer, which consists of a 50 Å GaAs single quantum well ($\lambda \sim 8250$ Å) centered in a 2450 Å parabolically graded $Al_xGa_{1-x}As$ layer ($0.20 \leqslant x \leqslant 0.85$). Successive epilayers were deposited uniformly over the nonplanar growth surface such that the corrugated contour of the growth surface remained essentially unchanged, as illustrated in Fig. 1, which shows a schematic cross section and a scanning electron micrograph of a portion of the laser array. Device wafers were mechanically thinned and polished, metallized, cleaved into bars of various lengths, and diced into individual diode arrays of various widths. The facets of the devices utilized in this study were left uncoated. No further processing or photolithographic steps were required either to define current injection or to suppress lateral lasing. The devices were mounted *p* side down in indium solder on Cu blocks with multiple wire bonds to contact the *n* side of the device and were tested under pulsed operation (400 ns, 1 kHz).

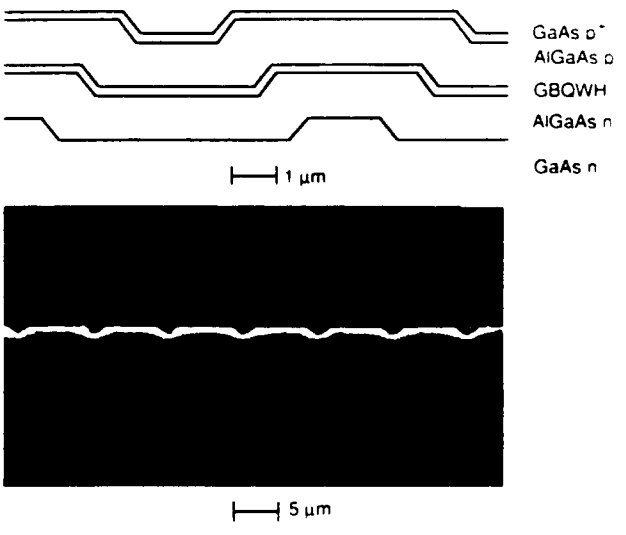

FIG. 1. Schematic diagram and scanning electron micrograph of the periodic nonplanar laser array grown by MOCVD on a corrugated etched substrate. The MOCVD growth over the nonplanar substrate results in a nonplanar active region which suppresses lateral lasing, allowing very wide laser bars.

 0003-6951/88/391159-03$01.00

Nonplanar quantum well heterostructure window laser

R. P. Bryan, L. M. Miller, T. M. Cockerill, and J. J. Coleman
Compound Semiconductor Microelectronics Laboratory and W. L. Everitt Laboratory, University of Illinois at Urbana–Champaign, 1406 West Green Street, Urbana, Illinois 61801

(Received 14 December 1988; accepted for publication 13 February 1989)

Data are presented on a nonplanar graded barrier quantum well heterostructure window laser formed by a single metalorganic chemical vapor deposition (MOCVD) growth. By utilizing a selectively etched substrate, a transparent window region is formed in the vicinity of the facets thereby relaxing the maximum power limit imposed by catastrophic optical degradation. The ultimate output power available from such devices is approximately 50% higher than from devices with the same structure but grown on unetched substrates. The processing required for device fabrication is minimized by taking advantage of the properties of MOCVD growth on nonplanar substrates.

Many of the degradation mechanisms of semiconductor lasers may be attributed to the presence of the active layer at the mirror facets.[1,2] During high-power operation optical absorption in the active region near the facets, which is enhanced by a high surface recombination velocity, leads to local heating in the region and may result in catastrophic optical degradation (COD). Furthermore, at lower intensity levels augmented generation of defects and facet oxidation degrade device performance. These degradation mechanisms may be eliminated or reduced by incorporating a nonabsorbing region between the active region and the mirror facets. The window region[3] reduces the local heating at the facets and decreases the optical intensity at a given output power by broadening the beam. Previously reported schemes[3–9] to produce window lasers require sophisticated fabrication processes or multiple growth steps. The diffused window stripe laser[3–5] requires precise control over its diffusion, the crank transverse junction stripe (TJS) laser[6] requires sophisticated selective etching, the V-channeled substrate inner stripe (VSIS) laser[7] and the large optical cavity buried heterostructure (LOC-BH) window laser[8,9] require two growth steps. Such complexities of the fabrication procedure reduce the laser yield, lower the device reliability, and limit the device structure.

In this letter we report the growth and fabrication of a simple nonplanar quantum well heterostructure window laser. In order to produce a nonabsorbing region in the vicinity of the facets at the active region, long mesas are etched in the substrate prior to growth. As a result of uniform[10–12] metalorganic chemical vapor deposition (MOCVD) growth over nonplanar surfaces, the active region is displaced toward the surface in the vicinity of the facets. Consequently, the optical field traverses the higher band-gap nonabsorbing confining layer in the vicinity of the mirror facets. Since the window region is a result of the nonplanar substrate, the type of laser structure grown is not restricted nor are sophisticated fabrication techniques or multiple growth steps required as in previously described window lasers. Data are presented on the light-current characteristics of devices with and without window regions which demonstrate a nearly 50% increase in the maximum output power. Near-field and far-field radiation patterns perpendicular to the junction which are presented clearly show a broadening of the optical field due to the window region.

GaAs:Si (100) substrates were prepared prior to epitaxial growth by delineating narrow mesa stripes (25 μm wide and 510 μm apart) with standard photolithography and wet chemical etching (1:8:80 H_2SO_4:H_2O_2:H_2O). The mesas, after growth, define the window region of the lasers. A graded barrier quantum well (GBQW) heterostructure laser[13,14] was grown in an atmospheric pressure MOCVD reactor[15,16] at a temperature of 800 °C. The laser structure consists of a 0.25 μm GaAs:n buffer layer, a 0.5 μm linearly graded ($0.0 \leqslant x \leqslant 0.85$) $Al_xGa_{1-x}As$:n buffer layer, a 1.0 μm $Al_{0.85}Ga_{0.15}As$:n confining layer, a 1200 Å parabolically graded ($0.85 \geqslant x \geqslant 0.20$) $Al_xGa_{1-x}As$:n layer, a 50 Å GaAs:u quantum well, a 1200 Å parabolically graded ($0.20 \leqslant x \leqslant 0.85$) $Al_xGa_{1-x}As$:p layer, a 1.0 μm $Al_{0.85}Ga_{0.15}As$:p confining layer, and a 0.2 μm GaAs:p^+ contact layer. The MOCVD growth is highly uniform[10–12] over the nonplanar substrate such that the substrate contours are maintained in the laser structure as illustrated in Fig. 1, which is a schematic cross section of the laser structure in the vicinity of the mirror facets. A planar substrate was loaded into the MOCVD reactor along with the etched substrate in order to directly compare the characteristics of

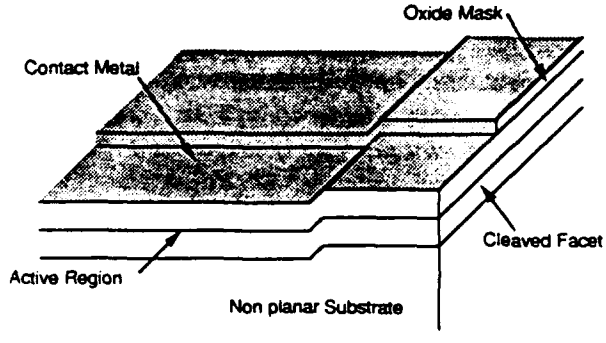

FIG. 1. Schematic of a nonplanar GBQW window laser grown by MOCVD on an etched substrate. The MOCVD growth follows the contours of the substrate resulting in a nonplanar active region and a nonabsorbing window region formed from the $Al_{0.85}Ga_{0.15}As$ confining layer between the active region and the mirror facet.

 0003-6951/89/171634-03$01.00

Optical Characteristics of High-Power Nonplanar Periodic Laser Arrays

CHARLES A. ZMUDZINSKI, STUDENT MEMBER, IEEE, MICHAEL E. GIVENS, ROBERT P. BRYAN, AND JAMES J. COLEMAN, SENIOR MEMBER, IEEE

Abstract—**Optical characteristics of high-power nonplanar periodic laser arrays are presented and analyzed. The nonplanar arrays, grown by metalorganic chemical vapor deposition, consist of a periodic array of mesas and grooves, which provides index guiding and prevents lateral lasing. The near- and far-field patterns are shown to be a strong function of the laser structure, particularly of the confining layer composition and effective index step. The near-field pattern determined by the structure affects the external differential quantum efficiency of these arrays relative to similar planar active region devices. Laser emission was generally confined to the mesa regions. A simple model is used as an aid to explain the observed near- and far-field patterns and to identify the mechanisms which confine the optical field to the mesa or groove region.**

I. Introduction

MULTIPLE-stripe laser arrays have proven to be a most promising source of high-power emission from semiconductor materials which are suitable for such applications as pumping solid-state Nd:YAG lasers [1]. Lateral lasing and amplified spontaneous emission in wide laser arrays can be suppressed by etching deep grooves at periodic intervals [2], [3] or by forming a nonplanar active region by metalorganic chemical vapor deposition (MOCVD) on an etched GaAs substrate [4], [5]. Either technique allows very wide lasers to be fabricated which emit over essentially the entire width of the facet. For nonplanar periodic laser arrays, the sharp bends in the active region provide large scattering losses for the lateral cavity modes, with no extra processing required to prevent lateral lasing. The purpose of this paper is to describe the characteristics of high-power nonplanar corrugated substrate laser arrays grown by MOCVD on etched GaAs substrates. An advantage of using MOCVD for the growth of these lasers is that the growth over the etched substrate follows the contour of the substrate more closely than with other growth methods [4]–[6].

In this paper, we discuss the fabrication, optical characteristics, and design considerations of nonplanar index-guided quantum well heterostructure periodic laser arrays which are suitable for high-power applications requiring optical power in excess of 10 W. In particular, we discuss the effects of fabrication parameters such as confining layer aluminum composition, active region structure, and the width of mesas and grooves on the threshold current, efficiency, and near- and far-field patterns of the laser array. We have experimentally observed a strong dependence of the near- and far-field patterns on the confining layer composition x_c of graded barrier quantum well heterostructure (GBQWH) [7], [8] periodic laser arrays, which in turn affects the external differential quantum efficiency of the laser arrays. In Section II, the fabrication process for the periodic laser arrays is described. Experimental results for lasers with various structures will be presented in Section III. In Section IV, a discussion of the experimental data is presented, and the results of this paper are summarized in Section V.

II. Laser Fabrication

The fabrication of nonplanar periodic laser arrays has been described previously [4], [5]. The resulting structure is shown in Fig. 1. The important features of the structure are the nonplanar active region with a series of grooves and mesas and a bent region connecting the grooves and mesas, which serves to provide index guiding and prevent lateral lasing and amplified spontaneous emission [4], [5]. Epitaxial growth was performed in an atmospheric pressure MOCVD reactor described previously [9]. Three different $Al_xGa_{1-x}As/GaAs$ GBQWH [7], [8] laser wafers were prepared on etched GaAs substrates for this study. All three structures consist of a 0.25 μm GaAs buffer layer ($n = 1 \times 10^{18}$), a 0.5 μm linearly graded $Al_xGa_{1-x}As$ buffer layer ($0.0 \leq x \leq x_c$, $n = 1 \times 10^{18}$), a 1.0 μm $Al_xGa_{1-x}As$ confining layer ($n = 1 \times 10^{18}$, $x = x_c$), a 1200 Å parabolically graded $Al_xGa_{1-x}As$ layer ($x_c \geq x \geq 0.20$, $n = 5 \times 10^{16}$), a 50 Å GaAs single quantum well (undoped), a 1200 Å parabolically graded $Al_xGa_{1-x}As$ layer ($0.20 \leq x \leq x_c$, $p = 1 \times 10^{17}$), a 1.0 μm $Al_xGa_{1-x}As$ confining layer ($p = 2 \times 10^{18}$, $x = x_c$), and a 0.2 μm GaAs contact layer ($p = 3 \times 10^{19}$). The first two wafers, one with $x_c = 0.85$ and one with $x_c = 0.40$, labeled wafer I and wafer II, respectively, were grown, with a mesa width of approximately 3.6 μm, a groove width of about 3.2 μm, and a bent region width of approximately 0.6 μm, resulting in a center-to-center spacing between adjacent mesas or grooves of 8 μm. Wafer III has the same structure as wafer I, except the

Manuscript received October 6, 1988; revised January 18, 1989. This work was supported in part by the National Science Foundation Engineering Research Center for Compound Semiconductor Microelectronics under Grant CDR 82-22666 and in part by the Naval Research Laboratory under Contract N00014-88-K-2005.

The authors are with the Compound Semiconductor Microelectronics Laboratory, University of Illinois at Urbana-Champaign, Urbana, IL 61801.

IEEE Log Number 8927326.

0018-9197/89/0600-1539$01.00 © 1989 IEEE

Loss in Heterostructure Waveguide Bends Formed on a Patterned Substrate

T. K. TANG, L. M. MILLER, E. ANDIDEH, T. COCKERILL, MEMBER, IEEE, P. D. SWANSON, R. BRYAN, T. A. DeTEMPLE, MEMBER, IEEE, I. ADESIDA, SENIOR MEMBER, IEEE, AND J. J. COLEMAN, SENIOR MEMBER, IEEE

Abstract—**An experimental comparison is made of the loss of Al$_x$Ga$_{1-x}$As heterostructure waveguide routing geometries at ≈860 nm patterned by two methods: Zn impurity induced layer disordering and native growth on a patterned substrate. Two multimode geometries were investigated: a raised cosine *s*-bend and a modified abrupt bend due to Shiina *et al.* [8, p. 736]. The measured transition distance for 3 dB loss was approximately 300 μm for 100 μm offset guides in the *s*-bend geometry for the patterned substrate samples using wet and dry etching methods. For the Shiina bend, the measured angle corresponding to the 3 dB loss was ≈ 13° also for both etching methods. These results represent significant improvements over the equivalent structures fabricated by impurity induced layer disordering primarily because of reduced free-carrier loss.**

RECENTLY, a method has been demonstrated for the fabrication of high-power, wide, multiple-stripe lasers on etched substrates on which the heterostructure is grown [1]–[3]. By this means, a lateral index difference, and hence waveguide, is achieved by the index of the upper confining layer which rolls over the substrate rib as is illustrated in the micrograph of Fig. 1. This approach is distinct from an etched regrowth approach in that the waveguide core, or active region, is surrounded by a native growth which should result in better metallurgical electrical and optical properties. It has also been demonstrated that multiple heterostructure active and passive waveguides can be grown in an optically self-aligned fashion suggesting this as a means for patterning a laser integrated with a waveguide which might also contain electrooptical elements such as modulators or routing elements [4].

In this paper, we report measurements of the passive routing properties of waveguide structures fabricated by the patterned substrate–native growth approach. In particular, we study one heterostructure with routing geometries which have been used to characterize impurity induced layer disordered structures so that we have a direct comparison to one existing fabrication method [5]–[7].

The heterostructure used in this study was comprised of a 1 μm thick superlattice (5 nm of GaAs and 5 nm of AlAs) which contains a centered 10 nm GaAs quantum well bounded by 10 nm AlAs barriers. The superlattice is bounded by 1.0 μm (bottom) and 0.75 μm (top) layers of $Al_{0.5}Ga_{0.5}As$, which formed the vertical waveguide cladding layers, and is capped by 100 nm of GaAs. The structure was grown, by metalorganic chemical vapor deposition, on an n-type GaAs substrate with 0.25 μm buffer layers and doped to form a p–i–n diode. The quantum well served to define the band-gap of the core and also synthesized an approximate laser-like structure.

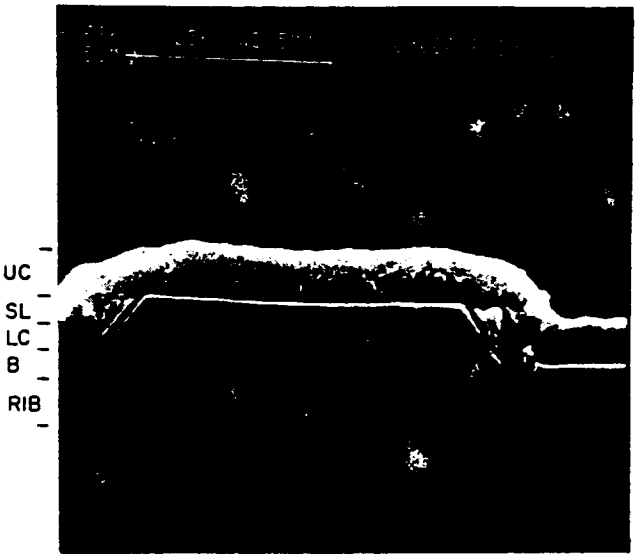

Fig. 1. Scanning electron microscope image of the cleaved and stained edge of a heterostructure grown on a patterned substrate. The labels indicate the buffer layer (*B*), lower (LC) and upper (UC) confining layers, and the superlattice core (SL).

The routing structures investigated in this study were a modified abrupt-like bend in the form of a Shiina geometry [8], shown in Fig. 2, and an *s*-bend in the form of a raised cosine pattern, shown in Fig. 3 [9]. The original structure, in the form of 10 μm linewidth masks, was patterned onto the substrate by both wet and dry methods. A wet etch, H_2SO_4:H_2O_2(30 percent):H_2O (1:8:80 by volume), was employed for the former method. For the dry etch method, a commercial reactive ion etch system (Plasma Technology RD80) with Freon 23 was used to transfer the photoresist pattern onto a SiO_2 masking layer followed by an etch of the GaAs substrate in an $SiCl_4$ (7 mTorr). The depth of both the wet

Manuscript received March 20, 1989. This work was supported in part by the National Science Foundation sponsored Engineering Research Center for Compound Semiconductor Microelectronics, CDR 85-22666, the U. S. Army Research Office: Durham, DAAL 03-86-K-0089, and the University of Illinois Industrial Affiliates Program.

The authors are with the Engineering Research Center for Compound Semiconductor Microelectronics and the Department of Electrical and Computer Engineering, University of Illinois, Urbana, IL 61801.

IEEE Log Number 8929018.

1041-1135/89/0600-0120$01.00

High-Power Pulsed Operation of an Optimized Nonplanar Corrugated Substrate Periodic Laser Diode Array

R. P. BRYAN, L. M. MILLER, T. M. COCKERILL, S. M. LANGSJOEN, AND J. J. COLEMAN

Abstract—**High-power pulsed operation of 14.1 W per uncoated facet from an optimized 3 mm wide (510 μm cavity length) nonplanar corrugated substrate periodic laser diode array is reported. Single-step metalorganic chemical vapor deposition growth over a selectively etched corrugated substrate provides suppressed lateral lasing and amplified spontaneous emission with a minimal number of processing steps. Higher external differential quantum efficiency, slope efficiency, and output power result from a design optimization with regard to the widths of the mesas and grooves of the corrugated substrate.**

MONOLITHIC multiple-stripe laser arrays have great potential as sources for high-power, high-efficiency operation. Applications for such devices include pumping of neodymium : yttrium aluminum garnet lasers [1], high-speed optical recording, and long-distance transmission. Although the maximum output optical power attainable from multiple-stripe laser diodes has increased dramatically in recent years, high-power operation is limited [2] by catastrophic optical degradation (COD). By increasing the aperture width of a laser diode, the intensity decreases for a given output power and, therefore, the total power at which COD occurs is increased. However, the maximum aperture width is generally restricted to being less than the cavity length because, as the width of the laser is made larger than the cavity length, lateral lasing and amplified spontaneous emission (ASE) become significant and the desired front facet emission is reduced. Lateral lasing and ASE can be suppressed by forming isolated regions of emitters thereby disrupting the propagation of the lateral modes. Previously reported [3]–[4] methods for achieving isolation require processing steps in addition to those required to form the actual array elements and also result in a portion of the array width which does not contribute to the laser output. In this letter we report optimized high-power, high-efficiency operation of a nonplanar multiple-stripe corrugated substrate laser array utilizing a graded-barrier quantum well (GBQW) [5], [6] structure. Metalorganic chemical vapor deposition (MOCVD) growth on a corrugated substrate is utilized [7]–[10] to form a nonplanar active region which effectively inhibits lateral lasing and ASE for the entire array. No additional processing steps, which may result in accelerated degradation due to the introduction of material defects, are required. Data presented within on the high-power pulsed operation (14.1 W per uncoated facet) of an optimized 3 mm wide corrugated substrate laser array represent a substantial improvement in device performance characteristics over previously obtained results on similar structures [7], [8], [11]. We report an increased maximum output power and linear power density; a highly uniform emission intensity across the structure; and a 40 percent improvement in the slope efficiency and differential quantum efficiency.

The GBQW structures were grown using an atmospheric MOCVD [12] system at 800°C following corrugated substrate preparation described previously [7]. The structure consists of a (100) GaAs : n substrate and buffer layer, a linearly graded AlGaAs : n layer, 1.0 μm $Al_{0.85}Ga_{0.15}As$ confining layers, a 2400 Å $Al_xGa_{1-x}As$ parabolically graded (x = 0.85 to 0.20) region, a 50 Å GaAs quantum well, and a GaAs : p^+ contact layer. The corrugated contours of the etched substrate are maintained throughout the epitaxial growth providing uniform formation of the active region (see Fig. 1) [7]–[9]. The nonplanar active region disrupts the propagation of the lateral cavity modes and no additional processing or photolithographic steps are necessary to either define current injection or to inhibit ASE or lateral lasing after the MOCVD growth. For comparison, 150 μm wide oxide stripe broad area lasers were fabricated from planar structures grown concurrently with each of the nonplanar substrates. The devices were mounted p side down in indium solder on Cu blocks with multiple Au wires to contact the n side and were tested using a 1 kHz pulsed current with a pulse duration of 225 ns. The facets of the devices described in this letter were left uncoated.

A typical near-field optical intensity pattern from a section of the nonplanar laser array is illustrated in Fig. 2. Shown also in Fig. 2 for reference as a dashed line is the relative size and position of the laser active region. The observed near-field pattern is uniformly distributed over the entire array width and is stable over a wide range of drive currents. Note that the emission is entirely from a double peak on each mesa [8], [9]. As a consequence of the negligible emission from the grooves there is a reduction in the efficiency [9] of nonplanar lasers relative to

Manuscript received July 27, 1989; revised October 2, 1989. This work was supported in part by Strategic Defense Initiative Organization/IST under Contract DAAL03-87-K-0013, by the Naval Research Laboratory under Contract N00014-88-K-2005, and by the National Science Foundation Engineering Research Center for Compound Semiconductor Microelectronics under Contract CDR 85-22666. The work of R. P. Bryan was supported in part by an AT&T Doctoral Fellowship. The work of T. M. Cockerill was supported in part by a Hughes Fellowship.

The authors are with the Compound Semiconductor Microelectronics Laboratory and the W. L. Everitt Laboratory, University of Illinois at Urbana-Champaign, Urbana, IL 61801.

IEEE Log Number 8932611.

Temperature dependence of compositional disordering of GaAs-AlAs superlattices during MeV Kr irradiation

R. P. Bryan, L. M. Miller, T. M. Cockerill, and J. J. Coleman
Materials Research Laboratory and Department of Electrical and Computer Engineering, University of Illinois at Urbana-Champaign, Urbana, Illinois 61801

J. L. Klatt and R. S. Averback
Department of Material Science and Engineering, University of Illinois at Urbana-Champaign, Urbana, Illinois 61801
(Received 14 August 1989)

The influence of the specimen temperature during MeV Kr irradiation on the extent of compositional disordering in GaAs-AlAs superlattices has been determined. For low-temperature irradiations (133–233 K), complete intermixing of the superlattice is observed. However, the mixing efficiency *decreases* with increasing specimen temperature between room temperature and 523 K. These results suggest the existence of a miscibility gap in the coherent-phase diagram of GaAs-AlAs superlattices with a critical temperature greater than 523 K.

Compositional disordering of III-V compound semiconductor epitaxial structures has great promise for the microfabrication of unique optical and electronic devices. One of the requirements for device fabrication is that the disordering be achieved selectively. Impurity-induced compositional disordering using Zn or Si diffusion or conventional ion implantation is often employed[1–3] for this purpose. However, in some cases, the incorporation of such electrically active impurities is undesirable.[4] Ion-beam mixing provides an alternative means for inducing selective compositional disordering, not limited to active impurities. Important considerations for ion-beam mixing are the damage the irradiation introduces into the sample, the ability to anneal such damage, and the efficiency with which the superlattice can be disordered. An important parameter for all three of these concerns is the sample temperature during the mixing irradiation.[5] This work focuses on the influence of sample temperature on the mixing efficiency. We will show the unexpected result that the mixing efficiency decreases with increasing substrate temperature between room temperature and 523 K, the highest temperature employed in this work. The implication of this observation is the existence of a miscibility gap in the coherent-phase diagram of the GaAs-AlAs superlattice system (wavelength ~400 Å) with a critical temperature greater than 523 K.

The technical implications of ion-beam mixing for the fabrication of thin-film devices and for surface treatments have been recognized[6] for several years, and a basic understanding of the physical processes underlying ion-beam mixing are beginning[7–9] to emerge. Two regimes are distinguishable[5,8–10] in the temperature dependence of ion-beam mixing. At lower temperatures, mixing is nearly independent of temperature and the system can be driven far from thermodynamic equilibrium. At higher temperatures, mixing is strongly (exponentially) dependent on temperature and the system moves toward equilibrium.

Ion-beam mixing in the low-temperature regime derives from the atomic rearrangement which occurs during the evolution of energetic displacement cascades. Early in the cascade evolution, atoms are displaced from their lattice sites by collisions with energies greater than ~5 eV. Later, when the initial recoil energy becomes partitioned among all atoms in the volume of the cascade, a thermal spike condition develops and diffusion takes place within the hot spike. Although questions about thermal spike dynamics remain, it is recognized[5,7,8] that atomic motion occurs while the atoms are highly excited, with atomic energies on the order of 1 eV. It is because the atomic rearrangements occur with such high energies relative to the ambient lattice temperature that a system can be driven far from equilibrium. In addition to creating atomic disorder, displacement cascades also produce point defects, i.e., vacancies and interstitial atoms. At elevated lattice temperatures, these defects are mobile and cause atomic diffusion, usually called radiation-enhanced diffusion. Since this diffusion process takes place long after the thermal spike has cooled and extends well beyond the original boundaries of the displacement event, radiation-enhanced diffusion tends to return the system to equilibrium. Although cascade mixing and radiation-enhanced diffusion both occur during high-temperature irradiations, the latter dominates at sufficiently high temperatures.[10] The transition between low- and high-temperature mixing occurs in the temperature range where both vacancies and interstitials become mobile, above room temperature in most cases. The experiments described here were undertaken to determine the transition-temperature range and to explore whether radiation-enhanced diffusion could be employed to enhance the disordering efficiency of the superlattice.

The samples used for these experiments were GaAs-AlAs superlattice (SL) structures grown[11] by atmospheric pressure metalorganic chemical vapor deposition at 800 °C. The substrates are (100)GaAs doped with silicon to a carrier concentration of 2×10^{18} cm^{-3}. The epitaxial structure consists of a 0.25-μm GaAs undoped buffer layer and a 50-period undoped SL of alternating layers of 200-Å GaAs and 200-Å AlAs. As a consequence of the growth temperature, the superlattice has a background p-

TEMPERATURE DEPENDENCE OF COMPOSITIONAL DISORDERING OF GAAS-ALAS SUPERLATTICES DURING MEV KR IRRADIATION

R. P. Bryan, L. M. Miller, T. M. Cockerill, J. J. Coleman, J. L. Klatt and R. S. Averback
Materials Research Laboratory
University of Illinois
Urbana, IL 61801

ABSTRACT

The influence of the specimen temperature during MeV Kr irradiation on the extent of compositional disordering in GaAs-AlAs superlattices (SLs) has been determined. We have investigated whether radiation-enhanced diffusion (RED) could be employed to reduce the dose required to completely disorder a SL by ion implanation. Metalorganic chemical vapor deposition grown GaAs-AlAs SLs were implanted with 0.75 MeV Kr to a dose of $2x10^{16}$ cm^{-2} at various sample temperatures ranging from 133 K to 523 K. The extent of disordering induced by the irradiations was determined by Rutherford backscattering spectrometry and secondary ion mass spectrometry. For low temperature irradiations (133 K to 233 K), complete intermixing of the SL is observed. However, the extent of intermixing of the SL *decreases* with increasing specimen temperature between room temperature and 523 K. We propose two possible explanations to interpret these results: (i) that the amount of ion beam mixing decreases with increasing temperature; and (ii) that the RED coefficient is negative which suggests the existence of a miscibility gap in the GaAs-AlAs SL system.

INTRODUCTION

Compositional disordering of III-V compound semiconductor epitaxial structures has great promise for the microfabrication of unique optical and electronic devices. In recent years, considerable interest has been shown in efforts directed towards fabricating buried heterostructure (BH) lasers [1] by compositional disordering of the active region of the device. The authors have previously reported [2] the fabrication of index-guided BH lasers in which we utilize the compositional disordering and semi-insulating characteristics [3] of MeV oxygen implanted AlGaAs layers. A single oxygen implant into a sample through a stripe mask results in lateral confinement of both the optical field and injected carriers (see Fig. 1). High dose oxygen implants (10^{17} cm^{-2}) are necessary [3], though, to induce the compositional disordering required to confine the optical field and, thereby, achieve index-guided laser operation. However, we observe that low dose implants (~10^{14} cm^{-2}) are sufficient [2] to compensate the layers. Therefore, the transverse straggle of the implant leads to a large compensated region under the implantation mask which results in a substantial increase in the threshold current of very narrow stripe width lasers. We have thus considered using radiation-enhanced diffusion to decrease the dose required to induce the compositional disordering of the AlGaAs heterostructure.

During an implantation, the temperature [4] of the sample significantly affects the diffusion of defects and, therefore, the extent of mixing. Three temperature regimes [4-7] are distinguishable in the chemical interdiffusion coefficient during implantation (see Fig. 2). At high temperatures, thermal diffusion is the most significant mixing mechanism but the diffusion coefficient decreases rapidly with decreasing temperature due to a high activation energy. At intermediate sample temperatures, radiation-enhanced diffusion dominates; it is also exponentially dependent on the sample temperature but the activation energy for the process is less than that of the thermal diffusion process. At lower sample temperatures, mixing is dominated by ion beam mixing which is usually assumed to be nearly independent of temperature.

Ion beam mixing [5-6,8] in the low temperature regime is a result of the diffusion which occurs during the dissipation of the energy transferred during collisions between the implanted ion and the target nuclei, *i.e.* a result of the mixing within the displacement cascades. Early in the cascade evolution, atoms are displaced from their lattice sites by collisions with energies greater than ~ 5 eV. Later, when the initial recoil energy becomes partitioned among all atoms in the volume of the cascade, a thermal spike condition develops and diffusion takes place within the hot spike. Although questions about thermal spike dynamics remain, it is recognized [4-5,8] that

In-phase operation of high-power nonplanar periodic laser arrays

R. P. Bryan, T. M. Cockerill, L. M. Miller, T. K. Tang, T. A. DeTemple, and J. J. Coleman
Compound Semiconductor Microelectronics Laboratory, University of Illinois, 208 North Wright Street, Urbana, Illinois 61801

(Received 29 May 1990; accepted for publication 17 October 1990)

The transformation of nonplanar periodic laser array modes from weakly locked out-of-phase to locked in-phase operation is investigated. A comparison study of near-field and far-field patterns is made for devices with differing mesa widths and heights. Data are presented which show that the mesa height and width can be adjusted to force in-phase operation. An array of 19 elements shows an essentially single-lobed far-field pattern centered at 0° with full width at half maximum of 1.6°, to output powers of more than 500 mW/uncoated facet.

Recently there has been considerable interest in developing high-power arrays[1-5] which may be used in such applications as pumping of solid-state lasers, long distance communication, lidar, high-speed modulation, and optical recording. In many applications, the optical output power needs to be a nearly diffraction limited single-lobed beam. However, coherent semiconductor laser arrays typically operate with each element locked out of phase which leads to a double-lobed far-field pattern. Several array structures including leaky waveguide arrays,[3] Y-coupled arrays,[1,6,7] diffraction-coupled arrays,[8] and offset stripe arrays[9] have been developed which exhibit stable, single-lobed far-field patterns. However, in general, these methods require some combination of multiple growths and sophisticated or complex processing. We report in this letter a relatively simple procedure to obtain high-power, in-phase operation of wide aperture laser arrays which require only simple processing and a single metalorganic chemical vapor deposition (MOCVD) growth. Index-guided laser structures grown on patterned substrates[10] can be formed into high power, wide aperture laser arrays[11,12] made possible by the incorporation of a nonplanar active region in the form of a regular pattern of mesas and grooves to suppress lateral lasing and amplified spontaneous emission. We have investigated the characteristics and, in particular, the far-field pattern of devices with various mesa heights and widths. By varying the width and the height of the mesas, we are able to transform the array elements from being weakly locked out of phase to being locked in phase. Consequently, we obtain a single-lobed far-field pattern from the laser array. Stable, near-diffraction-limited operation is obtained to over five times threshold with more than 500 mW/per facet of optical power for devices 150 μm wide and 380 μm long.

The laser device configuration utilized for this study is similar to nonplanar periodic laser arrays reported previously.[10,11] The laser structure is an AlGaAs-GaAs graded barrier quantum well heterostructure with a 50 Å quantum well grown by MOCVD. The first step in forming the array is wet chemical etching of a periodic pattern of mesa stripes into a GaAs substrate. We have investigated devices with shallow and deep mesas (0.3 μm and 0.6 μm etch depth respectively) as well as wide and narrow mesas (3.1 μm and 2 μm width at the active region, respectively). The center-to-center spacing between mesas was kept constant at 8 μm. Following etching, the devices are completed by a single MOCVD growth of the entire laser structure and contact metallization. In selected devices, 150-μm-wide oxide defined stripes were incorporated in order to accurately control the width and therefore the number of elements of the device. A schematic of the array structure and a scanning electron micrograph of the cross section are shown in Fig. 1 of the narrow, shallow mesa array. The MOCVD growth on a corrugated substrate forms a nonplanar active region which provides[10,11] definition of the individual emitters of the array, formation of a step in the effective index of refraction for stable mode operation, and suppression of the lateral lasing and the amplified spontaneous emission, thereby allowing high-power operation of wide aperture devices.

As reported previously,[12] the far-field patterns of devices with wide, deep mesas are very broad and double lobed. In order to determine the parameters which lead to the transformation from weakly locked out-of-phase to stable in-phase operation, we compared the far-field pattern of devices with different widths and heights of the mesas. For the comparison, the length and the width of the devices were kept relatively constant at 380 and 560 μm, respectively. Figure 2(a) shows the far-field pattern for a nonplanar laser array with mesas 0.6 μm high and 3.1 μm wide. The far-field pattern consists of two broad lobes at approximately $\pm 10°$. The full width at half maximum (FWHM) for each is $\sim 12°$ with no null at 0°. These patterns indicate that the emitters of the device are weakly locked out of phase. In the far field of the wide (3.1 μm), shallow (0.3 μm) mesa devices we observe a reduction of the width of the lobes as shown in Fig. 2(b). The far-field pattern is also double lobed with a narrower FWHM ($\sim 5°$) for these devices and the minimum at zero is more pronounced. For narrow (2 μm), shallow (0.3 μm) mesa devices the far-field pattern narrows to a predominantly single-lobed pattern. The FWHM for the main lobe is 2.2° with sidemodes spaced at 5.8–6.0° as shown in Fig. 2(c).

By reducing the mesa width at the active region from 3.1 to 2 μm and reducing the etch depth to only 0.3 μm, the far-field pattern switches from being a double-lobed pattern to a sharply peaked single-lobed pattern as seen in Fig. 2. Limiting the number of elements to nineteen with 150 μm oxide defined stripes further reduces the FWHM of the far-field pattern to 1.6° as shown in Fig. 3. Although

 0003-6951/91/020113-03$02.00

Characteristics of step-graded separate confinement quantum well lasers with direct and indirect barriers

L. M. Miller, K. J. Beernink, T. M. Cockerill, R. P. Bryan, M. E. Favaro, J. Kim, J. J. Coleman, and C. M. Wayman
Compound Semiconductor Microelectronics Laboratory and Materials Research Laboratory, University of Illinois, 1406 West Green Street, Urbana, Illinois 61801

(Received 12 February 1990; accepted for publication 14 May 1990)

Data are presented on step-graded separate confinement quantum well lasers with $Al_{0.85}Ga_{0.15}As$ outer confining layers, $Al_xGa_{1-x}As$ barriers and a 50-Å GaAs quantum well grown by metalorganic chemical vapor deposition. By varying x_b from 0.15 to 0.60, we show that, given an adequate optical waveguide confinement factor and sufficient cavity length, the collection of electrons in thin quantum wells with either direct or indirect barriers can be highly efficient, transfer of electrons from indirect barriers to thin direct wells does not degrade laser performance, and electron confinement in the separate confinement region plays no role in the operation of the laser.

I. INTRODUCTION

Quantum well heterostructure lasers have been extensively studied because of their excellent emission characteristics such as low threshold current density, high quantum efficiency and two-dimensional density of states. A topic of considerable discussion[1-9] is the mechanism of carrier capture by the quantum well. Holonyak *et al.*[1] determined that, for single well lasers, electrons within a diffusion length of the well will scatter into the well, provided the well width is larger than the mean free scattering length[2] of the electron. Shichijo *et al.*[3] concluded from the emission spectra of photopumped quantum well lasers that carrier collection becomes highly inefficient for well widths below 100 Å. Separate confinement heterostructure (SCH) lasers are thought[4] to improve carrier capture in the well by providing an intermediate or graded energy region of larger volume surrounding the well, thereby allowing for the use[5-8] of very thin quantum wells. Much of this work with SCH lasers has focused on the use of quantum wells with direct energy gap barriers and has not addressed the issue of electron transfer from indirect material. Theoretical work by Tang *et al.*[9] suggests that this transfer is no less efficient than transfer from direct barriers. In this study, we present data on the pulsed operation of AlGaAs/GaAs step-graded separate confinement quantum well lasers each with a 50-Å quantum well, $Al_xGa_{1-x}As$ inner barriers in which the composition x_b is varied from direct to indirect ($x = 0.15$–0.60), and outer confining layers of $Al_{0.85}Ga_{0.15}As$. By varying the waveguide and energy band characteristics in this way, we show that, given an adequate optical waveguide confinement factor and sufficient cavity length, (1) the collection of electrons in thin quantum wells with both direct and indirect barriers can be highly efficient, (2) transfer of electrons from indirect barriers to thin direct wells does not degrade laser performance, and (3) electron confinement in the separate confinement region plays no role in the operation of the laser. The relatively small increase in threshold current density observed with increasing barrier composition x_b is explained by increased free carrier absorption in the barrier layers and the outer confining layers.

II. EXPERIMENT

The laser structures studied here were grown at 800 °C in an atmospheric pressure metalorganic chemical vapor deposition (MOCVD) system[10] with a vertical chamber using trimethylgallium, trimethylaluminum and arsine for constituents and using disilane, magnesium, and intrinsic carbon as dopant sources. Growth rates varied from 2 μm/h for GaAs to 3.7 μm/h for $Al_{0.85}Ga_{0.15}As$. The basic structure consists of a GaAs:n substrate (Si doped, $n = 10^{18}cm^{-3}$), a GaAs:n^+ buffer layer (0.25 μm, $10^{18}cm^{-3}$), a graded $Al_xGa_{1-x}As:n^+$ layer ($0 < x < 0.85$, 0.5 μm, $1.5\times10^{18}cm^{-3}$), n- and p-$Al_{0.85}Ga_{0.15}As$ outer confining layers (1.5 μm, 1.5×10^{18} cm^{-3}), $Al_xGa_{1-x}As$ inner barrier layers (x_b, 0.1 μm), a single 50-Å GaAs quantum well, and a GaAs-p^+ cap layer (0.2 μm, 10^{19} cm^{-3}). Eight structures were grown varying only the composition of the inner barrier layers with compositions of $x_b = 0.15$, 0.20, 0.25, 0.30, 0.35, 0.40, 0.50, and 0.60. The undoped barrier layers have nominal background carbon doping levels ranging from $p\sim10^{16}$ cm^{-3} ($x_b = 0.15$) to $p\sim10^{18}cm^{-3}$ ($x_b = 0.60$) as determined by van der Pauw measurements of bulk samples grown under the same conditions. The barrier layers for the structures having $x_b = 0.50$ and 0.60 are counter doped[10] with Si on the n-side of the well to $n\sim3\times10^{17}cm^{-3}$ ($x_b = 0.50$) and $n\sim10^{18}cm^{-3}$ ($x_b = 0.60$). The total thickness of the barrier layers was chosen to be 0.2 μm to optimize[11] the optical waveguide confinement factor Γ. Cross-section specimens were examined by transmission electron microscopy (TEM) on a Philips 420 microscope in order to verify the quantum well thicknesses of 50 Å (±5 Å) in the structures containing the $x_b = 0.50$ and $x_b = 0.60$ barriers.

The as-grown wafers were processed into 150-μm-wide oxide-defined broad stripe lasers using standard photolithographic techniques. A relatively large cavity length

 0021-8979/90/171964-04$03.00

Depressed index cladding graded barrier separate confinement single quantum well heterostructure laser

T. M. Cockerill, J. Honig, T. A. DeTemple, and J. J. Coleman
Microelectronics Laboratory, University of Illinois, 208 North Wright Street, Urbana, Illinois 61801

(Received 26 July 1991; accepted for publication 26 August 1991)

In this letter, we present data for a novel depressed index cladding laser structure which provides reduced perpendicular far-field divergence angle with acceptable low-threshold current densities. Narrow perpendicular divergence angles of 27° full width at half maximum for a nearly perfect Gaussian beam shape have been measured, with a corresponding near-field spot size of 1.30 μm. Threshold current densities of 309 A/cm^2 are observed for 150 μm stripewidth, 780 μm long devices with 0.80 μm transverse spot sizes. Pulsed output powers for unmounted devices are greater than 0.9 W/uncoated facet.

Single quantum well heterostructure lasers are characterized by high quantum efficiency, low-threshold current, high output power, and quantum size effect wavelength selectivity. Thin single-well lasers are also characterized, however, by a relatively small near-field spot size and large beam divergence in the direction perpendicular to the junction plane. This results in relatively large coupling losses into optical fiber systems. Several methods for reducing the divergence angle have been demonstrated, including the large optical cavity (LOC) double-heterostructure laser[1] and monolithically stacked[2] multiple graded index quantum well heterostructure lasers. In this letter, we present data for a novel single quantum well heterostructure laser, the graded barrier depressed index cladding[3] (DC) laser, in which the perpendicular divergence angle is decreased while a reasonable threshold current density is maintained. The structure is formed by inserting high aluminum composition, low index, beam shaping layers adjacent to the graded index core of the quantum well structure. This geometry should provide lower coupling loss for integration with optical fibers[4] and, with the additional incorporation of some form of lateral patterning, should allow the realization of a quantum well laser with a nearly circular transverse emission profile. Additionally, the larger near-field spot size will increase the power level for the onset of catastrophic optical degradation (COD) by reducing the power density at the laser facets for a given drive current.

The DC lasers were grown by atmospheric pressure metalorganic chemical vapor deposition[5] in a vertical geometry, rotating disk reactor. The column III sources are trimethylgallium and trimethylaluminum and the column V source is 10% arsine in hydrogen. The *n*- and *p*-type dopants are disilane and diethylzinc, respectively. The growth temperature is 800 °C except for the top contacting layer which is grown at 650 °C to enhance the *p*-type dopant incorporation. Shown in Fig. 1(a) is the compositional profile of the structure which consists of a GaAs buffer layer and contact layer, 0.5 μm highly doped (2×10^{18} cm^{-3}) $Al_{0.30}Ga_{0.70}As$ outer cladding layers, highly doped (2×10^{18} cm^{-3}) $Al_{0.85}Ga_{0.15}As$ inner cladding layers of thickness $\delta\cdot T_{core}$, and an undoped 100 Å GaAs quantum well (QW) surrounded by parabolically graded undoped $Al_xGa_{1-x}As$ ($0.30>x>0.20$) barriers of thickness T_{core}. A series of lasers was grown with T_{core} of 0.5 and 0.8 μm and with $\delta = 0.3$ and 0.6. A series of lasers was also grown with $T_{core} = 0.3$ μm. The transverse index profile for these structures, however, resulted in a weakly confined optical field in the transverse direction. For comparison, we will make reference to a high performance[6,7] conventional graded index single quantum well structure. This structure consists of a GaAs buffer layer, a 0.5 μm linearly graded $Al_xGa_{1-x}As$ ($0<x<0.85$) layer, 1.5 μm highly doped (2×10^{18} cm^{-3}) $Al_{0.85}Ga_{0.15}As$ cladding layers, an undoped 100 Å GaAs QW surrounded by 1200 Å parabolically graded $Al_xGa_{1-x}As$ ($0.85>x>0.20$) barriers, and a GaAs top contact layer. The laser material was processed by standard photolithography into oxide defined stripe lasers with stripe widths of 4, 6, 8, 10, 12, 25, 50, and 150 μm. The wafers were then lapped and polished to ~4 mil thickness, metallized, and cleaved into bars of various lengths. Devices were tested unmounted and pulsed with a 2 kHz repetition rate and a 1.5 μs pulse. No facet coatings were applied.

Shown in Fig. 1(b) is the real refractive index profile for the DC laser. The insertion of the depressed index inner

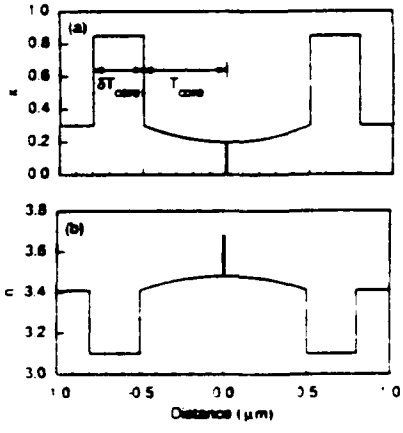

FIG. 1. Composition profile (a) and real refractive index profile (b) for a depressed cladding laser ($T_{core} = 0.5$ μm, $\delta = 0.3$). T_{core} is the waveguide half thickness and δT_{core} is the depressed cladding notch thickness.

 0003-6951/91/462694-03$02.00

Phase-locked ridge waveguide InGaAs-GaAs-AlGaAs strained-layer quantum well heterostructure laser arrays

K. J. Beernink, L. M. Miller, T. M. Cockerill, and J. J. Coleman
Microelectronics Laboratory, University of Illinois, 208 North Wright Street, Urbana, Illinois 61801

(Received 1 July 1991; accepted for publication 24 September 1991)

We report the characteristics of separate confinement heterostructure InGaAs/GaAs/AlGaAs strained-layer quantum well heterostructure ($\lambda > 1$ μm) ridge waveguide laser arrays grown by metalorganic chemical vapor deposition, and etched by reactive ion etching. The ten element arrays have ridge widths of 4 μm on 8 μm centers. Several etch depths are examined, covering the range from gain-guided to strongly index-guided elements. For these structures, values of effective index step, Δn_{eff}, below $\sim 6 \times 10^{-3}$ are necessary to achieve interelement coupling. For $\Delta n_{eff} = 1.3 \times 10^{-3}$, the devices lase in the highest array mode up to ~ 1.5 times threshold with a nearly diffraction-limited double-lobed far-field pattern. For higher currents, additional structure in the far-field pattern is observed, and is accompanied by splitting of the longitudinal modes due to operation in additional array modes.

Semiconductor laser arrays are attractive because of their ability to produce large optical power in narrow, coherent beams. Specifically, high power from InGaAs/GaAs/AlGaAs strained-layer lasers with $\lambda \sim 1$ μm is a useful source for second harmonic generation of visible light, and offers the opportunity for replacement of Nd-YAG at $\lambda \sim 1.06$ μm with a smaller, more efficient source. In order to avoid the highly astigmatic output pattern of gain-guided arrays, the use of index-guided elements is preferable. Previously, index-guided arrays of InGaAs/GaAs/AlGaAs lasers have been formed by metalorganic chemical vapor deposition (MOCVD) over corrugated substrates,[1] by impurity-induced layer disordering,[2] and by a two-step MOCVD process to form leaky mode arrays.[3] Ridge waveguides offer another means of forming index-guided arrays, and GaAs/AlGaAs ridge waveguide arrays have been reported.[4–6] In this letter, we report the operation of separate confinement heterostructure InGaAs/GaAs/AlGaAs strained-layer quantum well heterostructure ($\lambda > 1$ μm) ridge waveguide laser arrays grown by MOCVD and etched by reactive ion etching (RIE). By fabricating devices with several different etch depths, we investigate the range from gain-guided to strongly index-guided elements.

The separate confinement heterostructure quantum well laser structures were grown on GaAs ($n = 10^{18}$ cm^{-3}) substrates by atmospheric pressure MOCVD[7] and consist of a 0.25 μm GaAs buffer layer ($n = 10^{18}$ cm^{-3}), a 1.5 μm $Al_{0.2}Ga_{0.8}As$ cladding layer ($n = 10^{18}$ cm^{-3}), 0.1 μm GaAs inner barriers ($n = 10^{17}$ cm^{-3} and $p = 10^{17}$ cm^{-3}) surrounding a 70 Å $In_{0.31}Ga_{0.69}As$ quantum well, a 1.5 μm $Al_{0.2}Ga_{0.8}As$ cladding layer ($p = 10^{18}$ cm^{-3}), and a 0.2 μm GaAs ($p = 10^{19}$ cm^{-3}) ohmic contact layer. Growth conditions are described elsewhere.[7]

The ridge structure, shown schematically in Fig. 1, consists of 10 elements with 4 μm wide mesas on 8 μm centers. Standard photolithography and wet chemical etching were used to transfer the ridge pattern into a SiO_2 mask, then the GaAs cap and a portion of the top $Al_{0.2}Ga_{0.8}As$ cladding layer were removed using a $SiCl_4$ plasma in a RIE system. Etch times were varied to produce the desired etch depth. SiO_2 was then redeposited to cover the etched regions and contact windows were opened on top of the mesas by a self-aligned process. The devices were lapped and polished, and an alloyed Au/Ge contact and a Ti/Au contact were formed on the n- and p-sides, respectively. Individual diodes with 510 μm cavity length were mounted p-side down on Cu heat sinks using an In/Pb solder. Devices were tested both pulsed (1.5 μs, 2 kHz) and cw.

The thickness, T, of the residual $Al_{0.2}Ga_{0.8}As$ in the etched regions between ridges, the corresponding effective index steps, Δn_{eff}, and the emission wavelengths, λ, are listed in Table I for the five different etch depths. Structures D and E are from a different growth than the other three structures. Although the layers are nominally the same for the two growths, slight variations resulted in the difference in wavelength. The wavelength difference is also observed in broad area devices, and thus it is not a result of the different etch depths. Δn_{eff} is taken as the difference between the effective index of the transverse waveguides under the ridge and outside the ridge, and is calculated from layer thicknesses and refractive indices assuming that the electric field goes to zero at the metal contact layer.

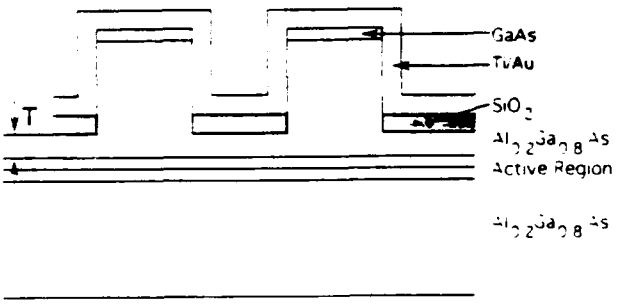

FIG. 1. Schematic diagram showing two elements of a ten element In$_x$Ga$_{1-x}$As/GaAs/Al$_y$Ga$_{1-y}$As strained-layer ridge waveguide array

 0003-6951/91/503222-03$02.00

InGaAs–GaAs–AlGaAs STRAINED-LAYER DISTRIBUTED FEEDBACK RIDGE WAVEGUIDE QUANTUM WELL HETEROSTRUCTURE LASER ARRAY

Indexing terms: Semiconductor lasers, Feedback, Lasers

Strained-layer DFB ridge waveguide laser arrays, requiring only a single MOCVD growth step, exhibit phase-locked emission in the highest order supermode. Uncoated 14 element arrays with CW threshold current of 110 mA and η_{ex} = 36% emit in a single longitudinal mode to above 190 mA. Peak pulsed and CW output powers are 400 mW and 53 mW, respectively.

Introduction: Semiconductor lasers in the form of high power laser arrays can replace solid state lasers in many applications because of their small size, high efficiency and low cost. Distributed feedback laser arrays have an added advantage over other semiconductor laser arrays in that they emit highly coherent light with high spectral and temperature stability, and relatively narrow linewidth. Use of strained-layer InGaAs–GaAs–AlGaAs quantum well heterostructures allows[1,2] reliable, high power operation at emission wavelengths in the range of 0·9–1·1 μm. We present a strained-layer InGaAs–GaAs–AlGaAs quantum well heterostructure distributed feedback ridge array, requiring only a single metal organic chemical vapour deposition (MOCVD) growth step, which is phase-locked in the highest order supermode of the array. A lateral grating on either side of an array element serves as an effective index step to eliminate antiguiding effects[4] and as a source of distributed feedback[3] to produce single longitudinal mode emission at λ = 1·0343 μm. Pulsed and continuous wave (CW) light–current, near-field, far-field and spectral data are presented for fourteen element arrays with cavity lengths of 430 μm and uncoated facets. By optimising the structure, improving the heat sink capacity of our test fixture, and extending the emission wavelength to 1·06 μm, this device may become a viable alternative to the Nd:YAG laser for some applications.

Device fabrication. The strained-layer InGaAs–GaAs–AlGaAs laser structure, grown[4] by atmospheric pressure metal organic chemical vapour deposition (MOCVD), consists of a 0·25 μm GaAs ($n = 10^{18}$ cm^{-3}) buffer layer, a 1·5 μm $Al_{0.2}Ga_{0.8}As$ ($n = 10^{18}$ cm^{-3}) lower cladding layer, 0·1 μm GaAs ($n = 10^{17}$ cm^{-3}, $p = 10^{17}$ cm^{-3}) inner barriers surrounding a 70 Å $In_{0.31}Ga_{0.69}As$ quantum well, a 0·75 μm $Al_{0.2}Ga_{0.8}As$ ($p = 10^{18}$ cm^{-3}) upper cladding layer, and a 0·1 μm GaAs

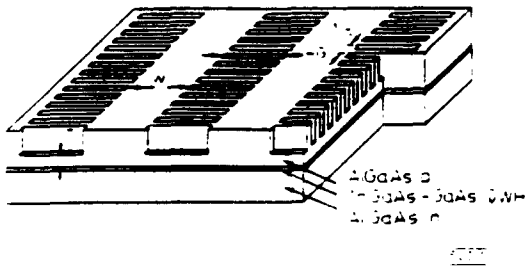

Fig. 1 *Schematic diagram of two element InGaAs–GaAs strained-layer DFB ridge waveguide laser array*

Portion of right grating has been removed for clarity

$p = 10^{19}$ cm^{-3}) ohmic contact layer. Growth conditions[5] have been described previously.

A portion of the DFB laser array is shown schematically in Fig. 1 with a section cut away in the gratings for clarity. Each array consists of 14 w = 2·11 μm mesas defined by lateral third-order gratings of length L_g = 2·01 μm. The third-order grating period, Λ_g = 0·4561 μm, was designed to satisfy the Bragg condition for the emission wavelength of broad area oxide-defined laser structures fabricated from the same laser material. The gratings[3] were patterned using direct write e-beam lithography and etched to within T = 0·10 μm of the upper GaAs inner barrier layer of the as-grown material by reactive ion etching (RIE). The ratio of the etched well width to the period of the grating is 53% which should nearly maximise[3] the coupling coefficient for a third-order grating. The SiO_2 used as the grating mask was stripped and 1500 Å of SiO_2 was redeposited to eliminate any direct contact to the gratings. Contact windows were then opened in the centre of the mesas, again using e-beam lithography. The wafer was lapped and polished to approximately 100 μm. Alloyed n-type Ge/Au/Ni/Au ohmic contacts and nonalloyed p-type Ti/Au contacts were formed on the back and top surfaces, the processed devices were cleaved into L = 430 μm cavities, scribed into individual diodes, and mounted onto Au-plated Cu blocks using In/Pb solder.

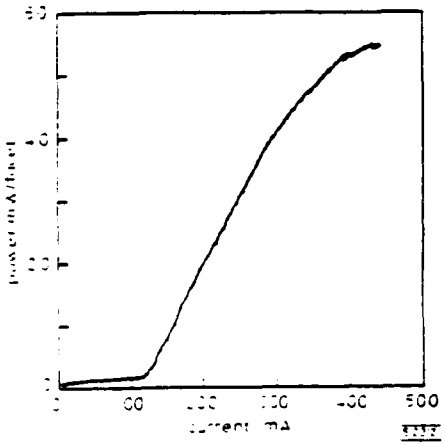

Fig. 2 *Output power as function of drive current of 14 element DFB ridge waveguide laser array operating under room temperature, CW conditions*

Results: The DFB laser arrays were tested under both pulsed (2 kHz, 1·5 μs) and CW conditions at room temperature. The CW output power against drive current (L–I) profile is shown in Fig. 2. The threshold current is 110 mA (< 8 mA/element), corresponding to a threshold current density of 455 A/cm^2, with an external quantum efficiency of η_{ex} = 36%. The L–I

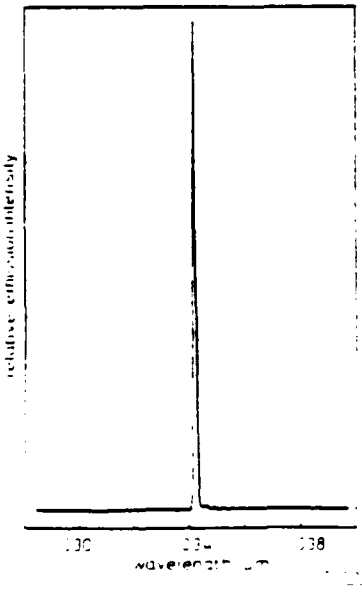

Fig. 3 *Room temperature, CW emission spectrum of 14 element DFB ridge waveguide laser array at I_{op}, λ = 1·0343 μm*

[*] BEERNINK, K. J., MILLER, L. M., COCKERILL, T. M., and COLEMAN, J. J.: Phase-locked ridge waveguide InGaAs–GaAs–AlGaAs strained-layer quantum well heterostructure laser arrays: unpublished

Reprinted from ELECTRONICS LETTERS 10th October 1991 Vol. 27 No. 21 pp. 1943-1944